ธรณีวิทยาใต้ผิวดินบริเวณส่วนใต้ของแอ่งตะกอนเมอร์กุยอายุเทอร์เชียรีทะเลอันดามัน

นางสาว ประภาพร เครือสีดา

วิทยานิพนธ์นี้เป็นส่วนหนึ่งของการศึกษาตามหลักสูตรปริญญาวิทยาศาสตรมหาบัณฑิต
สาขาวิชาธรณีวิทยา ภาควิชาธรณีวิทยา
คณะวิทยาศาสตร์ จุฬาลงกรณ์มหาวิทยาลัย
ปีการศึกษา. 2545

ISBN 947-17-3390-9

SUBSURFACE GEOLOGY OF THE SOUTHERN PART OF TERTIARY MERGUI BASIN, ANDAMAN SEA

Ms. Praphaporn Khursida

A Thesis Submitted in Partial Fulfillment of the Requirements
for the Degree of Master of Science in Geology
Department of Geology
Faculty of Science
Chulalongkorn University
Academic Year 2002

ISBN 974-17-3390-9

Thesis Title	Subsurface Geology of the Southern Part of the Tertiary Mergui Basin, Andaman Sea
By	Ms. Praphaporn Khursida
Field of Study	Geology
Thesis Advisor	Assistant Professor Nopadon Muangnoicharoen, Ph.D.
Thesis Co-advisor	Sunton Srigulwong

Accepted by the Faculty of Science, Chulalongkorn University in Partial Fulfillment of the Requirements for the Master's Degree

…….. Dean of Faculty of Science
(Associate Professor Wanchai Phothiphichitr, Ph.D.)

THESIS COMMITTEE

……..Chairman
(Associate Professor Visut Pisutha-Arnond, Ph.D.)

……..Thesis Advisor
(Assistant Professor Nopadon Muangnoicharoen, Ph.D.)

……..Thesis Co-advisor
(Sunton Srigulwong)

……. Member
(Assistant Professor Pongsak Phongprayoon)

ประภาพร เครือสีดา : ธรณีวิทยาใต้ผิวดินบริเวณส่วนใต้ของแอ่งตะกอนเมอร์กุยอายุเทอร์เชียรีทะเลอันดามัน (SUBSURFACE GEOLOGY OF THE SOUTHERN PART OF TERTIARY MERGUI BASIN, ANDAMAN SEA) อ. ที่ปรึกษา : ผ.ศ ดร. นภดล ม่วงน้อยเจริญ, อ. ที่ปรึกษาร่วม สุนทร ศรีกุลวงศ์ จำนวนหน้า 106 หน้า. ISBN 974-17-3390-9

การศึกษาธรณีวิทยาใต้ผิวดินบริเวณส่วนใต้ของแอ่งตะกอนอายุเทอร์เชียรีทะเลอันดามัน โดยศึกษาจากข้อมูลหลุมเจาะและข้อมูลการสำรวจธรณีฟิสิกส์ด้วยวิธีการวัดคลื่นไหวสะเทือน 2 มิติ เพื่ออธิบายธรณีวิทยาใต้ผิวดิน ธรณีวิทยาโครงสร้าง สภาพแวดล้อมของการสะสมตัว วิวัฒนาการของการเกิดแอ่งพร้อมทั้งประเมินศักยภาพปิโตรเลียมเบื้องต้น จากการศึกษาพบว่า มีรอยเลื่อนปกติวางตัวในแนวเหนือใต้เป็นปัจจัยควบคุมการเกิดแอ่ง ซึ่งรอยเลื่อนนี้เป็นผลจากแรงดึงซึ่งมีความสัมพันธ์กับการชนกันของแผ่นทวีปอินเดียและยูเรเซีย และมีความสัมพันธ์กับรอยเลื่อนตามแนวระดับในบริเวณนี้

การเรียงลำดับหินตะกอนอายุเทอร์เชียรีในบริเวณส่วนใต้ของแอ่งเมอร์กุย แบ่งออกได้เป็น 4 กลุ่ม คือ A B C และ D ส่วนล่างของกลุ่ม A ประกอบด้วยหินดินดาน บางส่วนแทรกสลับด้วยหินทรายแป้ง ส่วนกลางของกลุ่ม A ประกอบด้วยหินทรายบางส่วนแทรกสลับด้วยหินดินดาน ส่วนบนของกลุ่ม A ประกอบด้วยหินทรายแป้ง หินโคลน และหินดินดาน ส่วนกลุ่ม A ที่สะสมตัวในพื้นฐานที่ระดับสูงประกอบด้วยหินปูนในส่วนล่างและส่วนบนประกอบด้วยหินทรายแป้ง หินโคลน และหินดินดาน มีอายุในช่วงปลายสมัยโอลิโกซีนถึงช่วงต้นสมัยไมโอซีน และสภาพแวดล้อมของการสะสมตัวประกอบด้วยลักษณะปรากฏเป็นแบบแอ่งราบในส่วนนอกของทะเลน้ำตื้นถึงส่วนในของทะเลน้ำลึก การถล่มใต้ทะเลน้ำลึกและพืดหินใต้น้ำในทะเลน้ำตื้น กลุ่ม B ประกอบด้วยหินทรายแป้งและหินโคลน แทรกสลับด้วยหินปูน หินทรายและหินดินดาน มีอายุในปลายช่วงต้นสมัยไมโอซีนถึงช่วงกลางสมัยไมโอซีน และสภาพแวดล้อมของการสะสมตัวประกอบด้วยลักษณะปรากฏเป็นแบบแอ่งราบในส่วนบนถึงส่วนกลางของทะเลน้ำลึก กลุ่ม C ประกอบด้วยหินทรายแป้งและหินโคลน ส่วนกลุ่ม C ที่สะสมตัวในพื้นฐานที่ระดับสูงประกอบด้วยหินปูน มีอายุในช่วงปลายช่วงกลางสมัยไมโอซีนถึงช่วงสมัยไพลโอซีน และสภาพแวดล้อมของการสะสมตัวประกอบด้วยลักษณะปรากฏเป็นแบบแอ่งราบในส่วนบนถึงส่วนกลางของทะเลน้ำลึกและหินพืดใต้น้ำในทะเลน้ำตื้น กลุ่ม D ประกอบด้วยหินทรายแป้งและหินโคลน มีอายุในช่วงสมัยไพลสโตซีนถึงปัจจุบัน และสภาพแวดล้อมของการสะสมตัวประกอบด้วยลักษณะปรากฏเป็นแบบแอ่งราบในส่วนบนถึงส่วนกลางของทะเลน้ำลึก

ผลการวิเคราะห์ธรณีเคมีพบว่า หินดินดานที่สะสมตัวในทะเล และหินปูนที่สะสมตัวในปะการัง ในกลุ่มหิน A และ C มีศักยภาพที่จะให้น้ำมัน/ก๊าซและก๊าซ หินทรายและหินปูนในกลุ่มหิน A และ C เป็นหินกักเก็บที่มีคุณภาพพอใช้ถึงดี หินโคลน หินทรายแป้งและหินดินดานที่สะสมตัวในทะเลในทุกกลุ่มหินมีประสิทธิภาพที่จะเป็นหินปิดกั้น การกักเก็บปิโตรเลียมเป็นได้ทั้งแบบโครงสร้างกักเก็บและการเรียงลำดับชั้นหินกักเก็บ จากการศึกษาโดยวิธีการของโลปาแตง แสดงให้เห็นว่าช่วงการกำเนิดปิโตรเลียมอยู่ในระดับลึกมากกว่า 1000 เมตรในหลุมเจาะกันตัง และ 1200 ถึง 1300 เมตรในหลุมเจาะกระบุรี

ภาค……วิชาธรณีวิทยา…… ลายมือชื่อนิสิต……

สาขา……วิชาธรณีวิทยา…….. ลายมือชื่ออาจารย์ที่ปรึกษา……

ปีการศึกษา……..2545…….. ลายมือชื่ออาจารย์ที่ปรึกษาร่วม……..

##4372510023: MAJOR GEOLOGY/
KEY WORD: SUBSURFACE GEOLOGY /PETROLEUM/MERGUI BASIN/ANDAMAN SEA
PRAPHAPORN KHRUSIDA: SUBSURFACE GEOLOGY OF THE SOUTHERN PART OF TERTIARY MERGUI BASIN, ANDAMAN SEA. THESIS ADVISOR: ASSIST. PROF. NOPADON MUANGNOICHAROEN, Ph.D., THESIS CO-ADVISOR SUNTON SRIGULWONG. 110 pp. ISBN 947-17-3390-9

The study of subsurface geology of the southern part of the Tertiary Mergui basin, Andaman Sea, is based on well information and 2D seismic data set to explain subsurface geology, geologic structure, depositional environment and basin evolution with preliminary assessment on the petroleum potential within the study area.

The Mergui basin is located in the southern part of Andaman Sea. The development of basin is controlled by N-S normal faults that bound western edge of the basin. These normal faults are the result of the extension in this region that probably related to the collision of India with Eurasia plate and interaction of strike-slip faults in this region.

The Tertiary sedimentary sequence of the southern part of Mergui basin can be subdivided into 4 units, namely units A, B, C, and D. The unit A comprises outer neritic to middle bathyal shale in the lower part, upper bathyal sandstone in the middle part, and the upper part is outer neritic to middle bathyal siltstone claystone and shale that located in restricted sub-basin. The unit A that is located at the basement high is composed of limestone. This unit deposited in an outer neritic to middle bathyal basinal plain, mid-fan turbidite, and reef shallow-marine environment. The age is Late Oligocene to Early Miocene. Unit B consists of siltstone and claystone which occasionally interbeded with limestone, sandstone and shale. The age of this unit is Early Miocene to Middle Miocene. The environment of deposition is upper to middle bathyal basinal plain. Unit C consists of siltstone and claystone. The unit that located at the basement high is composed of limestone or carbonate builds up. The age of this unit is Middle Miocene to Pliocene. This unit deposited in upper to middle bathyal basinal plain, and reef of shallow-marine environment. Unit D consists of clayey siltstone. The age of this unit is Pliocene to Holocene. This unit deposited in upper to middle bathyal basinal plain with the shelf on the eastern part of study area.

The potential source rocks of the basin are marine shale and reef limestone in Units A and C., which, geochemicals analysis indicates oil and gas and gas prone types. The sandstone in unit A and reefal limestone in Units A and C are of fair to good quality reservoir. The marine claystone, siltstone and shale in all units are effective hydrocarbon seal. Most hydrocarbon accumulation is in structural and stratigraphic traps. The Lopatin's method and geothermal data suggest that petroleum generation might have been the oil generation at a depth below the oldest sedimentary unit, 1000 meters in Kantang-1a well and 1200 to 1300 meters in Kraburi-1 well.

Department……..Geology……. Student's signature……...

Field of study……Geology……. Advisor's signature……..

Academic year……2002……. Co-advisor's signature…….

ACKHOWLEDGEMENTS

The author is indebted to a number of individuals and organization for their constant support and encouragement toward the successful completion of this study.

The Graduate School and Department of Geology, Chulalongkorn University for financial support.Assistant Professor Dr. Nopadon Muangnoicharoen, thesis advisor and Mr. Sunton Srigulwong, co-advisor are thank for their guidance, encouragement, for his suggestions and valuable guidance throughout the study. Special acknowledgment goes Assistant Professor Pongsak Phongprayoon and Mrs.Malatee Taiyaqupt, are especially thanked for their valuable advises, comments and reading the manuscript.

The Department of Geology, Chulalongkorn University provides numerous facilities for the study. Energy Resource Information and Data Unit, Mineral Fuels Division, the Department of Mineral Resources of Thailand (DMR), allows the usage of data. Deep appreciation is given to Mrs. Malai Pitchayakul, Ms. Anongporn Intawong and Mr. Tananchai Mahattanachai for providing some data. Schlumberger's staffs for teaching and useful guidance the Charisma program.

Moreover, a great appreciation is directed to Ms. Ratrii Khruathao and Ms.Naiyana Naimolee for helping in the preparation of the manuscript.

Finally, this thesis could not be possible without the help and encouragement of her family and her best friends who patiently provide both moral and physical supports, especially her parents also appreciated for the timeless and throughout support to this study.

CONTENTS

CONTENTS(continued)

LIST OF TABLES

LIST OF FIGURES

LIST OF FIGURES(Cont.)

CHAPTER I

INTRODUCTION

Tertiary basins are probably the most attractive sedimentary basins of all different geological ages as they have been long known as the potential of the accumulation of mineral fuel and energy resources, especially oil, natural gas, oil shale and coal. The fact is, almost all coal mining and petroleum produced in Thailand are from Tertiary basins.

Of approximately 70 Tertiary basins in Thailand, 31 (Figure 1.1) are the interesting basins in terms of containing or possible possessing petroleum potential. These basins are distributed in all parts of Thailand, from the north, the central plain, to the south, as well as in the Gulf of Thailand, and in Andaman Sea in the west. There are five terrestrial basins, which have been known to contain commercial petroleum accumulation, namely Fang, Phisanulok, Phetchabun, Suphan Buri and Kamphaeng Saen. In addition, there are 4 basins in the Gulf of Thailand, namely Chumphon, Songkla, Pattani, and Malay basins, and 2 in Andaman Sea, ie Andaman and Mergui basins.

The southern part of Mergui basin has been selected for this study as it is lack of successful exploration within the Mergui basin in the past. And later on, there is additional information from the exploration programs, from both the drilling exploration and geophysical survey, which had been undertaken so that reasonable subsurface geological information is properly available. Hopefully, the findings from this study might benefit a further investigation for the petroleum occurring in this Tertiary basin and adjacent areas.

1.1 The study area

The study area covers the southern part of Mergui basin, Andaman Sea in the continental shelf part of Thailand as shown in Figure 1.2. The area lies approximately between Latitudes 6°45'N to 7°15'N and Longitudes 96°45'E to 97°40'E. It is approximately 5,000 square kilometers and covered by the W8/38 and W9/38

Concession blocks. The water depth ranges from 512 meters to over 1000 meters as shown in Figure 1.3.

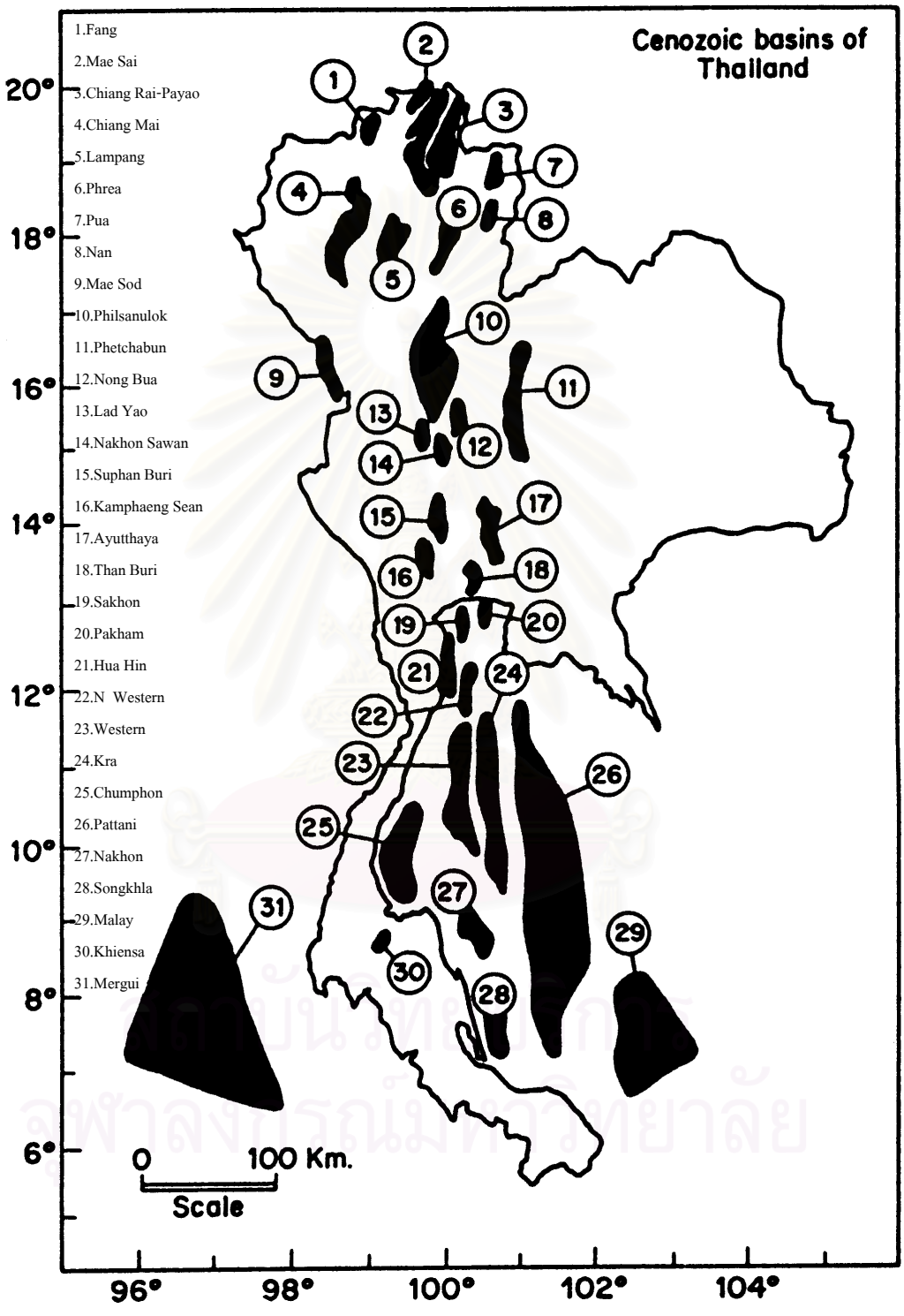

Figure 1.1 The Cenozoic basins of Thailand (from Chaodumrong, 1985).

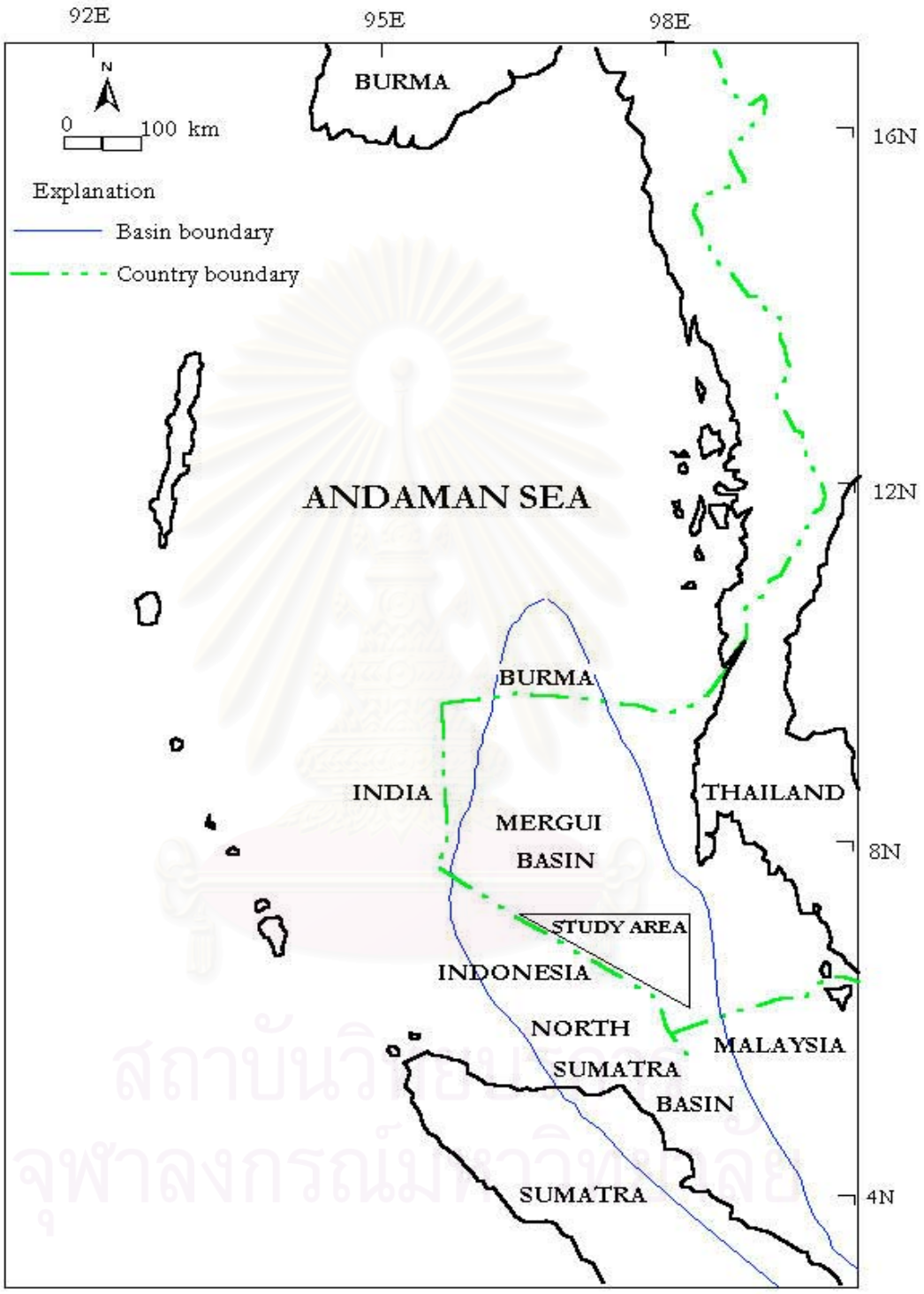

Figure 1.2 Location of study area.

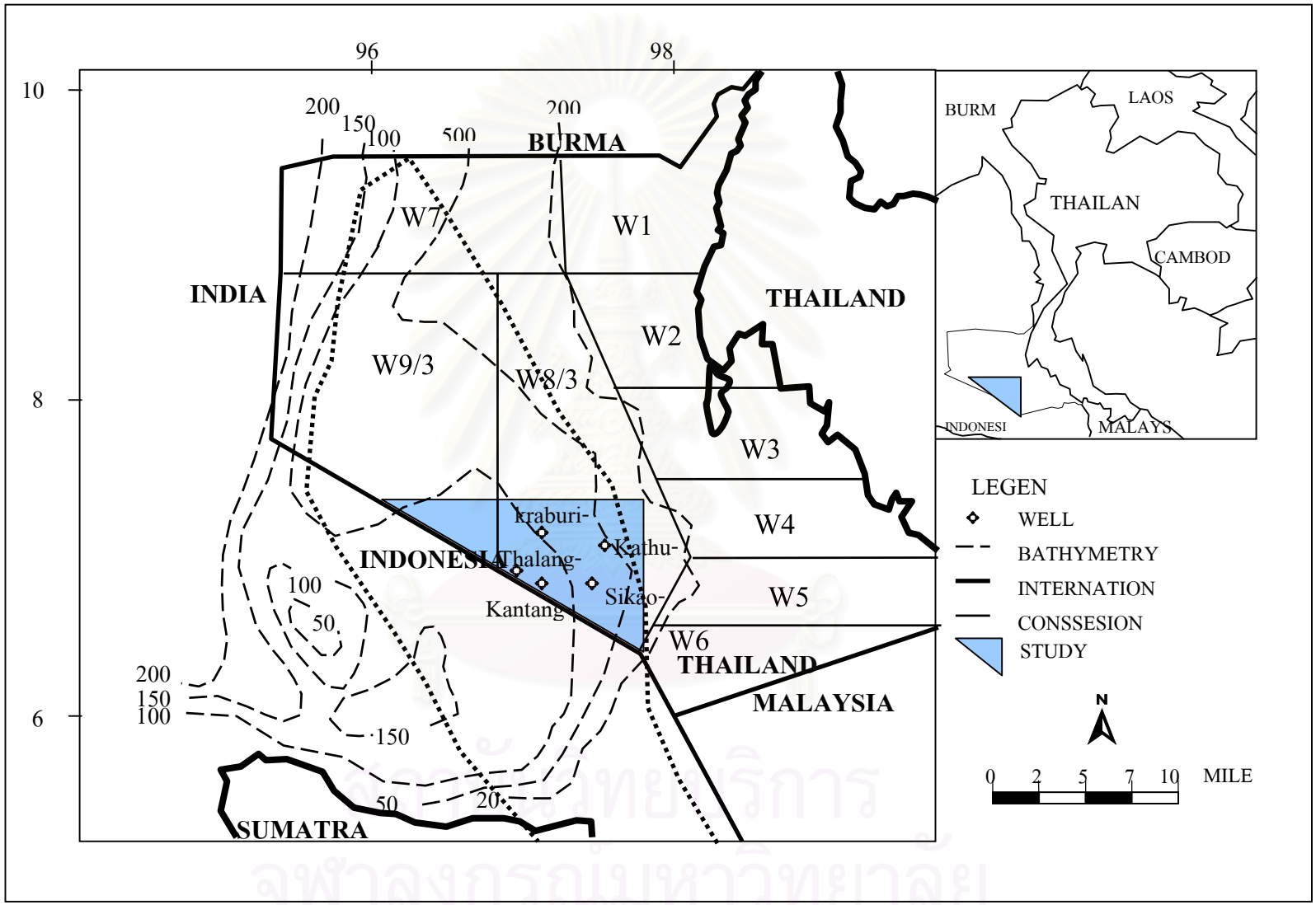

Figure 1.3 The exploratory well locations and bathymetic map.(modified from Polachan and Racey,1993)

1.2 Objective of the study

The purpose of this research is to assess the geological setting, geological structures, stratigraphy of Tertiary sediments and depositional evolution of the southern part of Mergui basin, as well as preliminary assessment of the petroleum source potential in the southern part of the Mergui basin. The analysis of Tertiary sedimentary sequence in order to reconstruct the depositional environment is well established to these objectives.

1.3 Data source

The studied data have been provided by the Mineral Fuels Division, Department of Mineral Resources, Thailand. The data consist of seismic data set, five final well reports, sidewall cores analysis reports, mud logs reports, biostratigraphy reports, geophysical logs and general geological data. The 2D reflection seismic data set is approximately 820 line–kilometers. The location of twenty reflection seismic lines and five exploratory wells are shown in Figure 1.4. The seismic sections have a vertical scale of 10cm/second and horizontal scale 1:250,000 with 25m shot point interval. The geophysical logs being available include the caliper, gamma ray, spontaneous potential, density, neutron and resistivity logs with scale 1:500 and 1:200.

In the study area, five exploratory wells, namely Kantang-1a, Thalang-1, Sikao-1, Kathu-1 and Kraburi-1 with the total depth of 10,648 meters were used for the study. Only Kantang-1a well is shown with minor gas trace.

1.4 Study methodology

All informations on regional geology of the Andaman Sea, Mergui basin and adjacent area are reviewed to serve as a background knowledge for the present study. The geological setting of the study area from previous studies has been reviewed in order to understand the geological history, tectonic evolution and general stratigraphy. The study was then focusing on the geological setting of southern part of Tertiary Mergui basin.

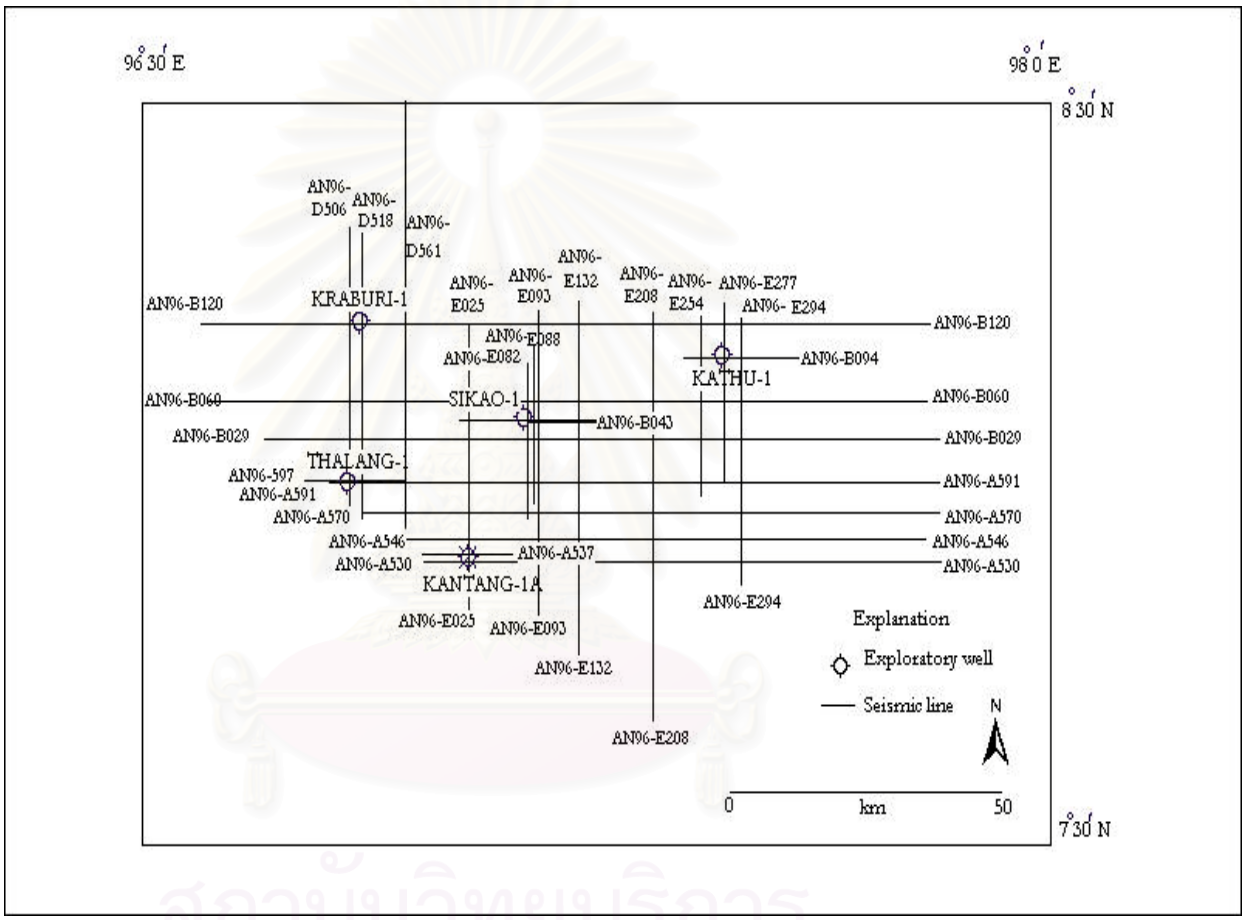

Figure 1.4 The location of seismic lines and exploratory wells in the study area.

The available data were selected and prepared for the study program as follow. The seismic data were selected and analyzed to search for the regional boundaries of depositional sequence and important geological structures. The seismic markers were identified by biostratigraphic data of the Kantang-1a, Thalang-1, Sikao-1, Kathu-1 and Kraburi-1 well. At the same time, the geophysical logs from five drilled holes were studied with mud logs, sidewall cores and biostratigraphic data. The results of these studies were compared and correlated to establish the Tertiary sedimentary units of Mergui basin. Then the sedimentary sequence studies were analyzed together with seismic data for depositional environments. Finally, the evolution of depositional system of the basin was reconstructed within the framework of geological setting of the study area.

In addition, the petroleum geochemical data, geothermal gradient and Lopatin's method were used to determine the maturation and potential to generate hydrocarbons. The results of the study were analyzed for the preliminary assessment of petroleum source potential of the southern part of the Mergui basin.

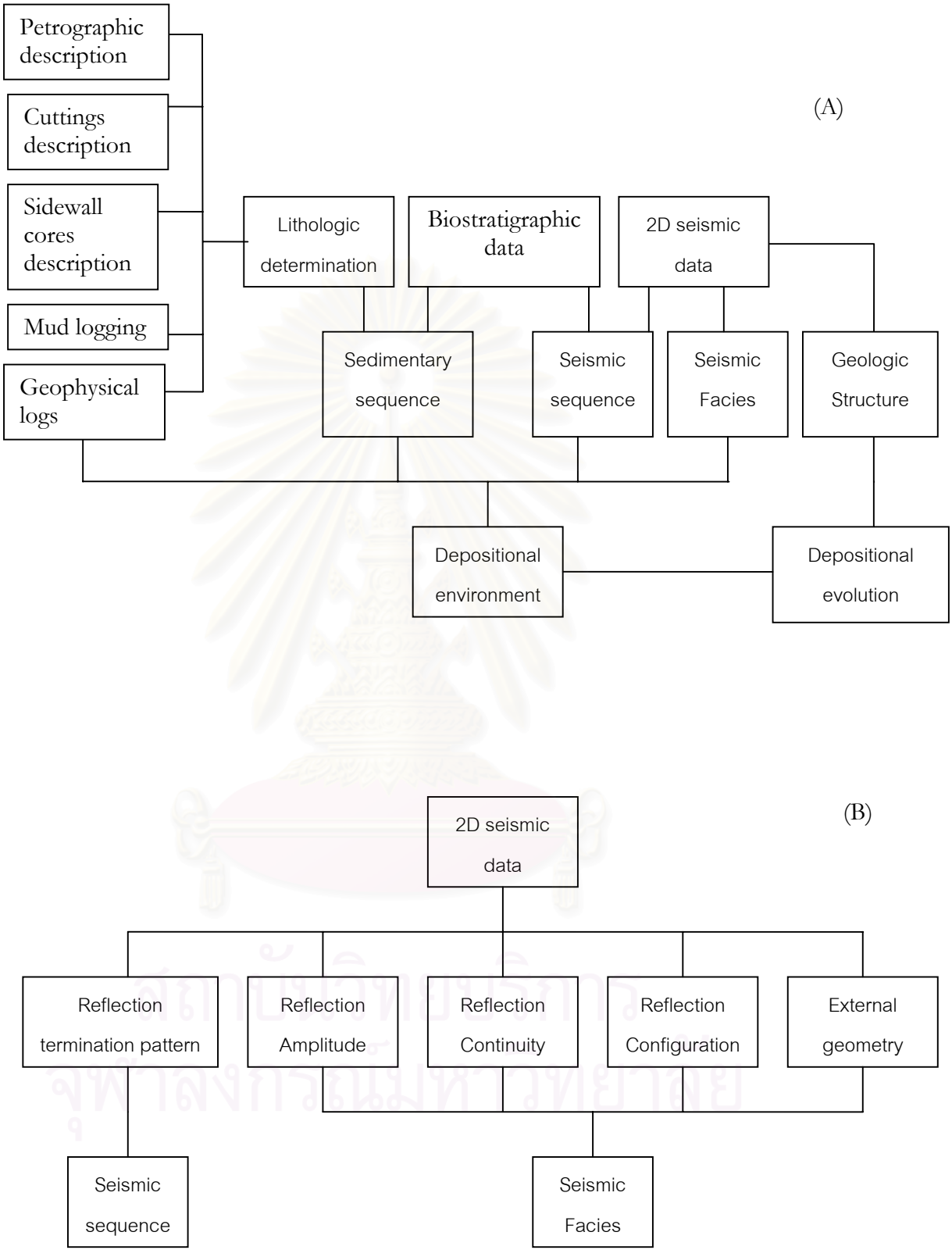

Figure 1.5 Flow charts illustrating the study methodology for (A) subsurface geology, and (B) seismic stratigraphy.

1.5 Exploration history

The petroleum concession block Nos.W7, W8 and W9 covered the Mergui basin (Fig.1.3). In 1974, the concession block No.W7 was awarded to Oceanic Exploration S.E.A., the concession block No.W8 to Union Oil Company of Thailand, and the concession block W9 to Esso Exploration Inc. In that year, 2D seismic survey was carried out on the concession block No.W7.

From late 1975 to 1976, 2D seismic surveys of totally 3,200 line – kilometers were conducted on the concession block No.W9. Five exploratory wells in the water depths ranged from 583 to 1,055 meters were drilled. They are W9-A-1, W9-B-1, W9-C-1, W9-D-1 and W9-E-1 with total depth of 16,535 meters. Non-commercial hydrocarbon was presented and Esso Exploration Inc. fully relinquished its concessions in 1982.

In 1976, 2D seismic surveys were carried out on the concession block No.W8. Six exploratory wells were drilled in the water depth ranged from 410 to 621 meters. They are Trang-1, Tai-1, Phangha-1, Mergui-1 and Payang-1. The sixth well, Surin-1 was abandoned because of mechanical problems. Only in Mergui-1 and Trang-1 wells that gas shows and trace were found. The grantee, Union Oil Company of Thailand relinquished this concession block in 1977.

In 1987, two exploratory wells were drilled in the concession block No.W8 that had the same name but different in shapes from the previous W8. The water depths were ranged from 618 to 655 meters. They are Yala-1 and Ranot-1.Before those wells were drilled, Hunt International Corp. carried out minor 2D seismic surveys of totally 834 line-kilometers in 1984. Both wells were found dry, with only minor gas shows was observed in Yala-1 well.

In 1995, The Department of Mineral Resource carried out the 2D seismic surveys covering the Andaman Sea using Geco-Prakla service.

In 1996, the concession W8 and W9 were again awarded to Unocal, Total and Statoil. Extensive 2D seismic surveys of total 11,737 line-kilometers were conducted, and five exploratory wells, namely Kantang-1a, Thalang-1, Sikao-1, Kathu-1 and

Kraburi-1 were drilled with the total depth of 10,648 meters. Non-commercial hydrocarbon was presented and then that concession was relinquished. These last survey results are the source data for the present study.

1.6 Previous works

Week et al. (1967) delineated the structural belt as major segment of the island arc system of the Andaman Sea from a sub-bottom profiler survey, bathymetry, gravity and magnetic measurement. The island arc system includes foredeep, outer sedimentary island arc, inner volcanic arc and associated rift valley, and backdeep.

Rodolfo (1969) reported the subaerial physiographic, geologic setting, bathymetry, marine geology of the Andaman Sea, and tectonic implications for Southeast Asia.

Achalabhuti (1975) discussed the petroleum potential in the Gulf and the West Coast of Thailand in terms of depositional systems. The expected potential petroleum producing trends include barrier bar-strandplain, shelf, shelf edge, and submarine fan.

Curray et al. (1978) reported the tectonic analysis of Andaman Sea and Burma based on the marine seismic reflection, refraction measurement, preliminary analyses of gravity, magnetic, heat flow, and bottom samples.

Nakanart and Mantajit (1983) studied and correlated the stratigraphic successions of the Mergui basin by the successions of the northern part of the straits of Malacca, and North Sumatra basin. Five formations from these two regions had been classified and correlated, namely Andaman and Parapat/Bampo Formations, Tai and Arun/Malacca Limestones, Trang and Bang Formations, Payang and Kentapang Formations, and Takua Pa and Seurula/Julu Rayen Formations.

Khantaprab and Sarapirome (1983) reviewed the geology of the Gulf of Thailand and Andaman Sea.

Dain et al. (1984) suggested two types of tectonic settings of Andaman Sea based on an interpretation of Landsat imagery and fault plane solutions of shallow and intermediate earthquakes. Tectonic settings, seafloor spreading and transform faulting suggested an eastward subduction of the Indian plate beneath the Andaman-Nicobar ridge.

Harding (1985) presented a definition of the negative flower structure from seismic profile examples from the Andaman Sea as shallow synform and the upward and outward spreading strains of a wrench fault.

Srigulwong (1986) proposed two types of faults, which have been developed in the southeastern part of Mergui basin. The major N-S normal faults with associated right-lateral movement and the minor NE-SW antithetic normal faults were noted from the studies of the structural evolution and sedimentation which occurred during the Oligocene time in the vicinity of the well W9-E-1 of the Mergui basin

Polachan (1988) studied the sedimentary, structural and tectonic evolution of the Mergui basin based on geological data from petroleum exploratory program in 1976.

Polachan and Sattayarak (1989) proposed the Tertiary basins to be predominantly transtensional basins based on the structural geometry, paleomagmetic data and recent earthquake analyses, which were related to the strain ellipsoid of dextral simple shear. The NW-SE and NNE-SSW trending faults had been interpreted as a conjugate set of strike slip movement.

Polachan and Racey (1993) described the Tai Formation of the Mergui Group, which was similar to the carbonates in Arun field of the same age that produced gas. They also discussed its petroleum potential.

Packham (1993) proposed the relationship between the plate tectonic evolution and the main phases of basinal development in western Southeast Asia from their genesis in Late Paleocene till Recent.

CHAPTER II

GEOLOGY

2.1 Physiography

The Mergui basin is located in the Thai part of Andaman Sea, which is bordered to the east by western coastal line of Thai – Malay Peninsula. It is limited to the west by the Indian area, to the north by the Myanmar and to the south by the Indonesian and Malaysian areas.

The northern part of Andaman Sea extend from Irrawaddy deltaic coast of central Burma and extending about 800 kilometers southward to North Sumatra and the Malacca strait. The maximum width of 650 kilometers from the western coast of the Thai-Malay Peninsula to Andaman and Nicobar Islands are as shown in Figure 2.1. Andaman Sea floor comprises two sedimentary basins, i.e. Andaman basin which locates to the northwestern and Mergui-North Sumatra basin to the southeastern part of the Andaman Sea. The water depth of the inner shelf along the western coast of the Malay Peninsula is less than 100 meters. A width of the northern end is about 130 kilometers. The width decreases toward the southern direction and is terminated by a minor slope which the relief is about 100 meters. The inner shelf of Phuket Island is only 35 kilometers. The Mergui terrace is widened, flattened and deepened from the north at 12 °N Latitude to the south at 9 °N Latitude, and becomes concave, bifurcated into Mergui bank on the western and Sumatra shelf basin on the east. A width of the Mergui bank is about 70 kilometers, and the length is about 200 kilometers. The Sumatra shelf is bound to the east and the south by the slopes off the Sunda shelf (Malacca strait) and the northern Sumatra, and it is opened to the continental slope at approximately 1300 meters water depth as shown in Figures 2.1 and 1.3. The continental shelf break is deepened southward. The shelf break marker is pinnacle with about 200 meters of the relief on the western edge of Mergui bank. Generally, the gradient is average 1.8° and steeper in the north. Between Sewell seamount and Matabun canyon, the continental slope abruptly ends in 2435 meters of the terrace, which gently in the west direction 60 kilometers to 2670 meters depth. And the bottom of central Andaman trough drops sharply to the 3035 meters depth.

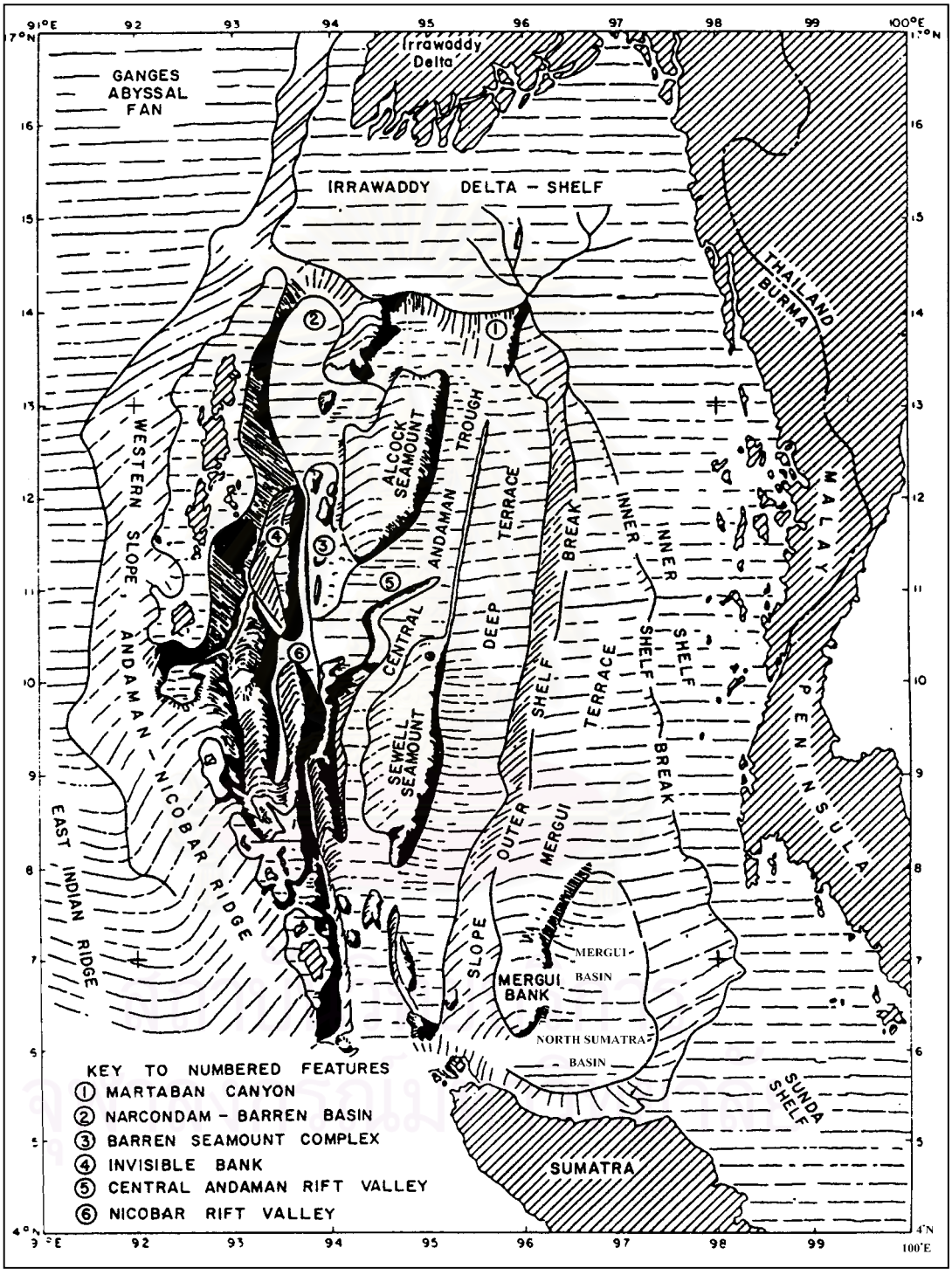

Figure 2.1 Physiography of the Andaman Sea (from Rodolfo, 1969).

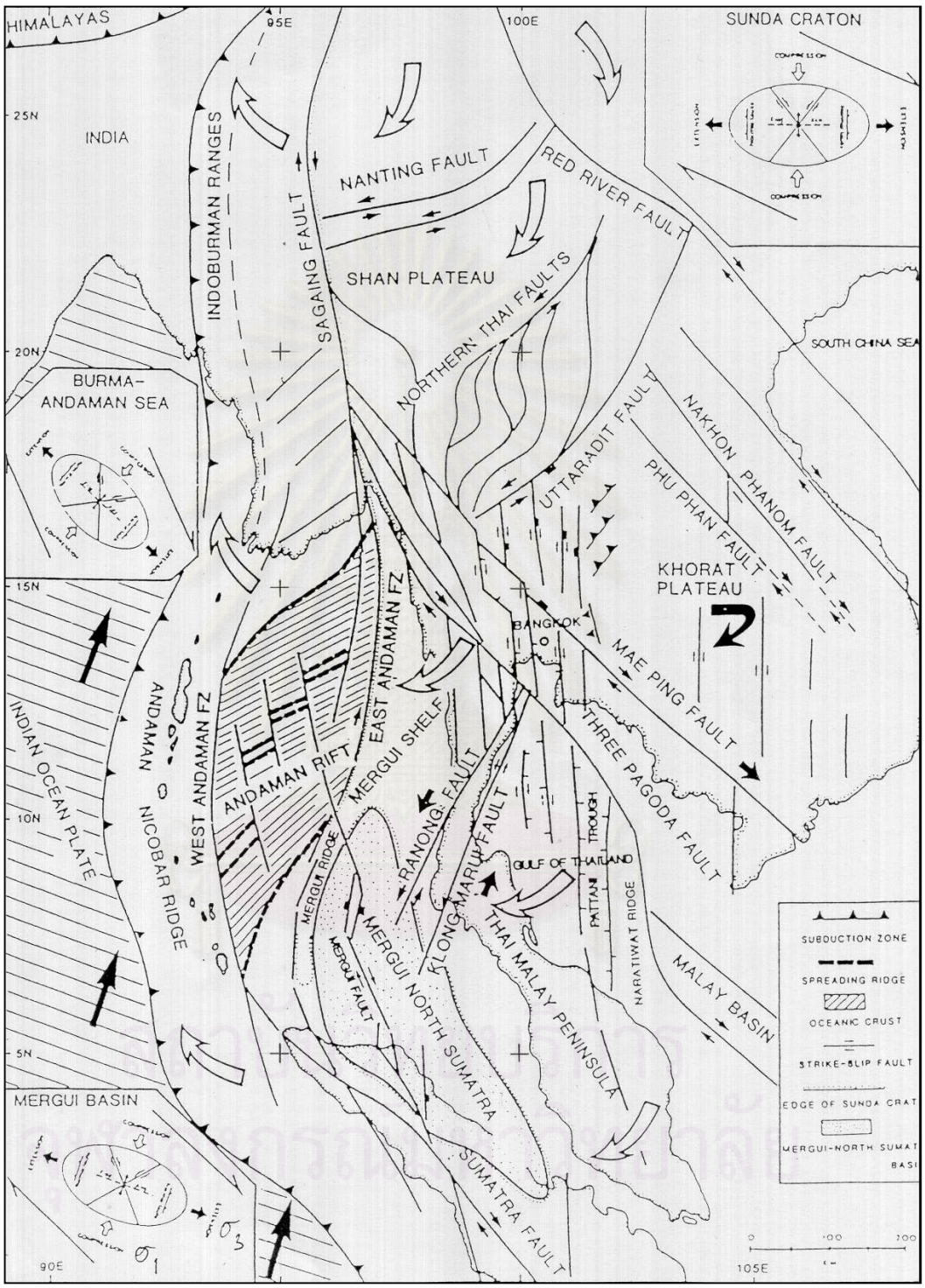

Figure 2.2 Regional tectonic feature of the Andaman Sea (from Polachan, 1988).

Andaman Sea area is one of the largest modern backarc basins, which is associated with the Sunda trench as shown in Figure 2.2. Sunda arc, between Burma and the Sunda land to the east of Java represents a 5000 kilometers long subduction zone of the Indian oceanic plate beneath the Eurasian plate. The northern and southern parts of this elongate basin which extend into Burma and Sumatra, respectively, lie on the continental crust, but the center of the basin is floored by the young oceanic crust. Thus, the present-day depositional environment of the basin changes from continental Burma to deltaic and oceanic Andaman Sea, which display a variety of sediment types including coarse-grained mass flow deposit, submarine fan turbidites and basinal turbidites, and again changes to continental condition in Sumatra (Rodolfo, 1969).

A detail analysis of the basin's sediments and sedimentary process were studied by Rodolfo, (1969). Generally, modern sediments in Andaman Sea are dominated by silty clay, silty clay with rare laminae and foraminifera ooze with rates of deposition about 5-30 centimeters per thousand years as shown in Figure 2.3. The highest rate of deposition is in the eastern deltaic shelf, which is about 200 centimeters per thousand years as shown in Figure 2.4. It is a principal source sediment for the Andaman basin. The coarse reef debris is presented all around the Andaman-Nicobar ridge which, in many place, the coral reefs and beaches are raised as high as 20 meters above sea level. The inner shelf and adjacent Mergui terrace is covered by approximately 200 meters thick of unconsolidated sediments. Particularly, Mergui terrace was made up with shelly quartz sands which contain Pleistocene and re-worked Miocene foraminifera. The small step-faults at the edge of Mergui terrace is freshly fractured unaltered basalt. The shelf break are the igneous rocks.

2.2 Geological setting of Mergui basin

The Mergui basin is located offshore off western peninsular Thailand in the southern part of Andaman Sea. It is inversed V-shape basin which is limited to the north by Mergui terrace of central Burma lowland and broader southward to the North Sumatra basin, with apparently continuous to the onshore portion. The basement of the Cenozoic basin in the Mergui basin comprises Eocene volcanic rocks, Late Eocene quartz – chlorite

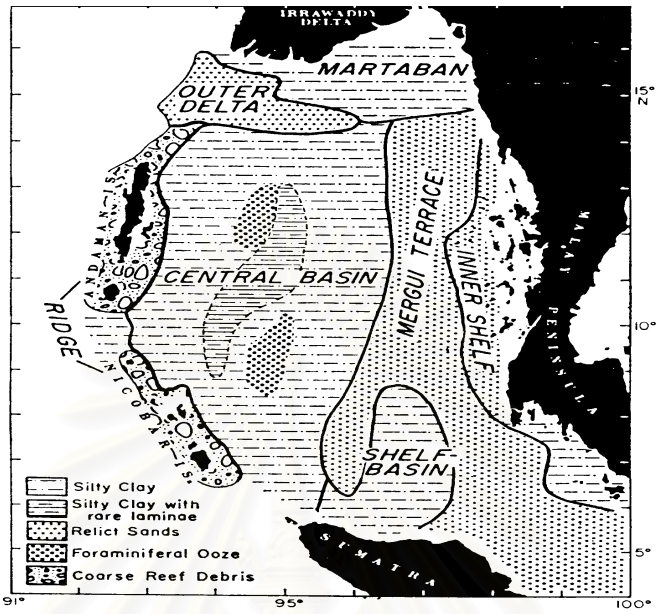

Figure 2.3 General surficial sedimentary basinal-floor forms of the Andaman Sea (Rodolfo, 1969).

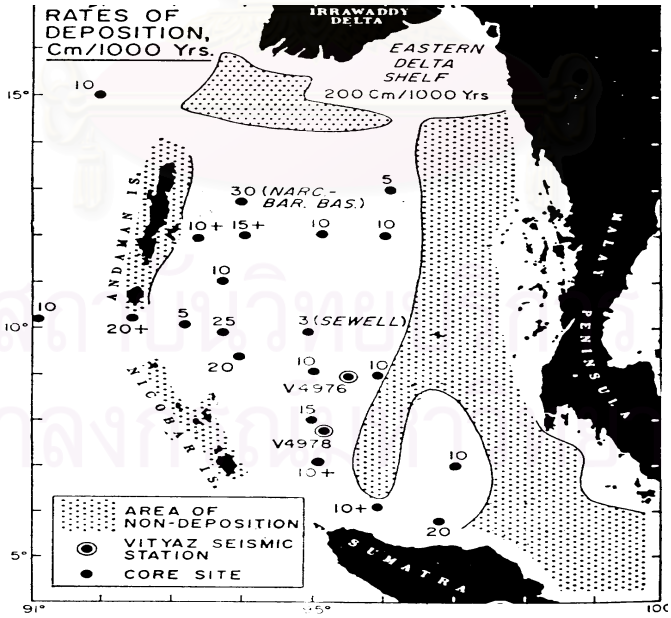

Figure 2.4 Depositional rate of the Andaman Sea. (Rodolfo, 1969).

schist and dacite/rhyodacitic composition (K/Ar dating 41 Ma in ages), Late Cretaceous quartz – monzonite basement, Pre-Tertiary quartzite, phyllite and low-grade metamorphic slate. In addition granite that is probably equivalent to the Paleozoic and Mesozoic rocks of the peninsular Thai-Malay, particularly, granites of late Cretaceous to early Tertiary age are common throughout western Malaysia, peninsular Thailand, and Myanmar.

The stratigraphy of the Tertiary sedimentary rocks of the Mergui basin can subdivided into nine formations of the Mergui Group according to Polachan, (1988), namely from bottom to top, Ranong, Yala, Kantang, Tai, Payang, Trang, Surin, Thalang, and Takua Pa formations. The last two formation formations of Late Oligocene-Earliest Miocene age are laterally equivalent and are equivalent to the Bampo formation in the North Sumatra basin. In ascend order, the next three formations are laterally equivalent formation of Earliest Miocene to Early Miocene age and are equivalent to the Peutu and Beluma formations in the North Sumatra basin. The next two upper formations are laterally equivalent formations of the Middle Miocene age and are equivalent to Baong formation in the North Sumatra basin. The upper part of Thalang formation is equivalent to Keutapang formation, and Takua Pa formation to Julu Payeu Seureula formation in the North Sumatra basin as shown in Figure 2.5. These formations overly the Pre-Tertiary basement and are varies in the environments of deposition, from non-marine sediments to deep marine sediments and submarine fan turbidities.

Also, the Tertiary sediments are divided into five chronostratigraphic units. At first, Late Oligocene-Earliest Miocene period is the time of the beginning of sedimentation. The Thai-Malay Peninsula supplied the sediment southward into the deeper parts of the basin. In the north, fluvio-deltaic sands were deposited, which shale and submarine fan were in the south. Secondly, the earliest Miocene to the end of Early Miocene period was when the water depth increased through time, and commenced rapid extension that created a basin-wide unconformity. Later the local sub-basin coalesced to form an extensive basin. The deep marine shale, some occasional turbiditic sandstone deposited over the entire basin, except that the structural high had been

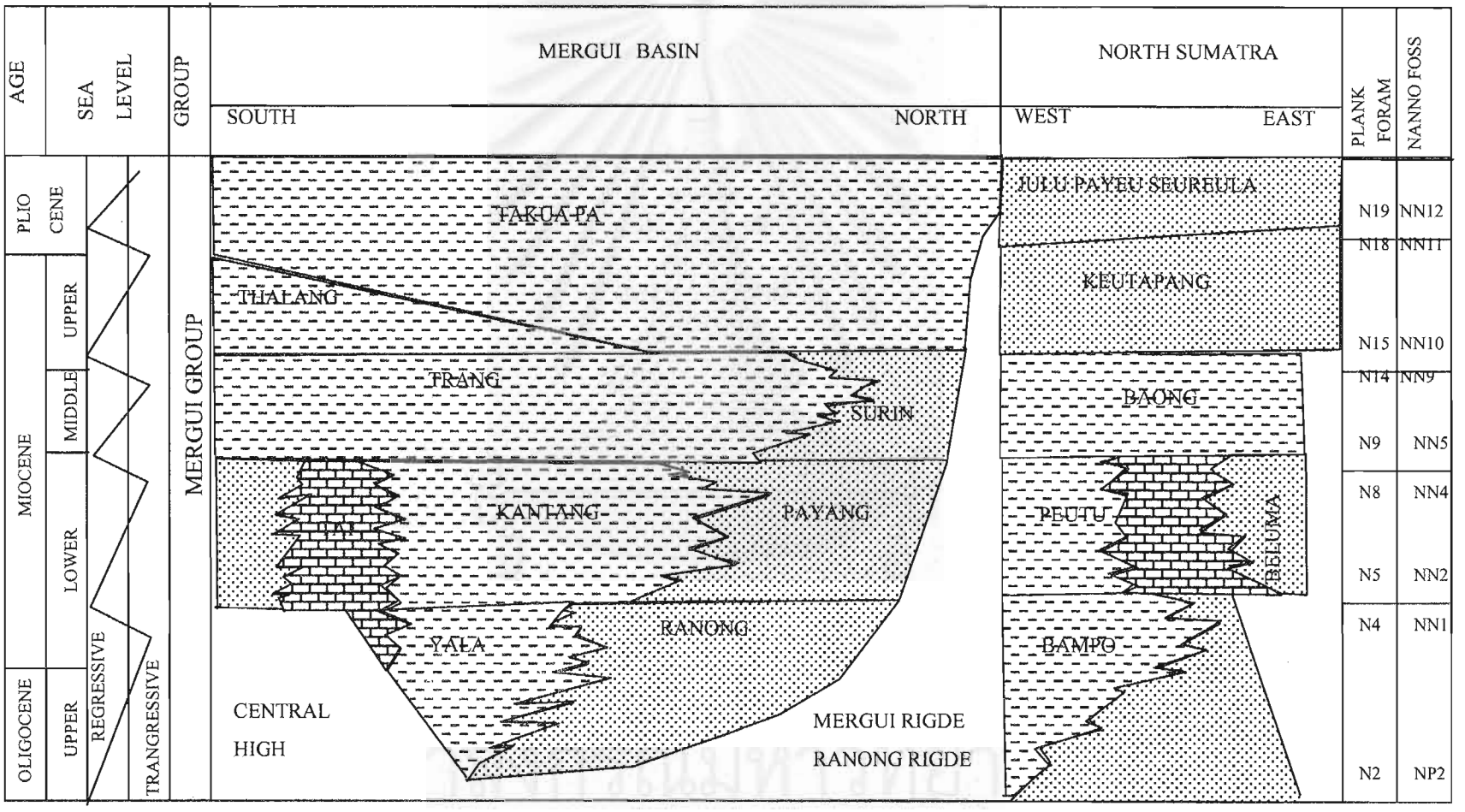

Figure 2.5. The stratigraphic correlation between the Mergui and North Sumatra basins (Polachan and Racey,1993).

formed by the reefs. The third unit in the Middle Miocene period is similarly to that in the previous cycle, i.e. the basinal shale and shallow marine sediments being deposited over the basin. For the forth, the deep marine shale continuously deposited in the southern part of basin, while most of the northern part of the basin was emerged. The fifth unit of the Pliocene to Recent is the completely submergence of the Mergui and Ranong Ridge. The extension and subsidence might have been continued until Recent. The marine shale had been deposited since then up till the present time.

It was noted that, the Tertiary sediments in the Mergui basin are both non-marine and marine types. The age range of the larger foraminifera, the first published record of the larger foraminifera of the Tai Formation in the Mergui Group were proposed by Polachan and Racey (1993) and shown in Figure 2.6. The nanofossil and foraminifera used in dating and correlating of the biostratigraphy as illustrated in Figure 2.7.

SPECIES AGE	UPPER Te LOWER MIOCENE	UPPER Tf MIDDLE MIOCENE
Cycloclypeus eidae	———————	?
Cycloclypeus sp. A	? ———————	?—? —
Lepidocyclina (Nephrolepidina) japonica	———————	———————
Lepidocyclina (Nephrolepidina) sp. A	? ———————	——— ?
Miogypsinaides sp. A	———————	
Miogypsina sp.	———————	———
Spiroclypeus yabeii	———————	
Heterostegina sp.A	—? —— ———	?
Amphistegina sp.	———————	———————
N4	TAI FORMATION N5 N8	N9

Figure 2.6 Age ranges of larger foraminifera recovered from Tai Formation, Mergui basin (Polachan and Racey, 1993).

Period	Epoch		Age	Ma		Biostratigraphic correlation		
						Foraminifera	Calc. Nannofossils	Radiolaria
Q	Early		Calabrian	2.0			Discoaster brouweri	
	Pliocene	L	Piacenzian		N.21	Pulleniatina obliquioculata	NN.18	Pte.p.
						Globorotalia margaritae	NN.17	
							NN.16	Spo.p.
					N.20		NN.15	
		E	Zanclian		N.19		NN.14	
							NN.13	Sti.p.
				5.1	N.18		NN.12	
	Miocene	L	Messinian		N.17	Globorotalia acostaensis	NN.11	Omm.p.
			Tortonian		N.16		NN.10	Omm.a.
				11.3	N.15	Globorotalia menardii	NN.9	
		M	Serravallian		N.14	Globorotalia siakensis	NN.8	Can.p.
					N.13	Globorotalia fohsi	NN.7	Dor.al.
					N.12	lobata-robusta	NN.6	
					N.11	Globorotalia fohsi fohsi	NN.5	
					N.10			
			Late Langhian	14.4	N.9	G. fohsi peripheroronda		Cal.c.
		E	Early Langhian		N.8	Praeorbulina glomerosa		
			Burdigalian		N.7	Globigerinatella insueta	NN.4	
					N.6	catapsydrax stainforthi	NN.3	Cal.v.
			Aquitanian		N.5	catapsydrax dissimilis	NN.2	
				24.6	N.4	Globorotalia kugleri	NN.1	Lyc.b.
	Oligocene	L	Chattian		P22	Globigerina ciperoensis	NP.25	
					P21a	Globorotalia opima opima	NP24	12
					P21b		NP23	13
				32.8	P20	Globigerina ampliapertura		

Figure 2.7 Paleogene and Neogene chronostratic scale and correlation .The figure is a combination of the works of Martini's(1971) and Blow's (1969).

2.3 Structural framework of Mergui basin

The Andaman Sea area is an extensional region that was formed by the seafloor spreading along short east-northeast trending spreading center that are offset by north-northwest striking transform faults (Curray et al., 1978). The West Andaman fault is of major significance throughout the whole region, which extends southwards to connect with the right-lateral Semangko Fault system of Sumatra, and northwards to connect with the right-lateral Sagaing Fault system of Burma. The spreading is shown as a rift valley in the seismic sections. The older strata are upturned along the margins of the rift valley, and indicated continuing spreading through time of the sediment deposition. The good magnetic anomalies is shown in the rift valley to the south, where there is little covered sediment which shows that the central basin began the opening 13 million years ago in the Middle Miocene time with the spreading rate having been calculated at 3.7 cm per year.

The Mergui basin is predominantly transtensional backarc basin that is prolonging to the North Sumatra basin to the south. The basin overlies the continental crust at the western edge of Sunda Craton. The basin rapidly developed as a series of N-S trending half-graben during the late Oligocene and rifting developed progressively northward. The syn-sedimentary faults are as a result of the transtensional right-lateral shearing along the NW-SE trending Sumatra fault system, and the left-lateral Ranong and Khlong Marui fault zones that are bound on the east. The shear was accommodated by the NNW-SSE trending Mergui fault zone and NNE-SSW en echelon normal faults as shown in Figure 2.2.

The general structural frameworks of the Mergui basin that defined by Polachan (1988) comprised six major structural elements as shown in Figure 2.8.

The Mergui Ridge is an approximately 70 kilometers-wide N-S trending structural high. It separates Mergui basin from Andaman basin. The N-S trending faults steeply dipping westward is bounded on the west of the ridge, and the gently eastward dipping slope of the Western Mergui basin is bounded to the east. Thin sediments were

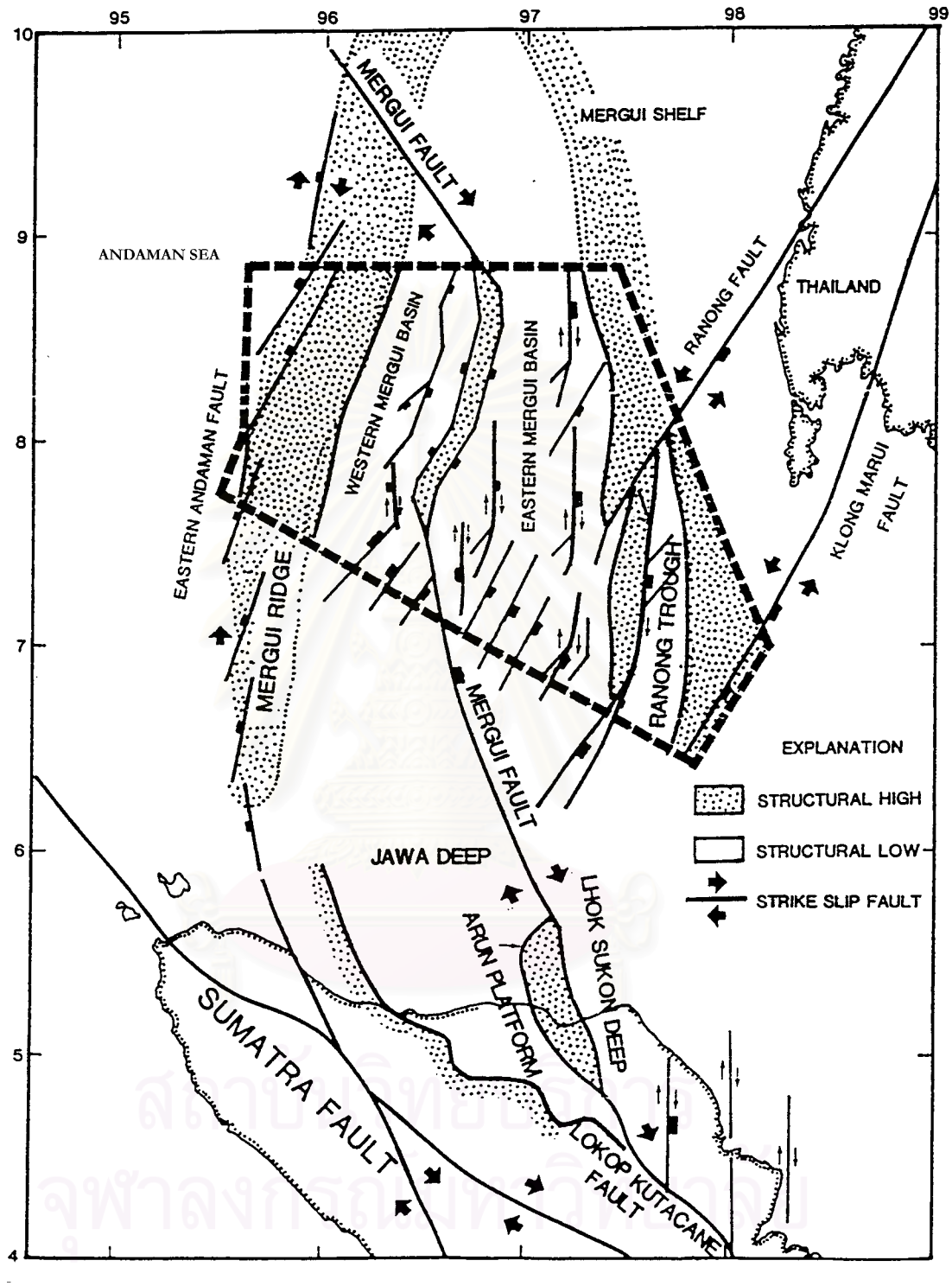

Figure 2.8 Structural map of the Mergui basin(Polachan, 1988)

deposited on the ridge, and mainly are Plio-Pleistocene in age. The Mergui ridge represents the western edge of Sunda Craton (Curray et al., 1979).

The Western Mergui Basin is N-S trending half graben-basin. It lies between the Mergui Ridge and Central High. The steep westward dipping Mergui Fault zone is bounded in the east. The estimated of 15,000-feet thick of sedimentary deposits from seismic section is laid down in this basin.

The Central High is N-S trending and bends into a SE trend in the south horst block, which extends along the Mergui Fault zone. The easterly dipping faults limit the horst in the east, and the westerly dipping faults in the west. On this ridge the reefal and carbonates rocks were deposited .

The Eastern Mergui Basin is N-S trending half-graben which separated by the easterly-dipping N-S trending normal fault. It lies between the west of the Central High and the Mergui shelf or the Ranong ridge in the east. This basin is the main part of the Mergui basin.

The Ranong Ridge is a westward tilting N-S trending basement high. The steeply eastward-dipping N-S trending normal fault is bounded on the east, by the NNE trending been left-lateral Ranong Fault zone. The thin sediments were deposited on the ridge, The sediements mainly are Plio-Pleistocene in age.

The Ranong Trough is a deep narrow westward tilting N-S trending half-graben. It lies between the Ranong ridge on the west and the Sunda shelf on the east. The trough is deepest in the southern portion and becomes shallower northward as the pointing V-shape. The sediments are thickening southward and westward toward Ranong ridge, and becomes thinning northward and eastward to the Sunda shelf.

The Mergui shelf is part of the continent. The thin and flat Tertiary sediments overly the pre-Tertiary basement rocks in this area.

CHAPTER III

SUBSURFACE GEOLOGY OF THE SOUTHERN PART OF TERTIARY MERGUI BASIN

The subsurface geology information in this study comprised geologic data from five exploratory wells with geophysical logs and 2D seismic reflection lines covering the southern part of Mergui basin. The biostratigraphic reports of all exploratory wells provided chronostratigraphic control to both well correlation and seismic correlation, and their palaeoenvironment was established on depositional setting. This information comprised microfossils and nannofossils analysis, which determined the biostratographic zones and palaeoenvironment. The mud logs, the summary of cuttings, and sidewall cores descriptions of all wells provided the lithological interpretation. The geophysical logs namely, gamma ray (GR), resistivity, density, neutron, and caliper logs of five wells are available in both hard copies and digital files. These informations are well established to determine the lithology and their pattern are further established to determine the depositional environment.

The seismic set of eighteen seismic sections is as an approximate grid spacing 5x5 km^2 covering the study area. There are five seismic sections that were shot a cross the exploratory wells. As a result, the time depth information from seismic section could be used for correlation between seismic data and well data. The wells Kraburi-1, Sikao-1, Thalang-1 and Kantang-1a are located in the Ranot trough, while only Sikao-1 well is located on the Ranong ridge. Kantang-1a is located at shotpoint 420 in the seismic dip line A537, and at shotpoint 1520 in the seismic strike line E025. Thalang-1 is located at shotpoint 330 in the seismic dip line A597, and at shotpoint 1580 in the seismic strike line D506. Sikao-1 is located at shotpoint 650 in the seismic dip line B403, and at shotpoint 445 in the seismic strike line E088. Kathu-1 is located at shotpoint 430 in the seismic dip line B094, and at shotpoint 380 in the seismic strike line E294. Kraburi-1 is located at shotpoint 1790 in the seismic dip line B120, and at shotpoint 660 in the seismic strike line D518. The geological structure is interpreted from these seismic data, with additional determination of the seismic sequence boundary and seismic facies for defining the depositional environment and correlated geological data throughout out the study area.

3.1 Sedimentary sequence

Form the lithologic data, geophysical logs, and biostratigraphic data, the stratigraphic framework of the southern part of Mergui basin can be established to be subdivided into four sedimentary sequences, namely, Unit A, B, C, and D in ascending order as shown in Table 3.1. Each unit is described in a detail as follows.

Unit A

Unit A is the lowest Tertiary stratigraphic unit in the southern part of Mergui basin. The unit overlies unconformably on the Pre-Tertiary basement rocks, and unconformably underlies Unit B. The typical sedimentary sequence of unit A is represent by the subsurface data from Kraburi-1 well and Thalang-1 well which is located on the deeper part of the eastern sub-basin. As well as Kantang-1A well and Sikao-1 well which are located on the west and east sides of the Ranot trough respectively. Unit A is absented in the Kathu-1 well.

Based on the lithologic data, geophysical logs, and biostratigraphic data, unit A is composed of three sub-units, namely, A1, A2, and A3 in the ascending order, which located on the deeper part of sub-basin, and Au which is not subdivided and locates on the basement high area. Each sub-units has the significant lithologically and paleoenvironment.

Sub-unit A1

A1 is the lowest lithostratigraphic unit that presents in Kraburi-1 well and Thalang-1. The subunit locates at the deeper part of the eastern sub-basin. This subunit overlies unconformably on the Pre-Tertiary basement and is conformed to subunit A2 above.

The base of sub-unit is defined by the lithological change from quartzitic rocks that appear at the top of the Pre-Tertiary basement in the Thalang-1 well, whereas the lower boundary at Kraburi-1 well did not reach the Pre-Tertiary basement. The top of sub-unit is defined by a lithological change from shale dominant sequence to sandstone

Table 3.1The sedimentary sequence in the exploratory wells

	Kraburi				Thalang				Kantang				Sikao				Kathu			
Unit	Depth(K.B.ft	Depth(ft.)	Thickness(ft.)	Marker	Depth(K.B.ft.)	Depth(ft.)	Thickness(ft.	Marker	Depth(K.B.ft.)	Depth(ft.)	Thickness(ft.	Marker	Depth(K.B.ft.)	Depth(ft.)	Thickness(ft.	Marker	Depth(K.B.ft	Depth(ft.)	Thickness(ft.	Marker
Bottom hole	10340	10257			8550	8467			6858	6775			5685	5602			3280	3197		
Top of BS	-	-			8528	8445	22		6764	6681	94		5625	5542	60		3250	3167	30	
Top of A1	9218	9135	1122	sh	7650	7567	878		-	-	-	-	-	-	-	-	-	-	-	-
Top of A2-1	8884	8801	334	sst	7540	7457	110		-	-	-	-	-	-	-	-	-	-	-	-
Top of A2-2	8618	8535	266	s-cst	-	-	-		-	-	-	-	-	-	-	-	-	-	-	-
Top of A2-3	8106	8023	512	sst	-	-	-		-	-	-	-	-	-	-	-	-	-	-	-
Top of A3	5830	5747	3054	bio(sh/cst)	6820	6737	720		6538	6455	226	lst	5225	5142	400	lst	-	-	-	-
	-	-	-	-	-	-	-		6300	6217	238	bio	5028	4945	197	cst	-	-	-	-
Top of Ax	-	-	-	-	-	-	-		6260	6177	40	cst	5010	4927	18	bio	-	-	-	-
Top of B	5300		530	seismic/bio	6400	6317	420	bio	5950	5867	350	bio	4450	4367	560	seiscmic	-	-	-	-
	-	-	-	-	-	-	-	-	-	-	-	-	-	-	-	-	3120	3037	130	lst/bio
	-	-	-	-	5620	5537	780	bio	5590	5507	360	bio	-	-	-	-	3110	3027	10	lst/bio
	-	-	-	-	5380	5297	240	bio	-	-	-	-	-	-	-	-	2865	2782	245	lst/bio
Top of C	3900	-	1400	seismic	4300	-	1320	seiscmic	4380	-	1210	seiscmic	3900	-	550	seiscmic	2650	-	460	seiscmic
Top of D (subsea)	3272	3189	628	seismic/bio	3490	3407	1890	seismic/bio	3561	3478	819	seiscmic	3272	3189	628	seiscmic	1765	1682	885	seiscmic

Remark: Biostratigraphic maker:bio

Seismic maker: seismic

Lithologic maker: sh, cst, lst, sst, s-cst

dominant sequence that is clearly observed in the geophysical logs by high value of the gamma ray and then by the abrupt offset at the top of unit.

Generally, the lithology of sub-unit A1 is characterized by predominantly shale with minor siltstone and trace of dolomite. Shale is light gray to gray, olive gray, greenish gray, grayish brown to dark brown in color. It is soft to firm, blocky to sub-fissile, moderately to a trace of very fine sand to silt, moderate to trace of coal, moderately to highly calcareous. Siltstone is olive gray to pale olive. It is soft, laminated in part, and strongly calcareous. Dolomite is white to pink. The thickness of this unit is 1122 feet or 342 meters in Kraburi-1 well and is 878 feet or 268 meters in Thalang-1 well as shown in Table 3.1 and Figures 3.1 and 3.2.

Sub-unit A2

The typical lithological sequence of sub-unit A2 is represented by the subsurface data from Thalang-1 and Kraburi-1 wells, which are located at deeper part of the eastern sub-basin. The unit overlies conformably sub–unit A1 and underlies conformably sub–unit A3. The top of unit is defined by a lithological change from sandstone dominant sequence to fine-grained sediment dominant sequence. It is clearly observed on the geophysical log by characteristically low value of gamma ray and then alternate with high to very high value of gamma ray.

Generally, the lithology of sub-unit A2 can be separated into 3 parts. The lithological sequence of sub-unit A2 is characterized by the thick sequence of clastic sediment that is restricted to the trough area of the southern part of Mergui basin.
The lowest part of this sub-unit is characterized by thick sequence of sandstone interbeded with shale, claystone and trace of argillaceous siltstone. The top of this part is recognized on the basis of a change in geophysical log response and the base coincides with a lithological change from a sandstone dominant sequence to a fine-grained clastic dominant sequence. Sandstone is white, light gray; greenish gray to dark brown; quartz is clears to milky, very fine to fine-grained occasional medium to coarse grained. It is soft, predominantly with loose quartz, moderately to poorly sorted, subangular to subrounded, friable to firm, argillaceous cement, moderate to trace chlorite, traces of fossils, carbonaceous in part, non-calcareous to moderately calcareous,

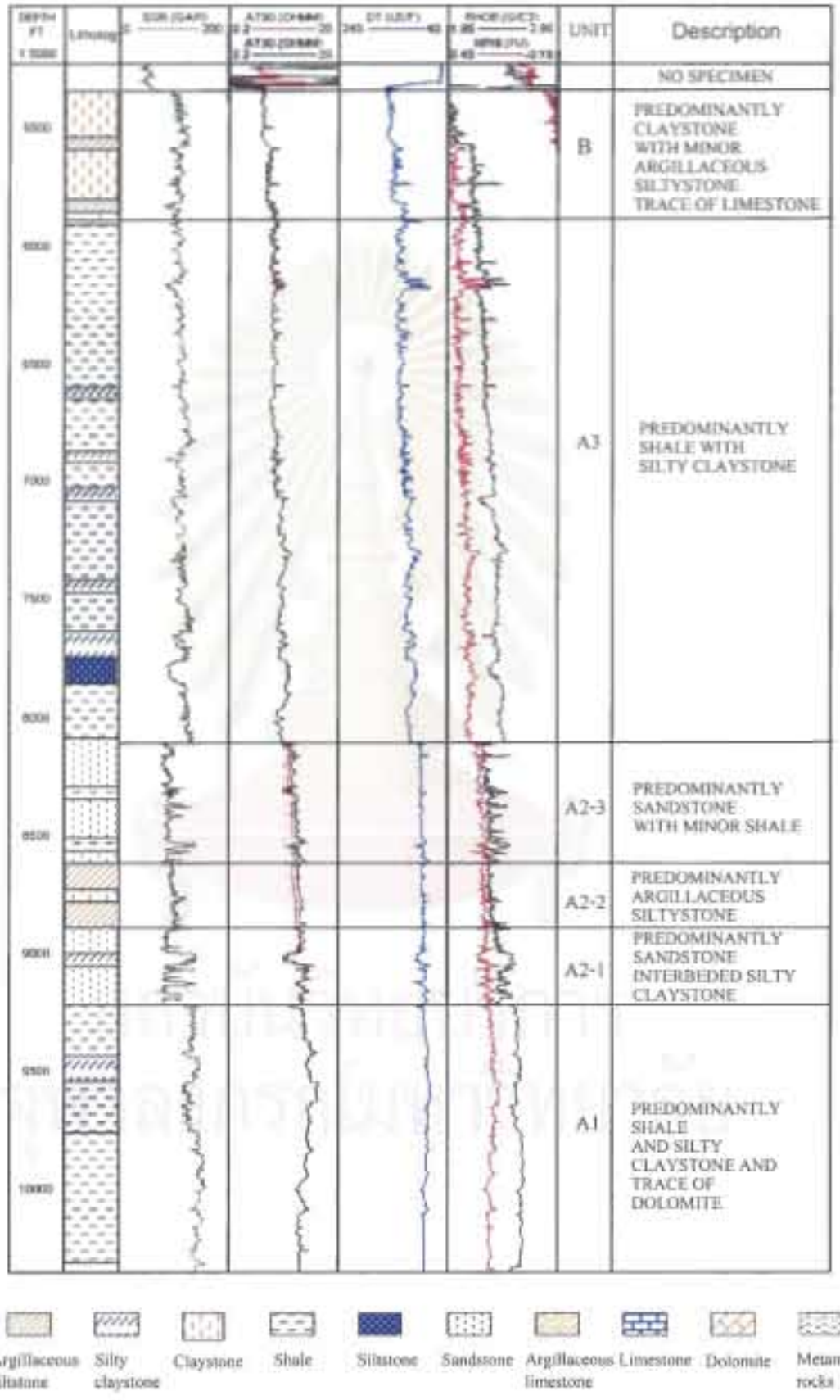

Figure 3.1 The geologic and geophysical log characteristics of Kraburi-1well.

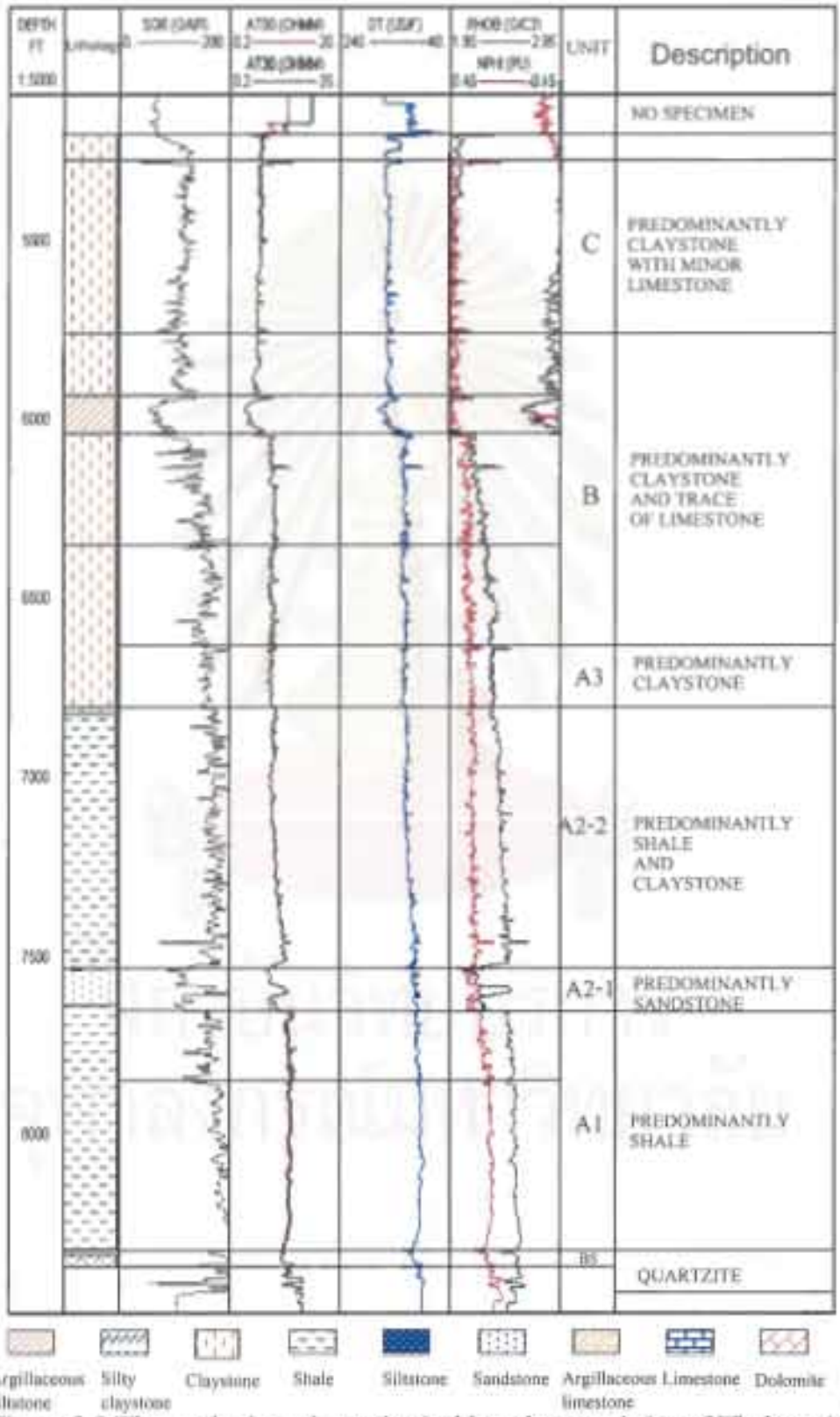

Figure 3.2 The geologic and geophysical log characteristics of Thalang-1well.

common coal, traces of rock fragments. Claystone is light to medium gray, moderately hard to soft, blocky to sub-blocky, in parts grading to shale, calcareous, silty in section.

Shale is olive to grayish brown. It is soft to firm, sub-block to sub-fissile, silty, carbonaceous in part, non-calcareous. Argillaceous siltstone is light olive to olive. It is soft, blocky, traces of quartz sand, rarely chlorite, sandy in part, non-calcareous. The thickness of this unit is 334 feet or 102 meters in Kraburi-1 well and is 110 feet or 33.5 meters in Thalang-1 well as shown in Table 3.1 and Figures 3.1 and 3.2.

Based on the petrographic analysis of sandstone at depth 8935 feet and 9163 feet from Kraburi-1 well, it was identified as feldspartic litharenite. It is fine-grained, moderately sorted, consists of quartz (51%) with lithic fragments of mainly metamorphic rocks and minor plutonic rocks and volcanic rocks (25-31%) and feldspar (18-24%). The visible porosity is about 5%-8%. It contains some plant fragments.

The petrographic analysis of sandstone at the depth 7540 feet to 7640 feet from Thalang-1 well was determined as litharenite. It is fine-grained, moderate to well sorted, comprising predominantly quartz (65-79%) with lithic fragments of mainly metamorphic rocks and minor plutonic rocks, volcanic rocks, chert and mudstone (17-33%) and feldspar (2-5%). The visible porosity is about (9-20%) as shown in an Appendix-1.

The middle part of sub-unit A2 is characterized by argillaceous siltstone with minor shale. The top of this part is recognized on the basis of a change in geophysical log response, and at the base the lithology changed from a uniform siltstone dominant sequence to sandstone with minor shale sequence. Argillaceous siltstone is light olive to olive and moderately brown. It is soft, blocky, traces of quartz grains, and rarely chlorites, sandy in part, non-calcareous. Shale is light olive gray to greenish gray. It is soft to firm, blocky to fissile, trace of chlorite, moderately calcareous, occasional graded to siltstone. The thickness of this unit is 266 feet or 81 meters in Kraburi-1 well as shown in Figure 3.1 and Table 3.1.

The upper part of the sub-unit A2 is characterized by sandstone with minor shale. Sandstone is light gray, greenish gray to dark brown, very fine to fine grained. It is

soft, predominantly loose quartz, moderate to poorly sorted, angular to rounded, friable, moderate to trace of chlorite, commonly with coal, trace of rock fragments. Shale is olive gray to grayish brown. It is soft to firm, subblocky to subfissile, silt, carbonaceous in part, non-calcareous. Number and thickness of sandstone layers of this part are less than the upper part. The thickness of this unit is 512 feet or 156 meters in Kraburi-1 well as shown in Figure 3.2 and Table 3.1.

Based on the petrographic analysis of sandstone at the depths 8190 feet, 8520 feet and 8812 feet from Kraburi-1 well it was determined as lithic arkose, lithic arkose/feldsparthic litharenite and feldsparthic litharenite. It is fine-grained, poor to moderately well sorted, consists of quartz is 37-54% with lithic fragments of mainly metamorphic rocks and minor plutonic rocks and volcanic rocks (23-33%) and feldspar (23-30%). The visible porosity is about 3-14% as shown in an Appendix.-1.

Sub-unit A3

The typical lithological sequence of sub-unit A3 is represented by the subsurface data from Kraburi-1 well and Thalang-1 well, which are located at deeper part of the eastern sub-basin. The unit overlies conformably the sub–unit A2 and underlies unconformably B–unit that is clearly observed on the seismic profile across the Kraburi-1 well as shown in Figures 3.3 and 3.5.

The sub-unit A3 is characterized by predominatedly claystone and shale with minor sand, shale and trace of limestone and dolomite. Claystone is light olive gray to olive. It is soft to firm, moderately hard, occasionally fissile, locally grading to siltstone, some grading to shale, slightly calcareous to non-calcareous. Shale is light olive gray to greenish gray. It is soft to firm, sub-blocky to sub-fissile, occasionally fissile, locally silty, trace of chlorite, slightly calcareous. Limestone is white and hard. Dolomite is white and white to pink, hard. The thickness of this unit is varies from 2276 feet or 694 meters in Kraburi-1 well to 720 feet or 219 meters in Thalang-1 well as shown in Figure 3.1, 3.2 and Table 3.1

Based on the petrographic analysis of sandstone at depth 7080 feet from Kraburi-1 well it was determined as feldsparthic litharenite. It is fine-grained, very poorly sorted, consists of quartz (58%) with lithic fragments of mainly metamorphic

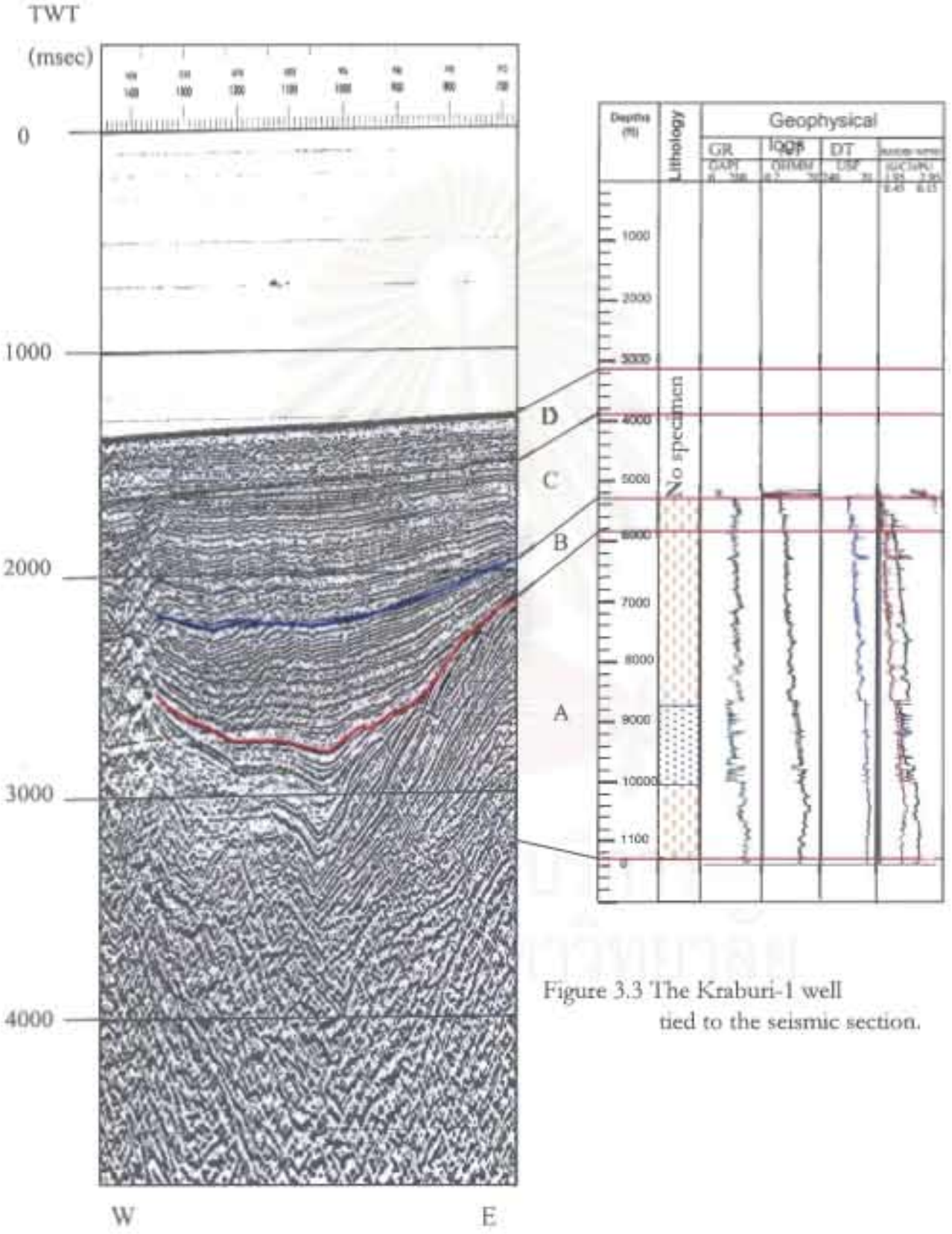

Figure 3.3 The Kraburi-1 well tied to the seismic section.

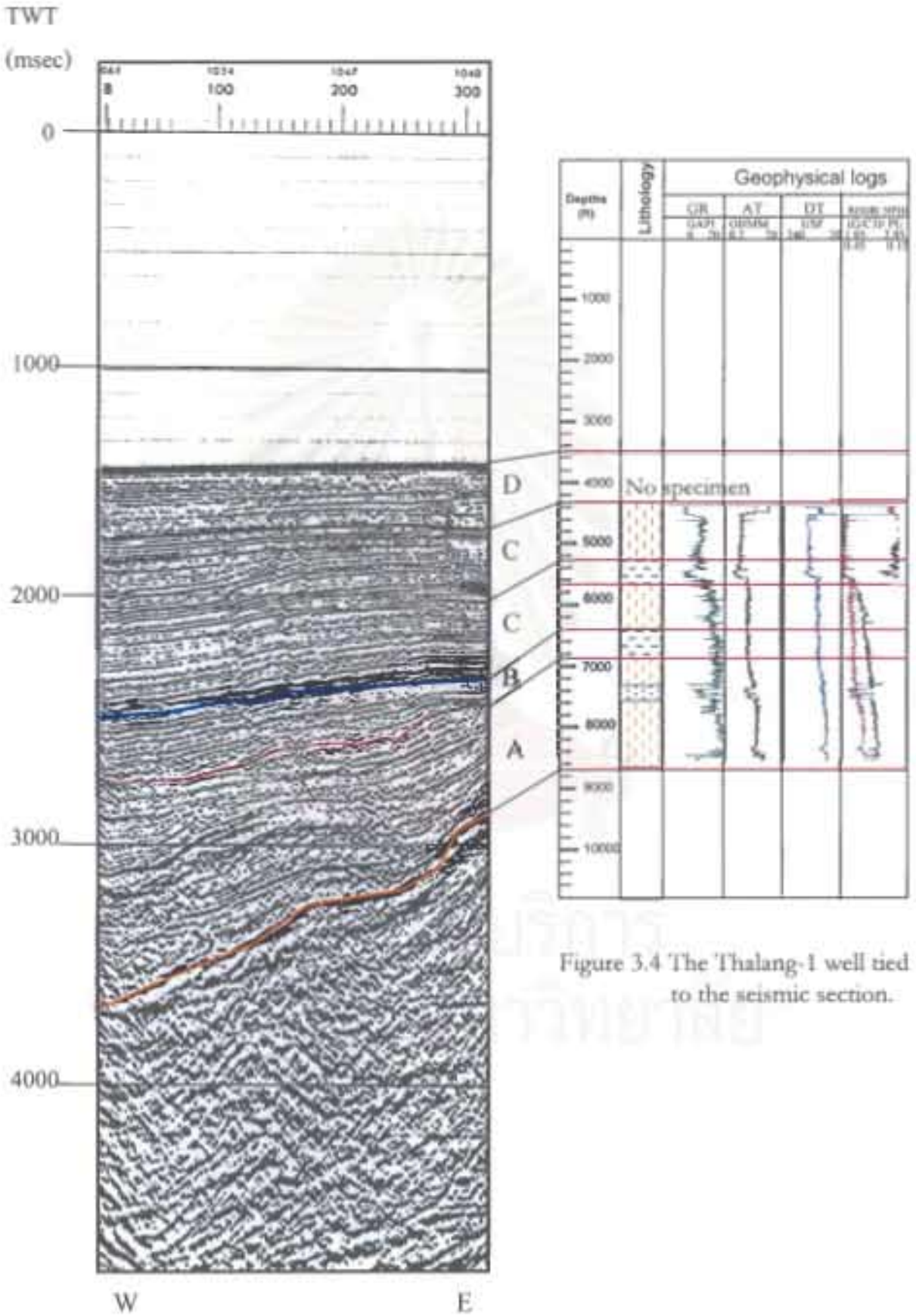

Figure 3.4 The Thalang-1 well tied to the seismic section.

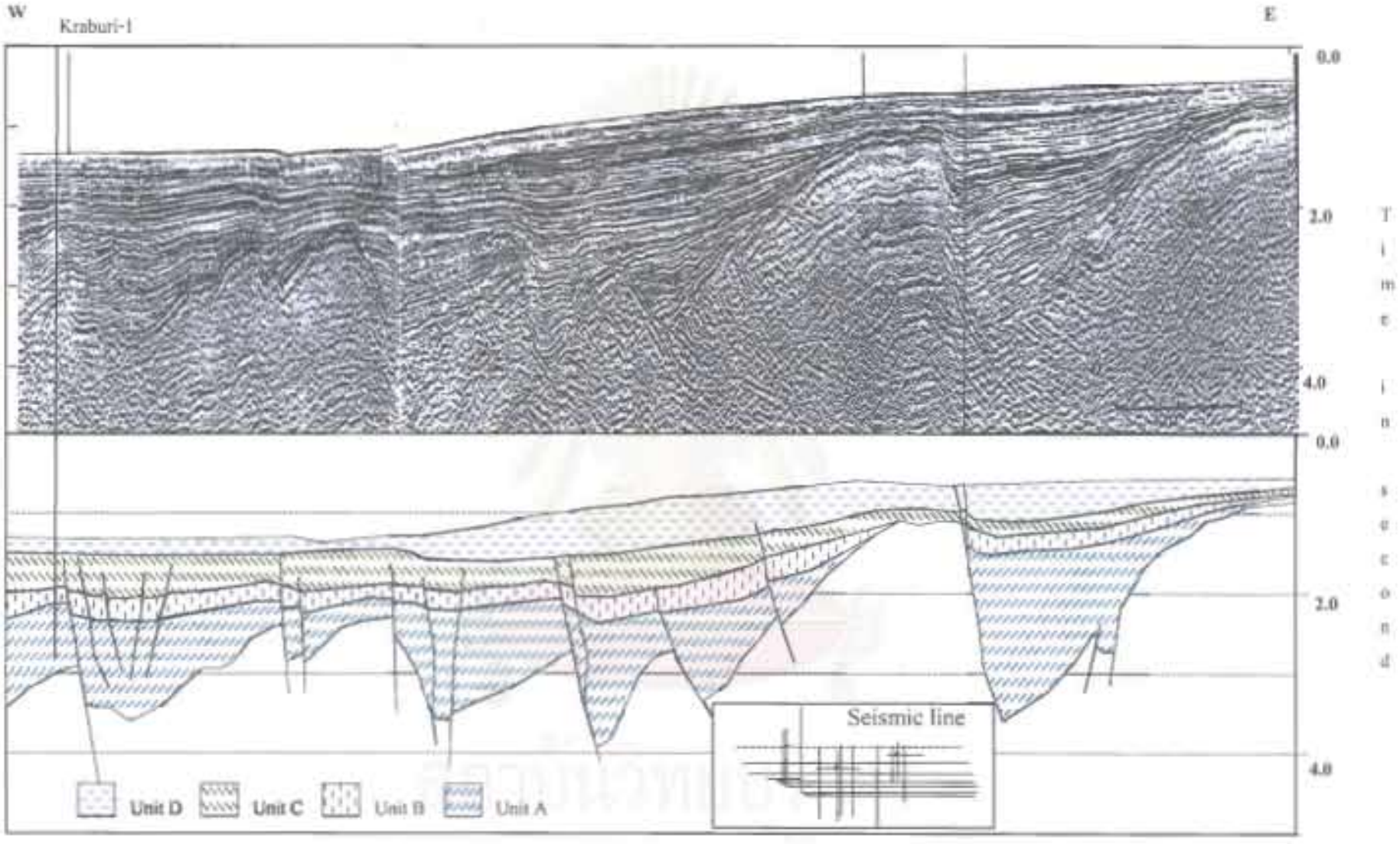

Figure 3.5 The seismic profile across Kraburi-1 well showing sedimentary unit in the southern part of Mergui basin.

rocks and minor plutonic rocks, volcanic rocks, chert and mudstone (22%) and feldspar (20%). The visible porosity is about 5%. It contains plant fragment 6% as shown in the Appendix-1.

Petrographic analysis of sandstone at depth 5831 feet from Kraburi-1 well was determined as lithic arkose. It is fine-grained, poorly sorted, consists of quartz (50%) with lithic fragments of mainly metamorphic rocks and minor plutonic rocks, volcanic rocks and mudstone (about 2%) and feldspar (about 48%). The visible porosity is about 9%. It contains plant fragment (3%) as shown in the Appendix-1.

The time-depth data from seismic section were used to convert biostratigraphic data from Kraburi-1 and Thalang-1 wells to seismic section that wells are located as shown in figure 3.3 and 3.4. Basically, the biostratigraphic data is used to date each of seismic sequences, which identified by the surface of reflection terminations that proposed by Mitchum et.al (1977) as chronostratgraphy. A seismic sequence and seismic facies are summary in table 3.2.

The seismic boundaries of the unit A interval are marked at the surface of the pre-Tertiary basement reflector that is generally reflected with very strong peak and marks between the overlying unconformity and the Pre-Tertiary basement. The top boundaries are marked by onlap on the Tertiary reflector on the Mergui shelf, the Ranong ridge, and the high basement between Ranot trough and the eastern sub-basin and concordant reflection termination in the basin. The base and top boundary can be identified clearly in seismic section, excepted the deeper basin.

Generally, the seismic facies within unit A interval can be separated into 4 sub-interval in ascending order such as: A1, A2, A3, and A4 as shown in Table 3.2.

Table 3.2 Summary of seismic facies characteristic.

Seismic Interval	Reflection Terminations	Reflection Configuration	External geometry	Depositional environment
D	Concordant/ Downlap at base	Moderately to low continuity Moderately to low amplitude Parallel/sigmoid stratified configuration	Slope-front Len/sheet	Basinal plain/ Shelf margin
C	Concordant at top Concordant at base	Moderately to low continuity Moderately to low amplitude Parallel stratified configuration	sheet	Basinal plain/ reef
B	Concordant at top Concordant at base	Moderately to low continuity high to low amplitude Parallel/ divergent stratified configuration	sheet	Basinal plain
A4	Onlap at top Concordant at base	Moderately to low continuity low amplitude divergent stratified configuration	Channel fill/ sheet	Basinal plain
A3	Onlap/Concordant at top Concordant at base	high to low continuity high amplitude chaotic lateral change to divergent stratified configuration	Channel fill/ sheet	Basinal plain/ reef
A2	Concordant at top Onlap at base	high to low continuity high amplitude chaotic lateral change to divergent stratified configuration	Channel fill/ sheet	Mid-fan turbidity
A1	Onlap at top	Moderately to low continuity high to moderately amplitude divergent stratified configuration	Fan-slope front/ Wedge	Basinal plain

Interval A1

The top of Pre-Tertiary basement configuration reflection defines the base boundaries of interval A1. The top is from onlap reflection.

Seismic facies within the interval A1 are characterized by divergent stratified configuration, lateral changed from high to moderate amplitude, and moderate to low continuity, the external geometry is fan-slope front as wedge shape as shown in Figure 3.5.

Interval A2

The base boundaries of interval A2 are defined by an onlap reflection. The top is concordant reflection.

Seismic facies within the interval A2 are characterized by lateral changed from divergent stratified to chaotic configuration, high amplitude, and lateral change from high to low continuity, the external geometry is channel fill as sheet shape as shown in Figure 3.5.

Interval A3

The base boundaries of interval A3 are defined by a concordant reflection. The top is onlap with lateral changed to concordant reflection.

Seismic facies within the interval A3 are characterized by lateral changed from divergent stratified to chaotic configuration, lateral changed from high to low amplitude, and lateral changed from high to low continuity, the external geometry is channel fill as sheet shape as shown in Figure 3.5.

Interval A4

The base boundaries of interval A4 are defined by a concordant reflection. The top is onlap.

Seismic facies within the interval A4 are characterized by divergent stratified configuration, low amplitude, and moderate to low continuity as shown in Figure 3.5. The external geometry is represented by channel shape filled.

Unit Au

The typical lithological sequence of unit Au is represented by the subsurface data from Kantang-1a and Sikao-1 wells are located at the basement high on the western and eastern side of Ranot trough, respectively. This unit overlies unconformably the Pre-Tertiary basement rock and underlies conformably the unit B.

Generally, the lithology of unit Au can be separated into 2 parts. The lithological sequence of Au unit is characterized by the thick sequence of carbonate and
Fine-grained clastic sediments that are restrictedly on the relative high area of the southern part of Mergui basin.

The lower part of unit Au is characterized by a sequence of limestone which is packstone or packstone grading to grainstone with depth, white to yellowish white, cryptocrystalline, hard and firm in parts, trace of pyrite, trace of chlorite, trace of fossils, trace of microfracture. The thickness of this unit varies from 226 feet or 69 meters in Kantang-1a well to 400 feet or 122 meters in Sikao-1 well as shown in Figure 3.6 and 3.7 and Table 3.1.

The upper part of sub-unit Au is characterized by predominantly claystone with minor sand, shale and trace of limestone and dolomite. Claystone is light olive gray to olive. It is soft to firm, some are of moderately hard, occasionally fissile, locally grading to siltstone, some grading to shale, slight calcareous to non-calcareous. Shale is light olive gray to greenish gray. It is soft to firm, sub-blocky to sub-fissile, occasionally fissile, locally silty, trace of chlorite, slightly calcareous. Limestone is white. Dolomite is white to pink, hard. The thickness of this unit is varies from 278 feet or 85 meters in Kantang-1A well to 205 feet or 65 meters in Sikao-1 well as shown in Figure 3.6 and 3.7 and Table 3.2

The planktonic foraminifera indicate the Late Oligocene; *Globorotalia siakensis* (N14), *Globorotalia opima opima*(P21) *Globigerina selli aff.*(N1,P19/20) *Globorotalia opima opima*(P21) *Globigerina ciperoensis aff.*(N4) *Globigerina angulisuturalis*(P21) were recovered from this unit. Late Oligocene calcareous nannofossils are *Triquetrorhabdulus carinatus* (NN1) also found as shown in Table 3.3.

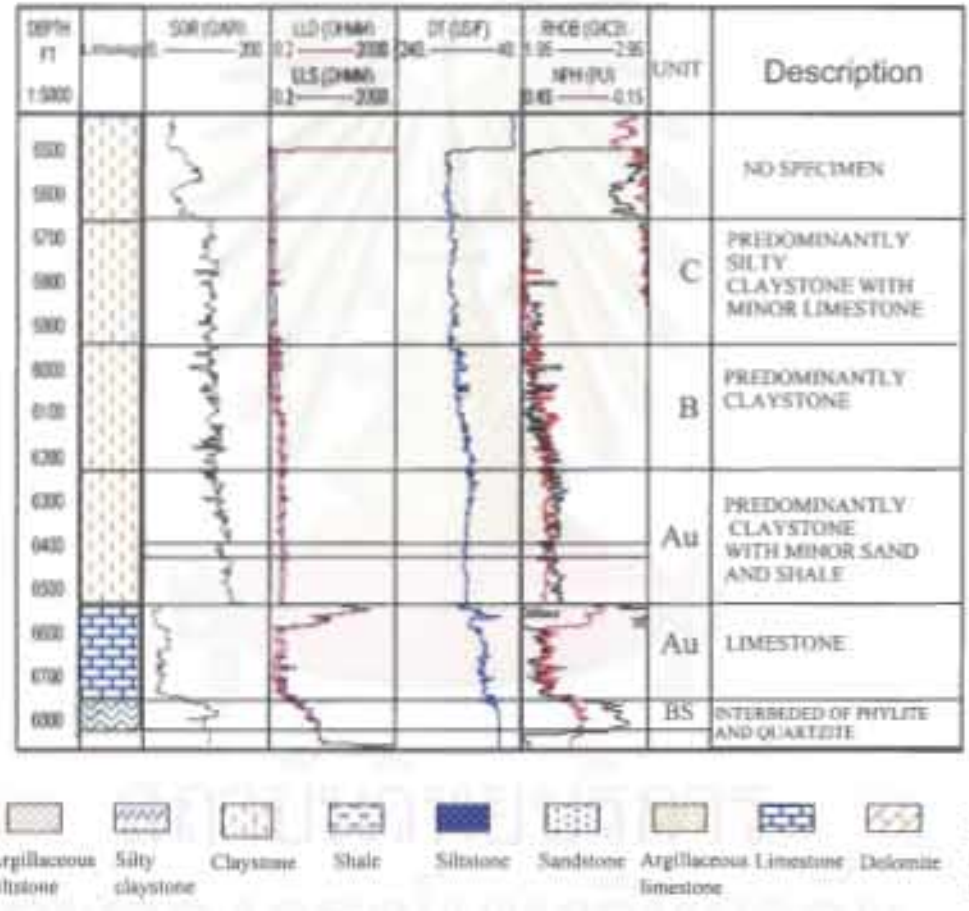

Figure 3.6 The geologic and geophysical log characteristics of Kantang-1a well.

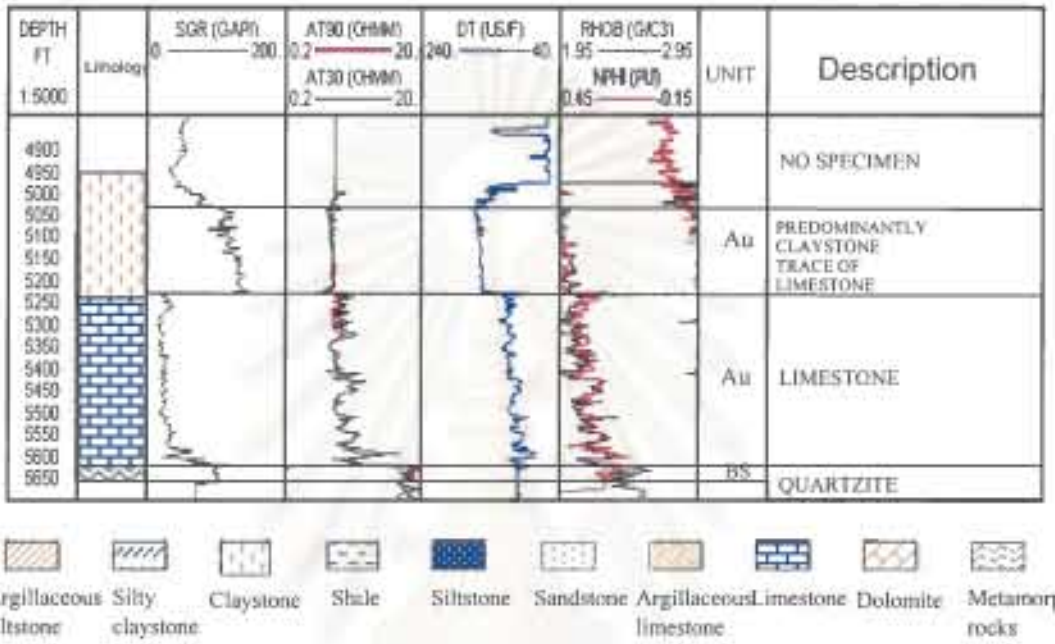

Figure 3.7 The geologic and geophysical log characteristics of Sikao-1

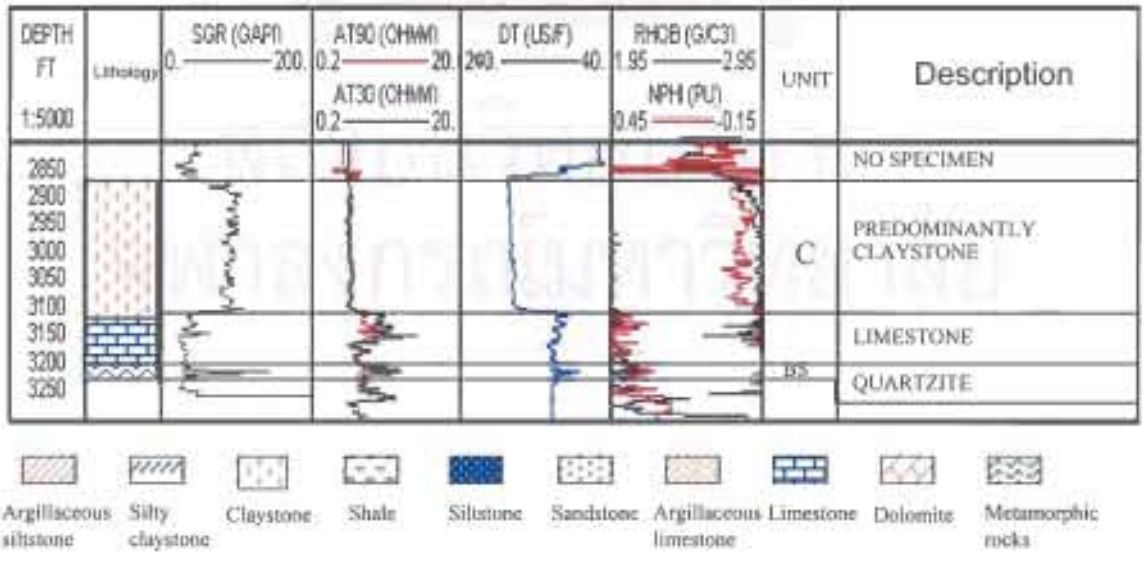

Figure 3.8 The geologic and geophysical log characteristics of Kathu-1

Table 3.3. Biostratigraphic summary of the wells in the study area.

(a) Kantang-1a well

Depths	Lithology	Nannofossil	Depths	Lithology	Foraminiferal	Facies	Depositional environment	Ages
5530	clayey siltstone	*Discoaster hamatus(NN9)*	5530	clayey siltstone	*Globorotalia siakensis(N14)*	C	basinal plain	Late Miocene
			5530	clayey siltstone	*Globoquadrina altispira altispira(N19)*			
5650-5770	clayey siltstone	*Discoaster kugleni(NN7)*	5650		*Globoquadrina altispira globosa(N19)*	C	basinal plain	Middle Miocene
5770-5950	claystone	*Sphenolithus heteromorphus (NN5)*	5710-5770	claystone	*Shaeroidinella subdehiscens(N13)*			
			5710-5772	claystone	*Globorotalia praefohsi(N11)*			
			5710-5772	claystone	*Globerotalia peripheroacuta(N10)*			
			5772	claystone	*Globorotalia peripheroronda(N9)*			
			5772	claystone	*Globigerinoides sicanus(N8)*			
5950-6300	clayey siltstone	*Helicopontosphaera ampliaperta(NN4)*				B	basinal plain	Early Miocene
6338	shale	*Triquetrorhabdulus carinatus(NN1)*				A2	basinal plian	Late Oligocene

(b) Kathu-1 well

Depths	Lithology	Nannofossil	Depths	Lithology	Foraminiferal	Facies	Depositional environment	Ages
2880-3000	claystone	*Discoaster quinqueramus(NN11)*				C	basinal plain	Late Miocene to Middle Miocene
3000-3120	claystone	*Discoaster quinqueramus(NN11)*	3000-3120	claystone	*Sphaeroidinellopsis subdehiscens subdehiscens(N13)*	C	basinal plain	Middle Miocene

(c) Sikao-1 well

Depths	Lithology	Nannofossil	Depths	Lithology	Foraminiferal	Facies	Depositional environment	Ages
5010-5190	claystone	*Triquetrorhabdulus carinatus(NN1)*	5010-5190	claystone	*Globorotalia siakensis(N14)*	A2	basinal plain	Late Oligocene to Early Miocene

Table 3.3. (cont.)
(d) Kraburi-1 well

Depths	Lithology	Nannofossil	Depths	Lithology	Foraminiferal	Facies	Depositional environment	Ages
5350	silty claystone	*Helicopontosphaera ampliapertura (NN4)*	5350	silty claystone	*Globigerinoides sicanus(N8)*	B	basinal plain	Early Miocene
			7215	shale	*Globorotalia opima opima(P21)*	Au	basinal plain	Late Oligocene

(e) Thalang-1 well

Depths	Lithology	Nannofossil	Depths	Lithology	Foraminiferal	Facies	Depositional environment	Ages
5380-5620	claystone	*Discoaster hamatus(NN9)*	5260	claystone	*Globoquadrina altispira globosa(N19)*	C	basinal plain	Late Miocene
			5320	claystone	*Globoquadrina altispira altispira(N19)*			
5620-5740	claystone	*Discoaster kugleni(NN7)*				C	basinal plain	Middle Miocene
			6142	claystone	*Globorotalia siakensis(N14)*	C	basinal plain	
6280-6540	claystone	*Discoaster exilis(NN6)*	6340-6400	claystone	*Globorotalia praefohsi(N11)*			
6280-6482	claystone	*Helicopontosphaera ampliaperta(NN4)*	6340-6400	claystone	*Globerotalia peripheroronda(N10)*			
6280-6480	claystone	*Discoaster exilis(NN6)*	6460	claystone	*Globerotalia peripheroronda(N10)*			
6580	claystone	*Sphenolithus heteromorphus (NN5)*	6580	claytone	*Globigerinoids sicanus(N8)*	B	basinal plain	Early Miocene
6647-6800	claystone	*Helicopontosphaera ampliaperta(NN4)*						
			6970	claystone	*Globigerina ciperoensis aff.(N4)*	A3	basinal plain	Early Miocene to Late Oligocene
			7180	claystone	*Globigerina angulisuturalis(P21)*			
			7480-7540	claystone	*Globigerina selli aff.(N1,P19/20)*	A3	basinal plain	Late Oligocene
			7660-8528	claystone	*Globorotalia opima opima(P21)*	A1		

Unit B

The combination of subsurface data from Thalang-1, Kraburi-1, and Kantang-1a wells represented the typical lithological sequence of B-unit. The unit overlies unconformably the sub-unit A3 in the Kraburi-1 well and Thalang-1 well and overlies conformably Au unit in the Kantang-1a. As well as it underlies conformably the unit C.

The unit B is characterized as a sequence of fine-grained clastic sediment claystone alternated with siltstone and limestone. Claystone is light gray to grayish green and olive gray. It is soft, sticky, from trace to no coal, trace of highly calcareous. Siltstone is olive gray, no fissility, soft, and trace of coal, strong to very strong calcareous. Limestone is packstone, white, soft to firm, cryptocrystalline, abundant of fossil, and calcite crystals. The thickness of this unit varies from 350 feet or 107 meters in Kantang-1A well to 420 feet or 128 meters in Thalang-1 well as shown in Table 3.1 and Figure 3.1, 3.2 and 3.6.

The unit B is Early Miocene in age because it contains *Globigerinoids sicanus* (N8) And calcareous nanofossil comprise *Helicopontosphaera ampliaperta (NN4), Sphenolithus heteromorphus* (NN5) as shown in Table 3.3.

The time-depth data from seismic section were used to convert the biostratigraphic data from Sikao-1 and Kantang-1a wells to seismic section that wells are located as shown in Figures 3.9, 3.10 and 3.11. Basically, the biostratigraphic data is used to date each of seismic sequences as chronostratgraphy.

The base and top sequence boundaries of unit B interval are defined by a concordant reflection.

Seismic facies within the interval B are characterized by lateral changed from parallel to divergent stratified configuration, lateral changed from high to low amplitude, and moderate to low continuity as shown in Figure 3.12. The external geometry is represented by sheet shape filled.

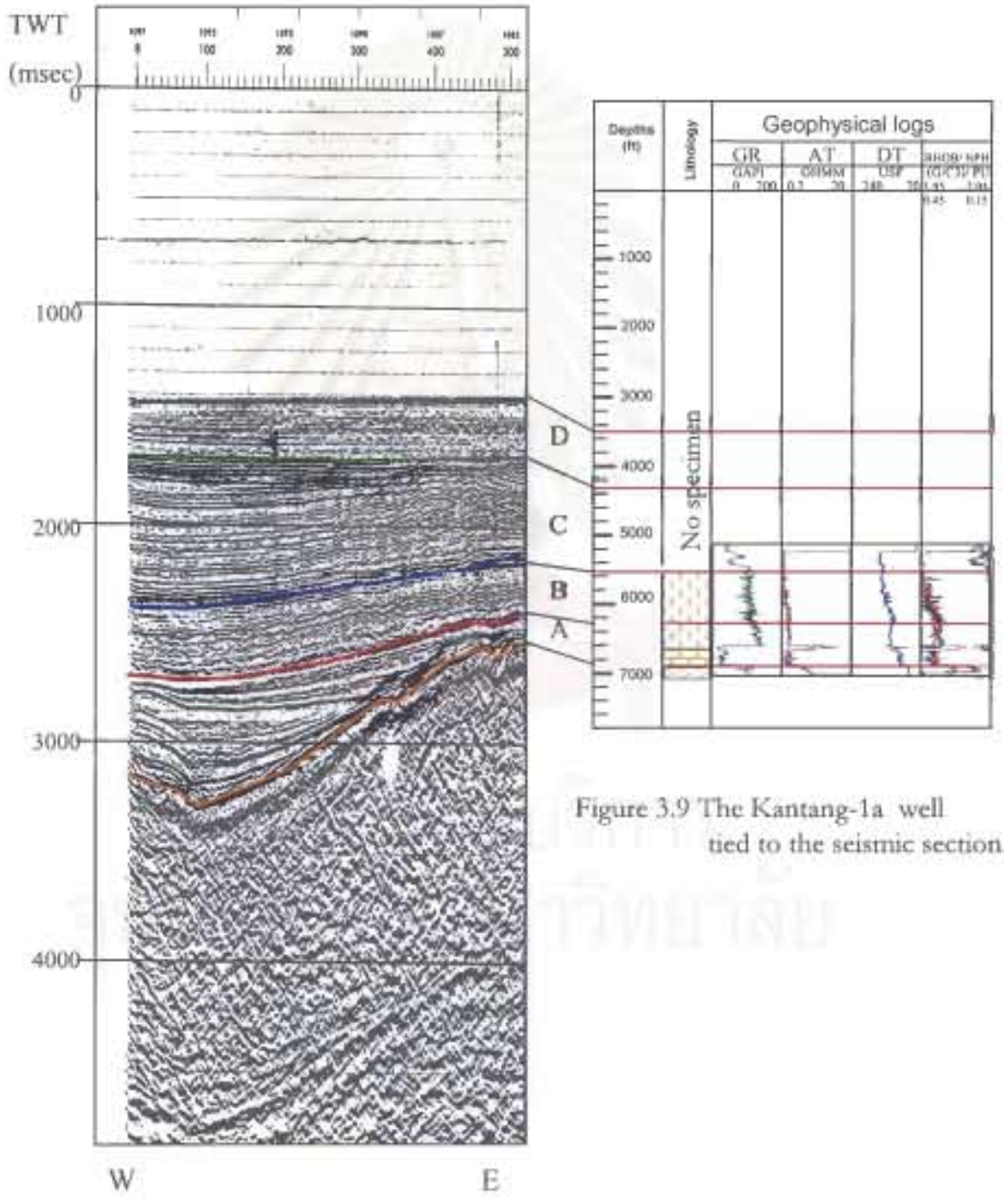

Figure 3.9 The Kantang-1a well tied to the seismic section.

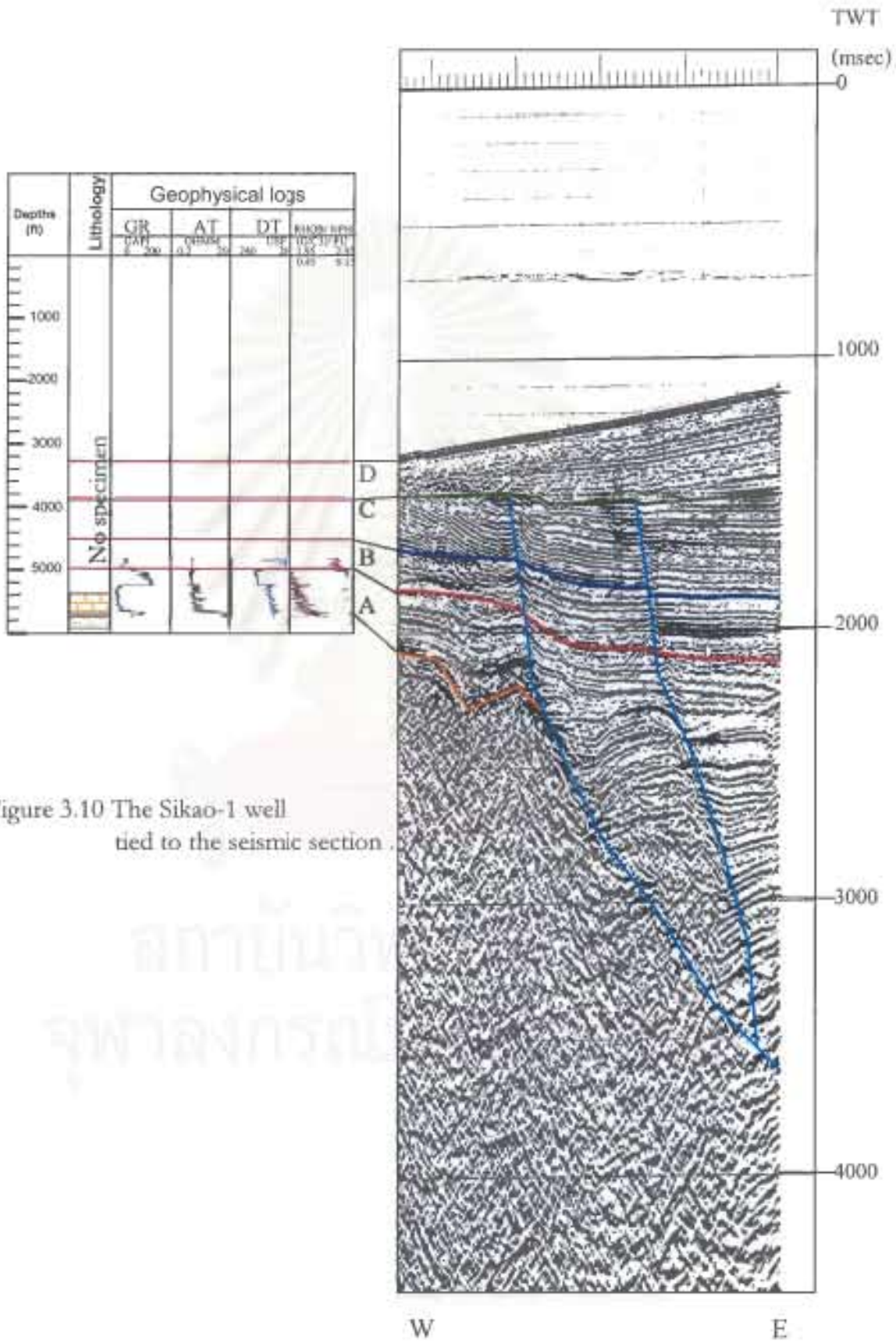

Figure 3.10 The Sikao-1 well tied to the seismic section .

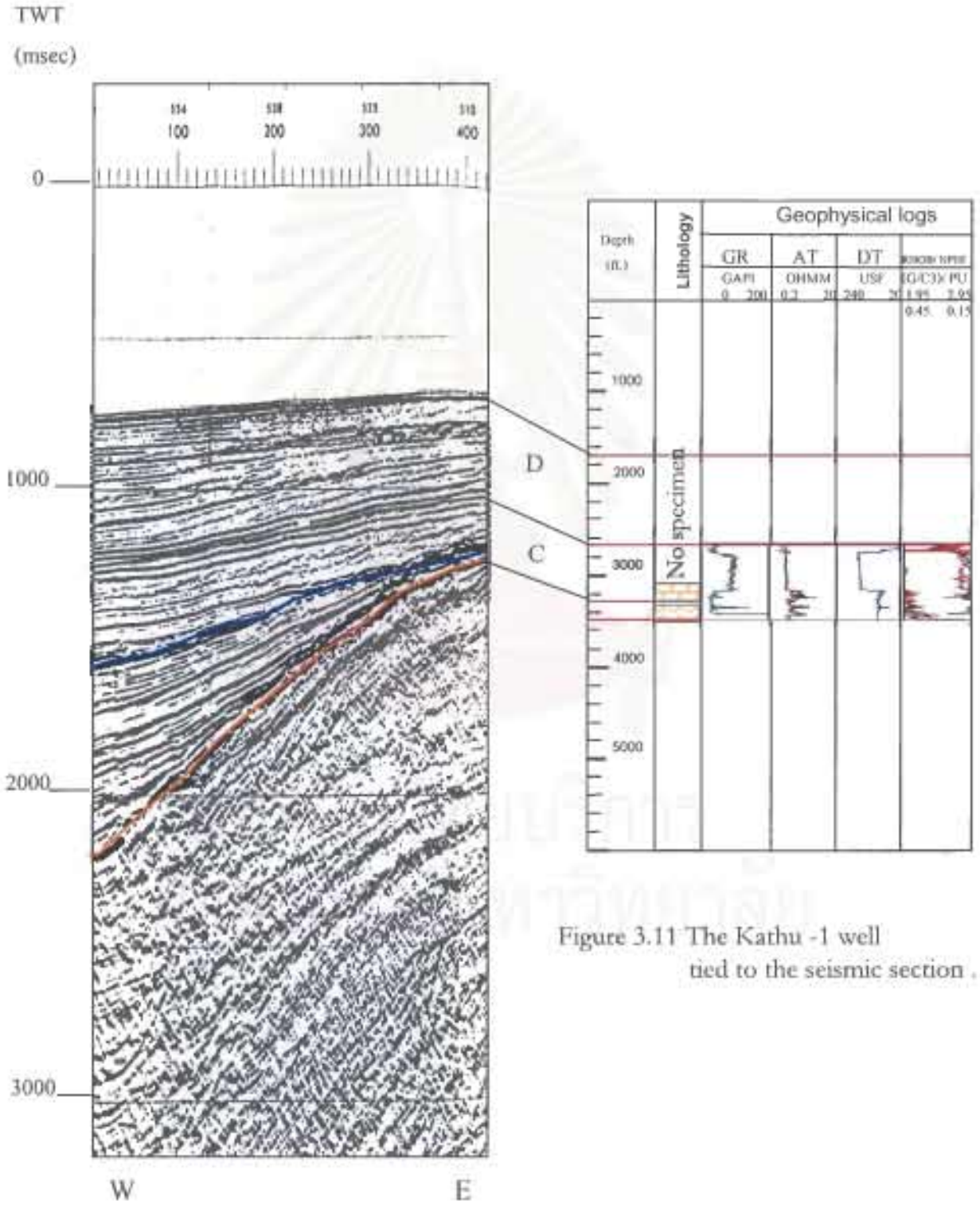

Figure 3.11 The Kathu -1 well tied to the seismic section .

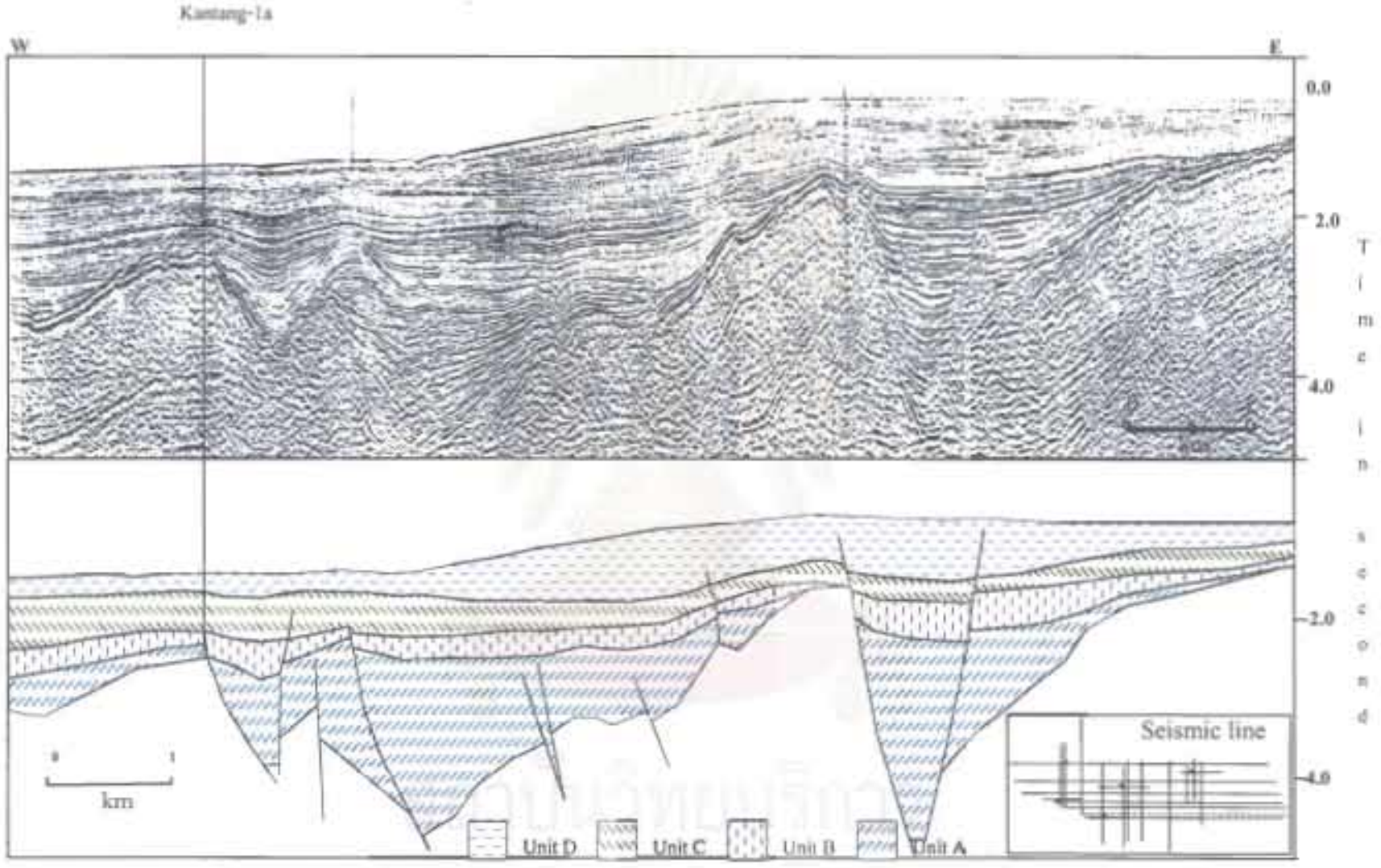

Figure 3.12 The seismic profile across Kantang-1a wellshowing sedimentary unit in the southern part of Mergui basin.

Unit C

The typical lithological sequence of unit C is represented by the combination of the subsurface data from all exploratory wells in the study area. The unit overlies conformably unit B and underlies conformably unit D in the Kraburi-1, Thalang-1, and Kantang-1A wells. The unit also overlies unconformably the Pre-Tertiary basement in Kathu-1 well on Ranong ridge. Generally, the lithology of unitC can be separated into 2 parts. The lithologic sequence of C-unit is characterized by the sequence of both fine-grained clastics which spread all over the study area and non-clastic sediment that appeared at the lowest portion of the unit at Ranong ridge in the Kathu-1 well.

The lowest part of the unit C in the Kathu-1 well is characterized by sequence of limestone, which is packstone. It is white, bluish white and light gray, soft to hard, cryptocrystalline with trace of pyrite.

Above the lower part of unit C is the higher part of the unit. The lithological sequence is characterized by silty claystone with minor limestone and siltstone at the top. Silty claystone is light olive gray to gray. It is soft to moderately hard, sub-blocky, moderate to highly calcareous, trace of coal and trace of carbonaceous matter.

The thickness of this Unit C varies from over 2100 feet or 640 meters in Thalang-1 well as shown in Figure 3.6, to 470 feet or 143 meters in Kathu-1 well as shown in Table 3.1 and Figures 3.2 and 3.7. It tends to be thinning to the eastern part of study area.

The unit C are group in Middle Miocene to Late Miocene age because it contains *Globigerinoides sicanus* (N8)*, Globorotalia peripheroronda*(N9) *,Globerotalia peripheroacuta* (N10),*Globorotalia praefohsi*(N11)*, Sphaeroidinellopsis subdehiscens subdehiscens* (N13)*, Globoquadrina altispira globosa*(N19).And calcareous nanofossil comprises *Helicopontosphaera ampliaperta (NN4), Sphenolithus heteromorphus* (NN5)*, and Discoaster exilis* (NN6) that indicate Middle Miocene age. As well as foraminifera conclude *Globoquadrina altispira globosa*(N19), *Globoquadrina altispira altispira*(N19) *Globorotalia siakensis*(N14), and nanofossil comprises *Discoaster hamatus*(NN9) represents Late Miocene in age as shown in Table 3.3

The base and top sequence boundaries of unit C interval are defined by both concordant reflections.

Seismic facies within the interval C are characterized by parallel configuration, moderate to low amplitude, and moderate to low continuity as shown in Figure 3.12. The external geometry is represented by sheet shape filled.

Unit D

The uppermost portion of sedimentary sequence of the southern part of Tertiary Mergui basin generally covers throughout the study area. The unit is defined by seismic configuration only because there are no data available in all exploratory wells. The reason of the absent data is because the wells are separated from the formation by the preventing casing.

The base sequence boundaries of unit D interval are defined by downlap surface on the shelf lateral changed to concordant reflection in the basinward. The top is a concordant reflection

Seismic facies within the interval D are characterized by lateral change from parallel to sigmoidal stratified configuration, moderate to low amplitude, and moderate to low continuity as shown in Figure 3.12. Sheet shape filled represent the external geometry.

The correlation between all exploratory wells within the southern part of Mergui basin is shown in Figures 3.13 and 3.14.

3.2 Depositional environment

Basically, the concept of facies model is an important tool to determine a depositional environment. Additionally, their palaeobathyals and seismic facies are well-established tools used to interpret the environment. The facies models apply in this study are described in Walker (1978) for shelf and shallow marine sand, Mutti and Ricci

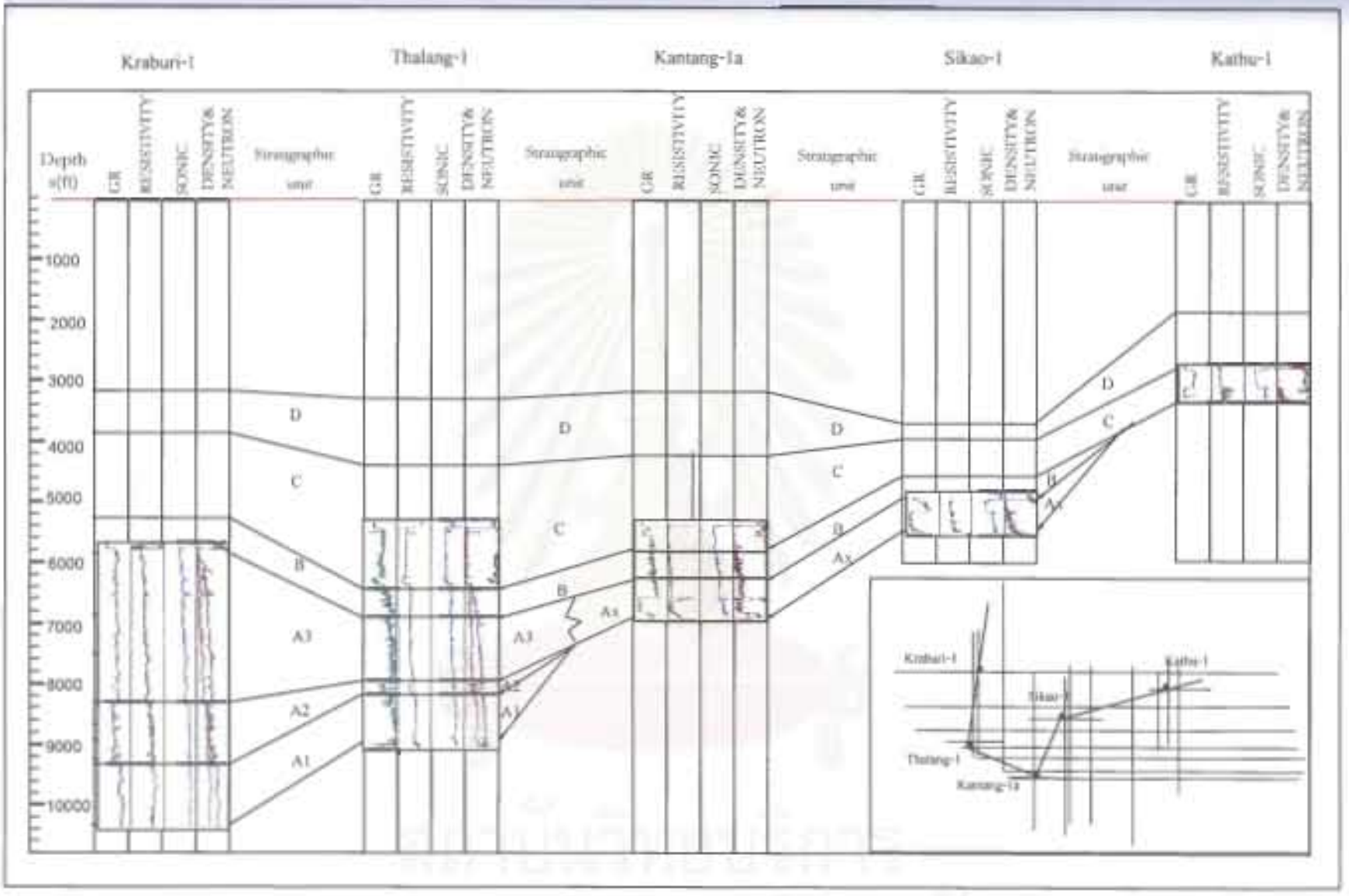

Figure 3.13 Well logs stratigraphic correlation of the southern part of Mergui basin..

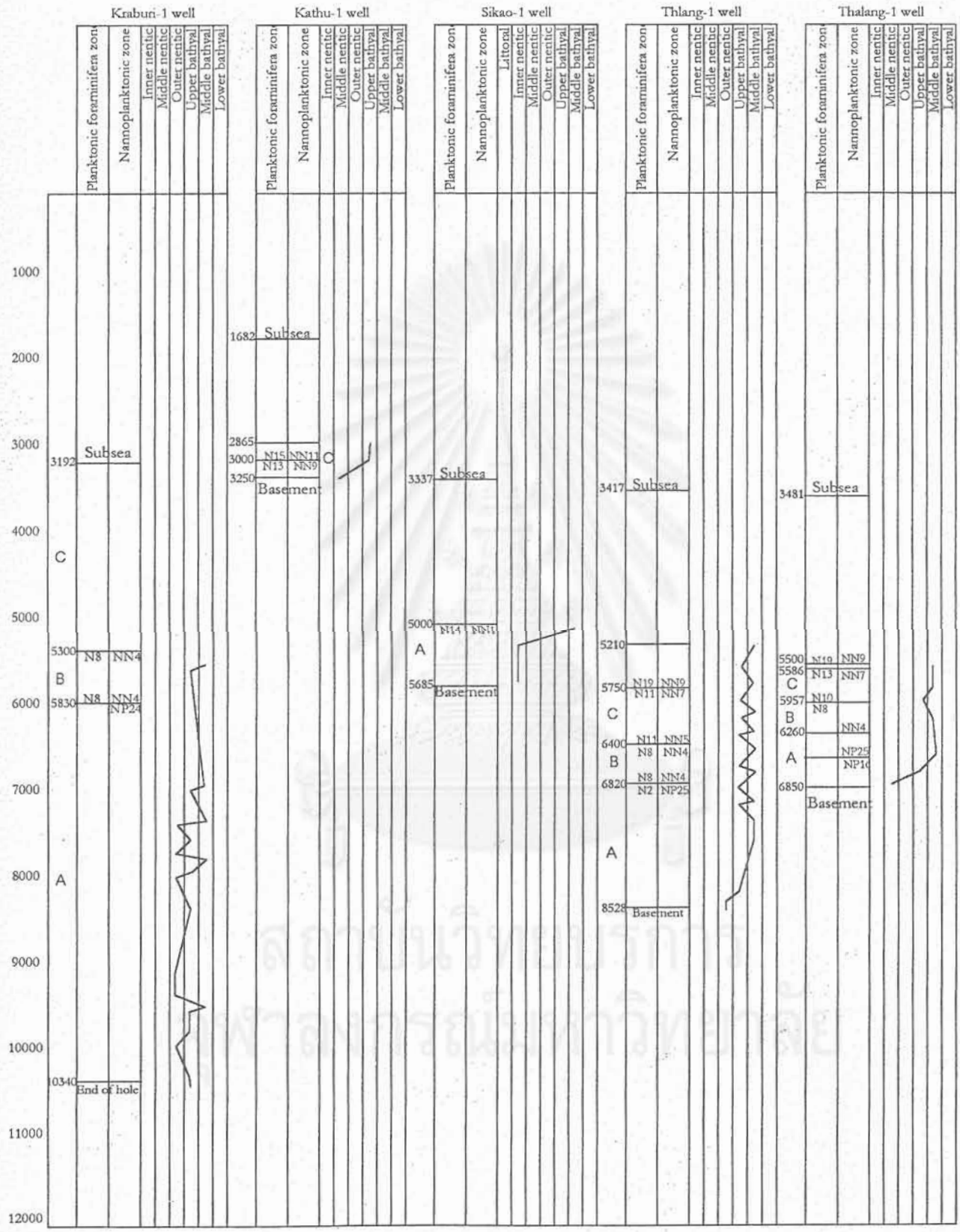

Figure 3.14 Palaeobathymetric chart of the exploratory wells.

(1972), Selley (1979), Walker (1984) and Nelson (1989) for turbidite facies with three association facies, such as slope, fan, and basinal plain.

Additionally, the sequence boundaries as seismic sequence and seismic facies are based on and derived from seismic reflection sections, as well as biostratigraphic data, which obtained from five exploratory wells. The four seismic sequence boundaries are identified and picked for the surface of reflection termination in terms of reflection termination that proposed by Payton (1977), Mitchum et al. (1977), Sheriff (1980) , Posamentier et al. (1993),such as lapout, erosional truncation, base lap, toplap, onlap and downlap and then tie to others line in the seismic data set. Each of seismic sequence were identified as seismic facies by recognition of the reflection geometry, continuity, amplitude, frequency and interval velocity, as well as the external form of groups of reflection, which contained information of stratigraphic significance.

Sub–unit A1

The depositional system of the sub-unit A1 is characterized by wedge shape, with high to moderate amplitude reflections, and divergent stratified configuration that suggested uniform rates of deposition on the basinal plain setting. This depositional system occurs after the relative sea level rise. The high amplitude reflectors observed on the seismic data were interpreted to indicate interbedding between shale and siltstone. The over all vertical succession observed in the well log shows a uniform pattern and the fine grained clastic sediment with this unit comprising thick shale and silty shale alternating with siltstone so indicating that sedimentary unit was deposited in low energy condition of basin plain.

The most common significant fossils found in this unit consists of foraminifera, nanofossil, that suggested two cycles of vertical succession of shallower upward from upper bathyal to outer neritic basinal plain environment as shown in Figures 3.15, 3.16 and 3.17.

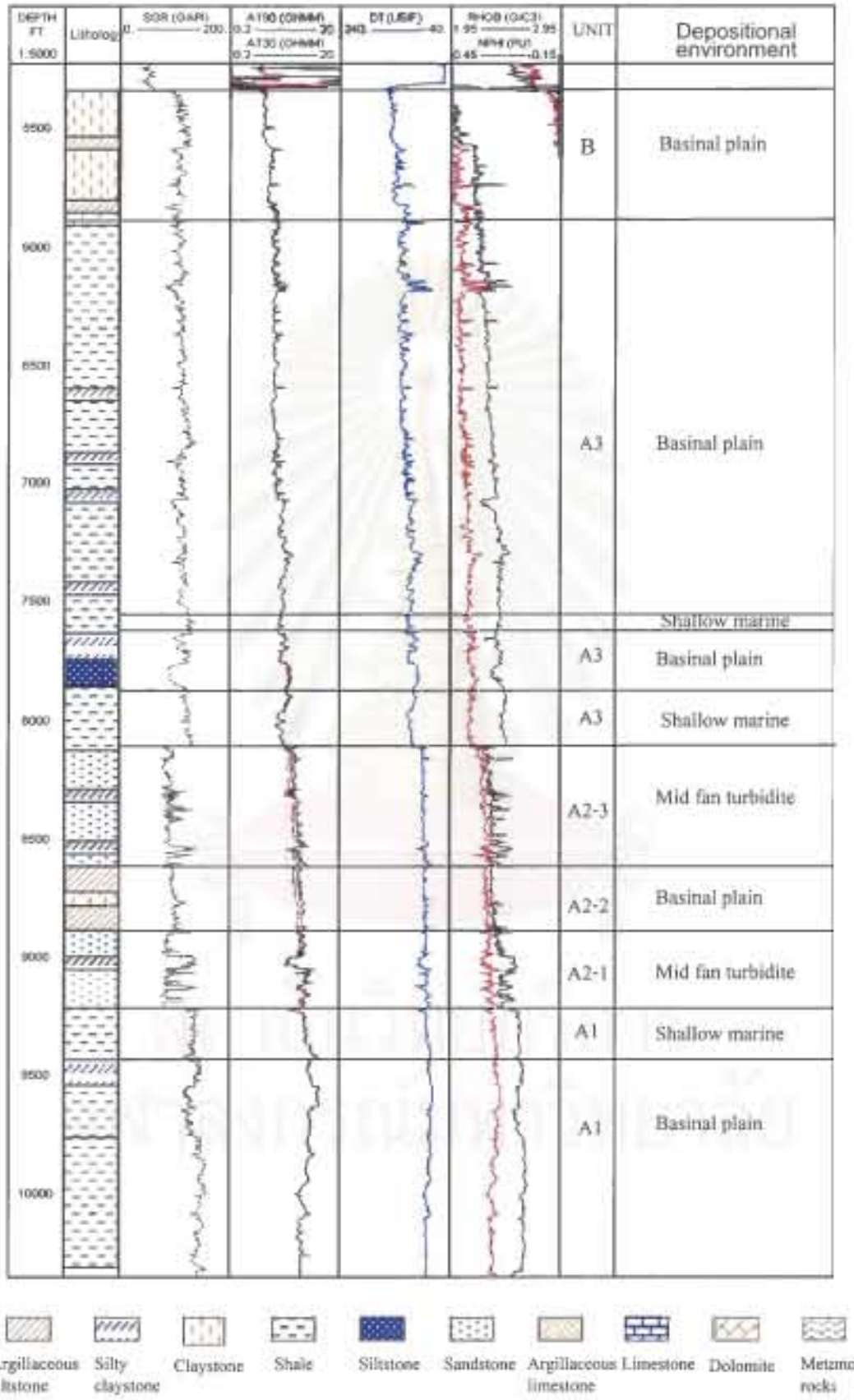

Figure 3.15 The sedimentary sequence and depositional environment of Kraburi-1well

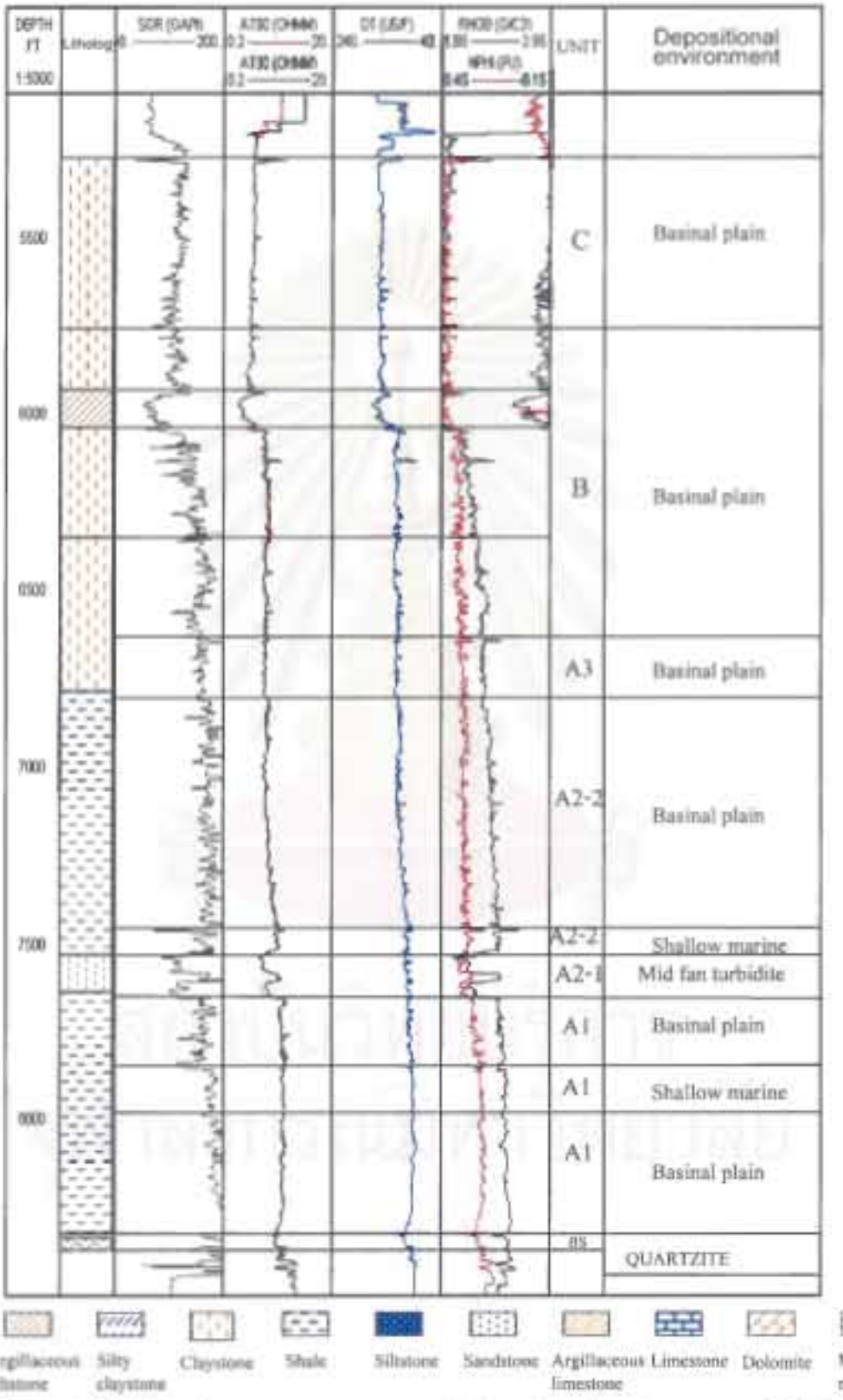

Figure 3.16 The sedimentary sequence and depositional environment of Thalang-1well

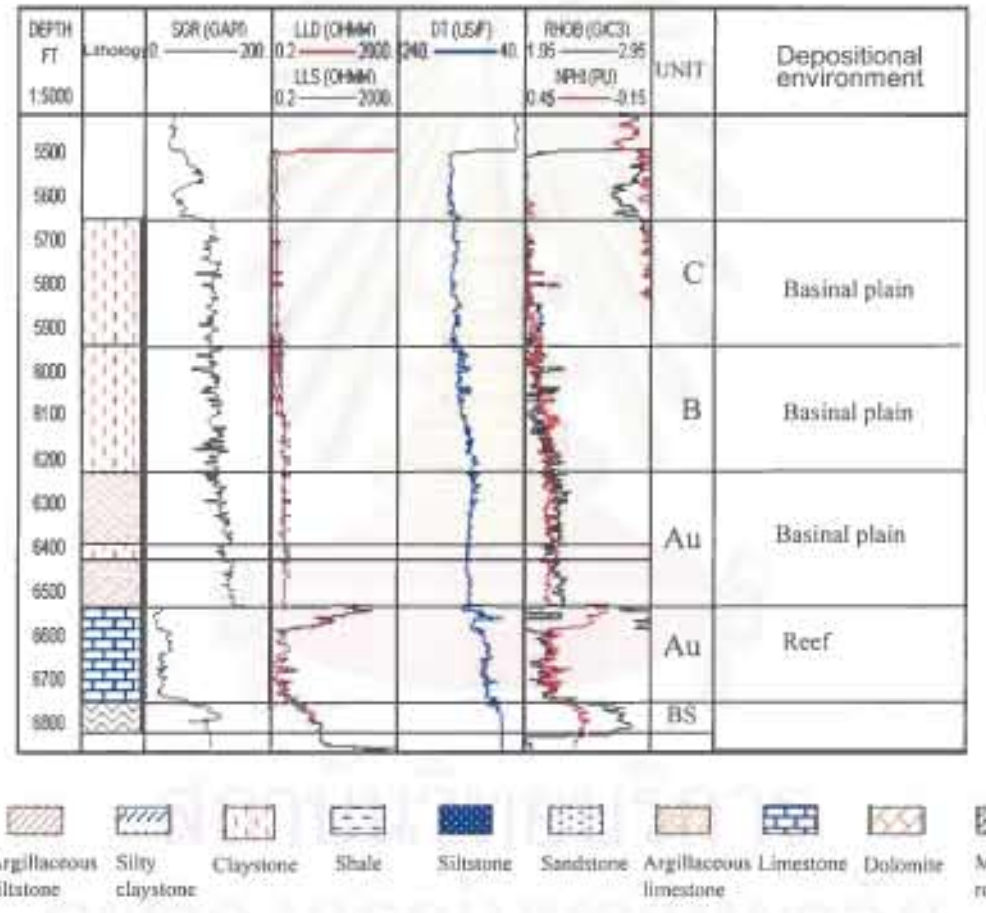

Figure 3.17 The sedimentary sequence and depositional environment of Kantang-1A well

Sub–unit A2

The depositional system of the first part of sub-unit A2 is characterized by channel filled and sheet shape, with high amplitude reflections, and chaotic lateral change to divergent stratified configuration which suggest uniform rates of deposition on the basinal plain setting. This deposition system occurs after the relative sea level rise. The chaotic configuration, which characterized this sedimentary unit, was for the deposition in condition of fan turbidite. The high amplitude reflectors observed on the seismic data were interpreted to indicate interbedding between thick sandstone and shale and siltstone. The over all vertical succession observed in the well log shows an alternating cylindrical pattern and finning- upward pattern and the lithology of this unit comprise thick sandstone alternating with siltstone and shale thus indicated this sedimentary unit was progressively deposited in high energy condition of mid fan turbidite overlying basinal plain of unit A1 as shown in Figures 3.15, 3.16 and 3.17.

.

The most common significant fossils found in this unit consist of foraminifera, nanofossil, supporting an upper bathyal mid-fan turbidite environment as shown in figure 3.14.

The depositional system of second part of the sub-unit A2 is characterized by channel filled and sheet, with high amplitude reflections and divergent stratified configuration which suggest a uniform rate of deposition on the basinal plain setting. This depositional system occurs after the relative sea level rise. The high amplitude reflections observed on the seismic data were interpreted to indicate interbedding between shale and siltstone. The over all vertical succession observed in the well log shows a uniform pattern, and the lithology in this unit comprise thick shale and silty shale alternating with siltstone that indicates that sedimentary unit was deposited in low energy condition of basinal plain. As well, the most common significant fossils found in this unit consist of foraminifera, nannofossil, supporting an upper bathyal basinal plain environment as shown in Figures 3.15, 3.16 and 3.17.

The depositional system of the third part of sub-unit A2 is characterized by channel filled and sheet shape, with amplitude reflections, and chaotic lateral changed to divergent stratified configuration that suggested uniform rates of deposition on the

basin plain setting. This depositional system occurs after the relative sea level rise. The chaotic configuration, which suggested and indicated this sedimentary unit, was deposited in condition of mid-fan turbidite. The reflections observed on the seismic data were interpreted to indicate interbedding between thick sandstone and shale and siltstone. The over all vertical succession observed in the well logs shows an alternate cylindrical pattern and finning- upward pattern and the lithology of this unit comprise thick sandstone alternating with siltstone and shale that indicated this sedimentary unit was progressively deposited in high energy condition of mid-fan turbidite overlies the upper bathyal basinal plain of subunit A2-2.

The most common significant fossils found in this unit consist of foraminifera, nanofossil, suggested the upper bathyal mid-fan turbidite environment as shown in Figures 3.15, 3.16 and 3.17.

Sub–unit A3

The depositional system of the sub-unit A3 is characterized by channel filled and sheet shape, with high amplitude reflections, and divergent stratified configuration, which suggested uniform rates of deposition on the basinal plain setting. This depositional system occurred after the relative sea level rise. The high amplitude reflectors observed on the seismic data were interpreted to indicate interbedding between shale and claystone, siltstone, and trace of sandstone. The over all vertical succession observed in the well log shows a uniform pattern and fining upward sequence and the lithology of this unit comprise thick shale and silty shale alternating with siltstone that indicated this sedimentary unit was deposited in low energy condition of basinal plain.

The most common significant fossils found in this unit consist of foraminifera, nannofossil, supporting three cycles of deeper upward form outer neritic to middle bathyal basinal plain environment and shown in Figures 3.15, 3.16 and 3.17.

Unit Au

The depositional system of the lower of unit Au is characterized by channel fill and sheet shape, with high amplitude reflections, and free configuration lateral change to divergent stratified configuration which suggested carbonate build up laterally with a uniform rates of deposition on the basinal plain setting. This deposition system occurs after the relative sea level rise. The free configuration which characterizes this sedimentary unit, suggests the deposition in condition of shallow marine with generally rising eustatic sea level during this period allowed the accumulation of the thick reeftal units. The over all vertical succession observed in the well log shows a uniform pattern with very low to low gamma ray and the lithology with this unit comprise thick limestone that indicated this sedimentary unit was deposited in quiet condition of shallow marine.

The most common significant fossils found in this unit consist of foraminifera, nanofossil, supporting an outer neritic reeftal environment as shown in the Figure 3.14.

The depositional system of the upper part of unit Au **is** characterized by channel fill and sheet shape, with high amplitude reflections, and divergent stratified configuration which suggested a uniform rates of deposition on the basinal plain setting. This depositional system occurred after the relative sea level rise. The high amplitude reflections observed on the seismic data were interpreted to indicate interbedding between shale and claystone, siltstone, and trace of sandstone. The over all vertical succession observed in the well log shows a uniform pattern and fining upward sequence and the lithology with this unit comprise thick shale and silty shale alternating with siltstone that indicated this sedimentary unit was deposited in low energy condition of basinal plain. The most common significant fossils found in this unit consist of foraminifera, nannofossil, supporting an upper to middle bathyal basinal plain environment as shown in the Figure 3.14.

Unit B

The depositional system of the unit B is characterized by sheet shape, with high to low amplitude reflections, and divergent stratified configuration which suggested

uniform rates of deposition on the basinal plain setting. This depositional system occurred after the relative sea level rise. The high amplitude reflections observed on the seismic data were interpreted to indicate interbedding between shale and claystone, siltstone, and trace of sandstone. The over all vertical succession observed in the well log shows a uniform pattern and fining upward sequence and the lithology of this unit comprise thick shale and silty shale alternating with siltstone that indicated this sedimentary unit was deposited in low energy condition of basinal plain.

The most common significant fossils found in this unit consist of foraminifera, nanofossil, supporting an upper to middle bathyal environment as shown in Figure 3.14.

Unit C

The depositional system of lower part of unit C is characterized by sheet shape, with moderate to low amplitude reflections, and free configuration lateral changed to divergent stratified configuration which suggested carbonate build up laterally with a uniform rates of deposition on the basinal plain setting. This depositional system occurred after the relative sea level rise. The free configuration, which suggested this sedimentary unit, was deposited in condition of shallow marine with generally rising eustatic sea level during this period allowed the accumulation of the thick reeftal units. The over all vertical succession observed in the well log shows a uniform pattern with very low to low gamma ray and the lithology of this unit comprise thick limestone that indicated this sedimentary unit was deposited in quiet condition of shallow marine.

The most common significant fossils found in this unit consist of foraminifera, nanofossil, supporting an inner neritic reeftal environment as shown in figure 3.14.

The depositional system of the upper part of unit C is characterized by sheet shape, with moderate to low amplitude reflections, and parallel stratified configuration which suggested uniform rates of deposition on the basinal plain setting. This depositional system occurred after the relative sea level rise. The over all vertical succession observed in the well log shows a uniform pattern and fining upward sequence and the lithology of this unit comprise thick shale and silty shale alternating

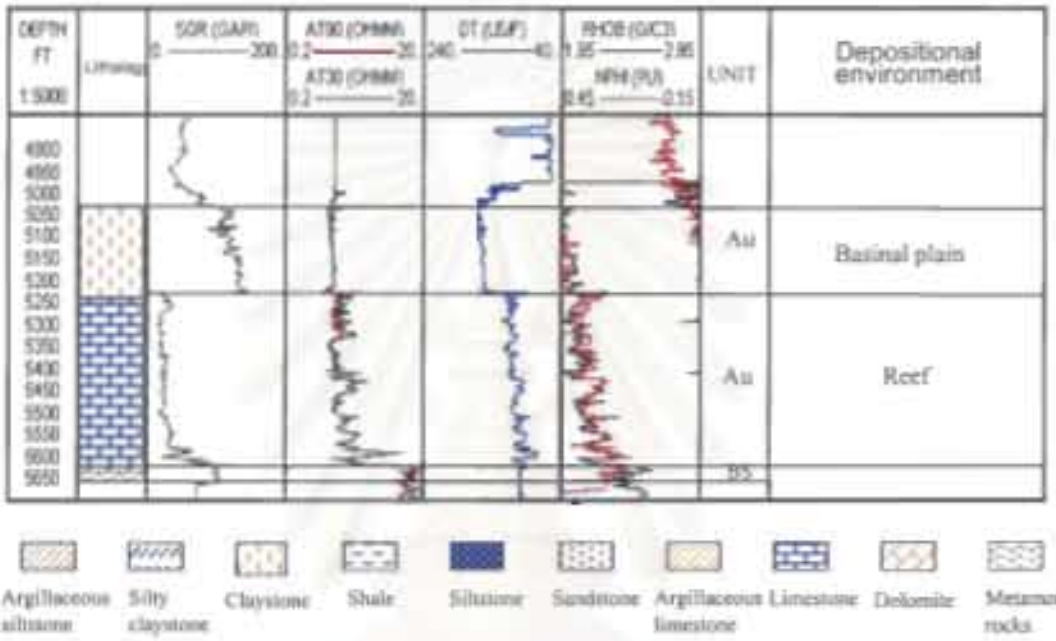

Figure 3.18 The sedimentary sequence and depositional environment of Sikao-1 well

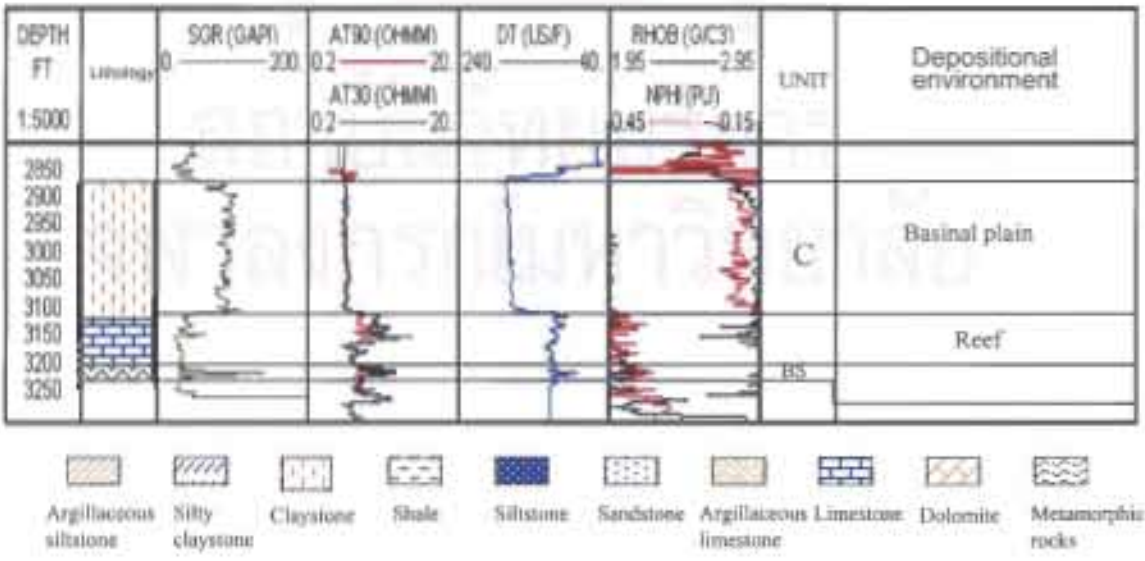

Figure 3.19 The sedimentary sequence and depositional environment of Kathu-1 well

with siltstone that indicated this sedimentary unit was deposited in low energy condition of basinal plain.

The most common significant fossils found in this unit consist of foraminifera, nanofossil, supporting an upper to middle bathyal environment and shown in Figures 3.14, 3.16, 3.17 and 3.19.

Unit D

The depositional system of the unit D is characterized by slope-front, lens and sheet shape, with moderate to low amplitude reflections, and parallel changed to sigmoidal stratified configuration which suggested a uniform rates of deposition on a uniformly subsiding shelf or the basinal plain stable setting change laterally to prograding. This depositional system occurs after the relative sea level rise. The high amplitude reflections observed on the seismic data were interpreted to indicate interbedding between shale and claystone, siltstone, and trace of sandstone.

3.3 Geological structure

The southern part of Mergui basin comprises three main subbasins, namely, Eastern sub-basin, Ranot trough, and Ranong trough. They are small, narrow and elongate basins, which forms as a series of N-S trending half graben. The important geological structures are as follow.

1. Normal faults

The series of N-S trending normal faults is principally controlled by the development of the basin, then forming the N-S trending half-graben geometry of the Ranong and Ranot troughs at the same time of sedimentation as shown in figure 3.20. The depocenters, which influenced the sedimentation thickening into the western margin of the sub-basin, suggests that the normal faults are growth fault as that affected rate of sedimentation and they themselves have been partly controlled by sedimentary loading which are known as growth faults.

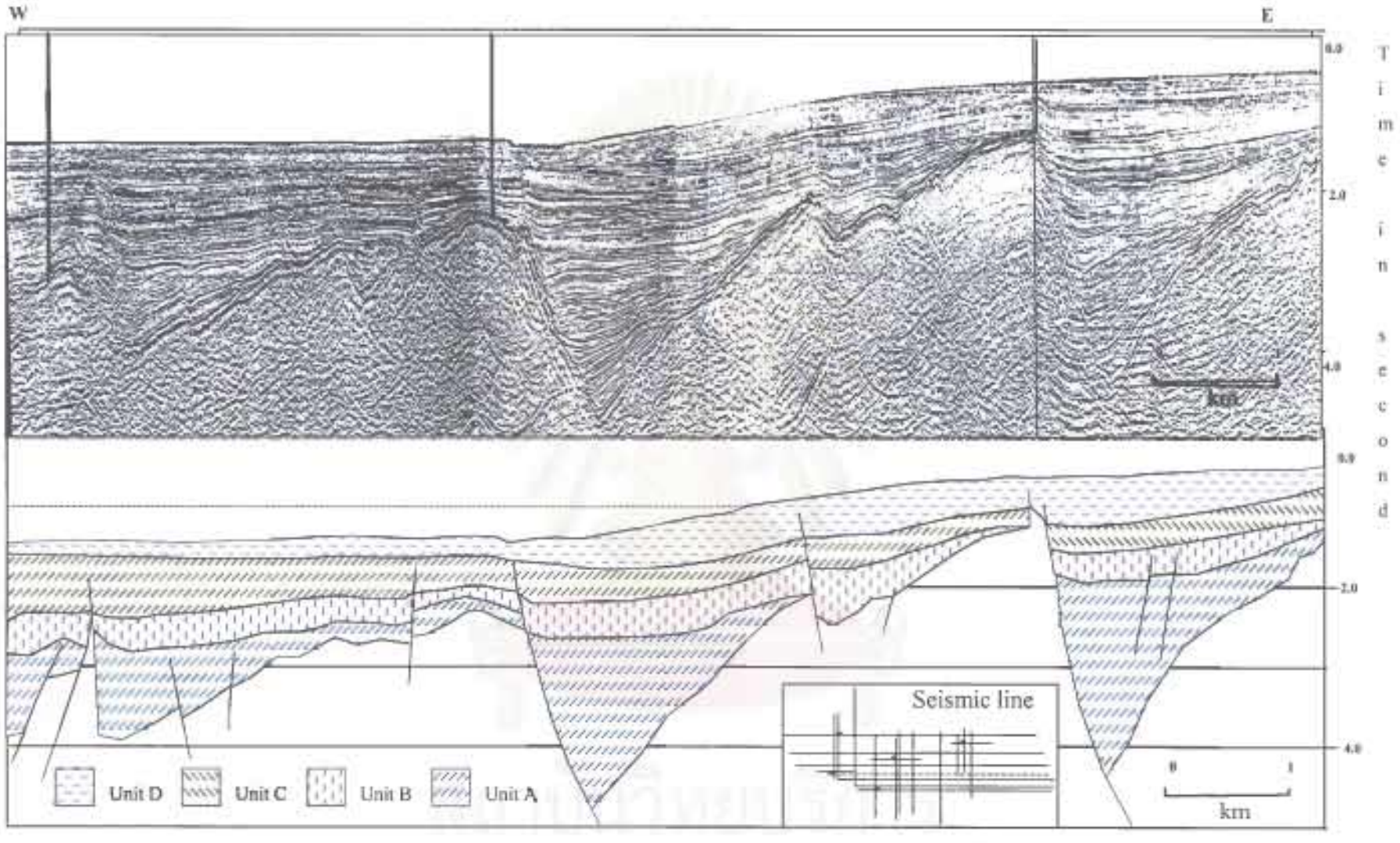

Figure 3.20 The seismic profile showing half-graben geometry subbasins in the southern part of Mergui basin.

These faults are characterized by the western boundary faults with the eastern dipping. The faults cross cut all the entire Tertiary sequence and through the pre-Tertiary basement as shown in figure 3.21.

2. Rollover anticlines

Rollover anticline is the simplest structure that occurs associated to the listric normal fault. It is developed on the hanging wall of the listric normal fault. The surface at the top of the hanging wall formed an anticline or roll-over as a result of the sagging down of the sedimentary strata to the fault, therefore beds has to rotated and dips in hanging wall have been steeper than in the foot wall. Basically, the rollover anticlines are clearly seen between the sequence of Late Oligocene to Early Miocene in age, particularly in Ranot trough.

3. Negative flower structure

Negative flower structure are defined as linear, shallow synform that are displaced by upward-diverging strands of a wrench fault having normal separation (Harding et al., 1983) which occur east side of Eastern sub-basin as shown in seismic profile of figure 3.22. These structures demonstrate important criteria to identify the structural style of wrench-fault of this region.

The structural elements of southern part of Mergui basin have been illustrated by the seismic profile and the two-way time structure map, which produced based on a reflector at the top of basement, unit A, unit B and unit D as shown in figures 3.23 to 3.26.

3.4 Depositional evolution of the southern part of Tertiary Mergui basin

The southern part of Mergui basin was commencing rifting in the Late Oligocene with N-S trending haft-graben. The sediment fills within the basin are entirely marine sediments which both of shallow marine as neritic zone and deep marine (bathyal marine). The depositional environments are composed of basinal plain, mid fan

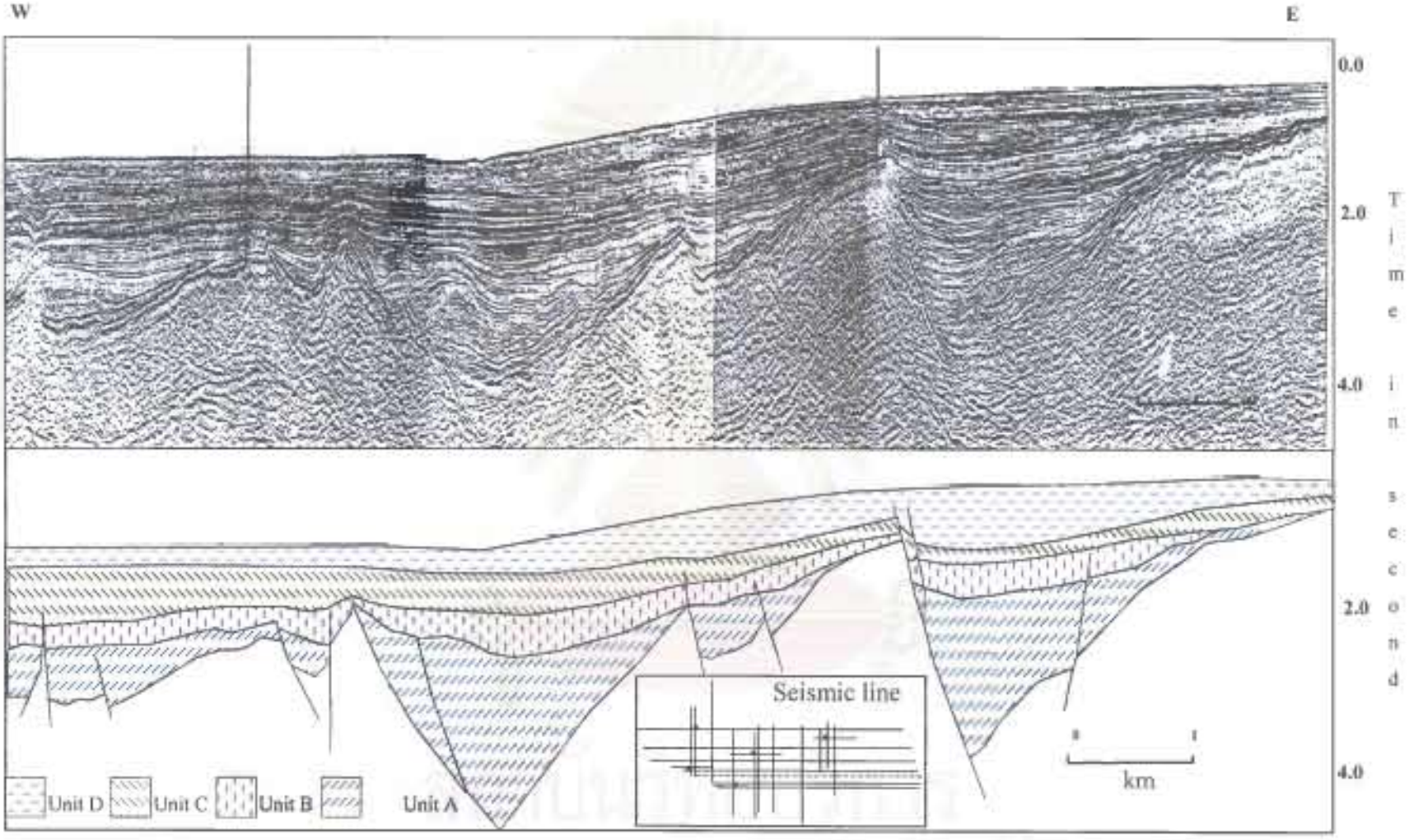

Figure 3.21 The seismic profile showing east dipping normal fault in the southern part of Mergui basin.

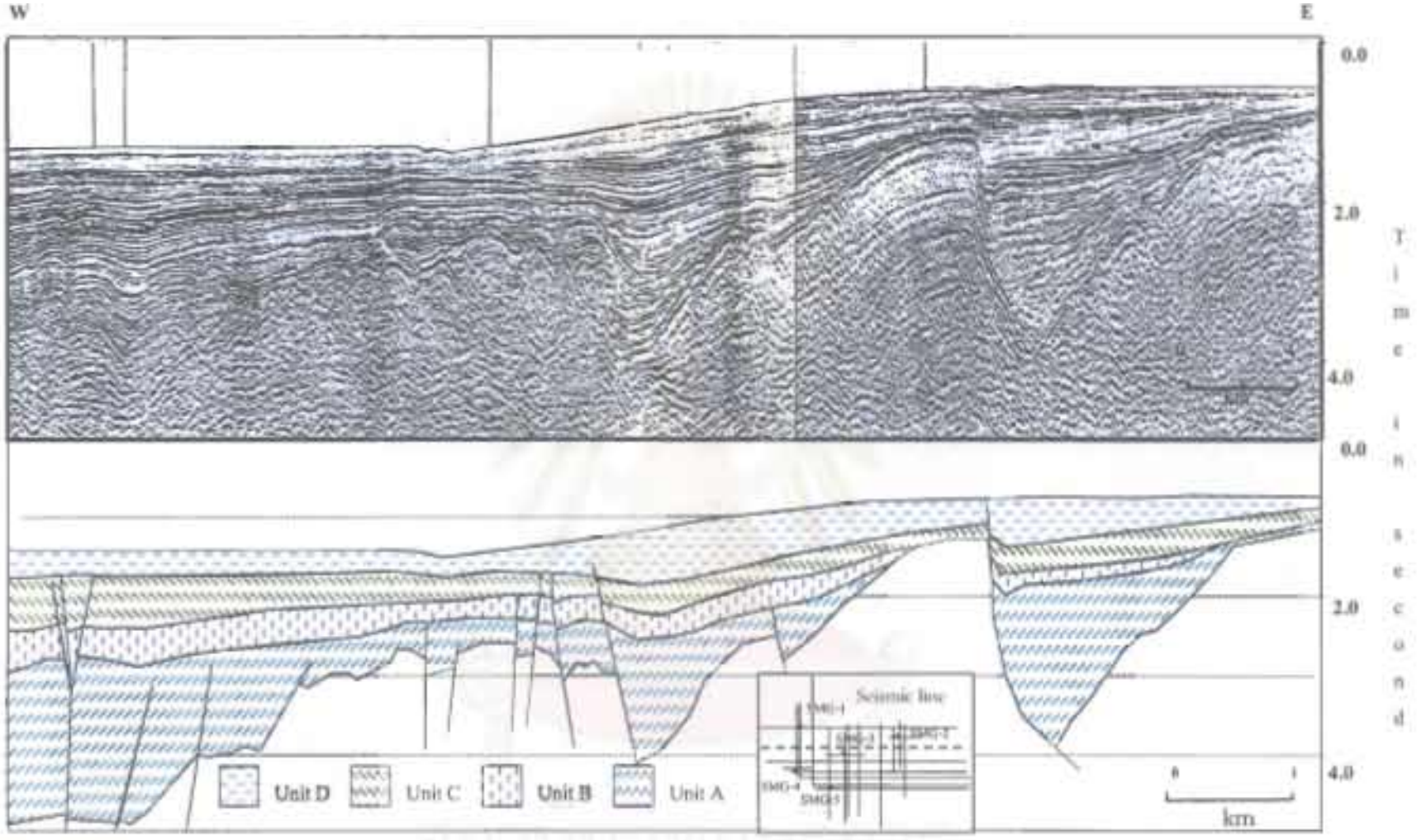

Figure 2.22The seismic profile showing nagative flower structure in the southern part of Mergui basin

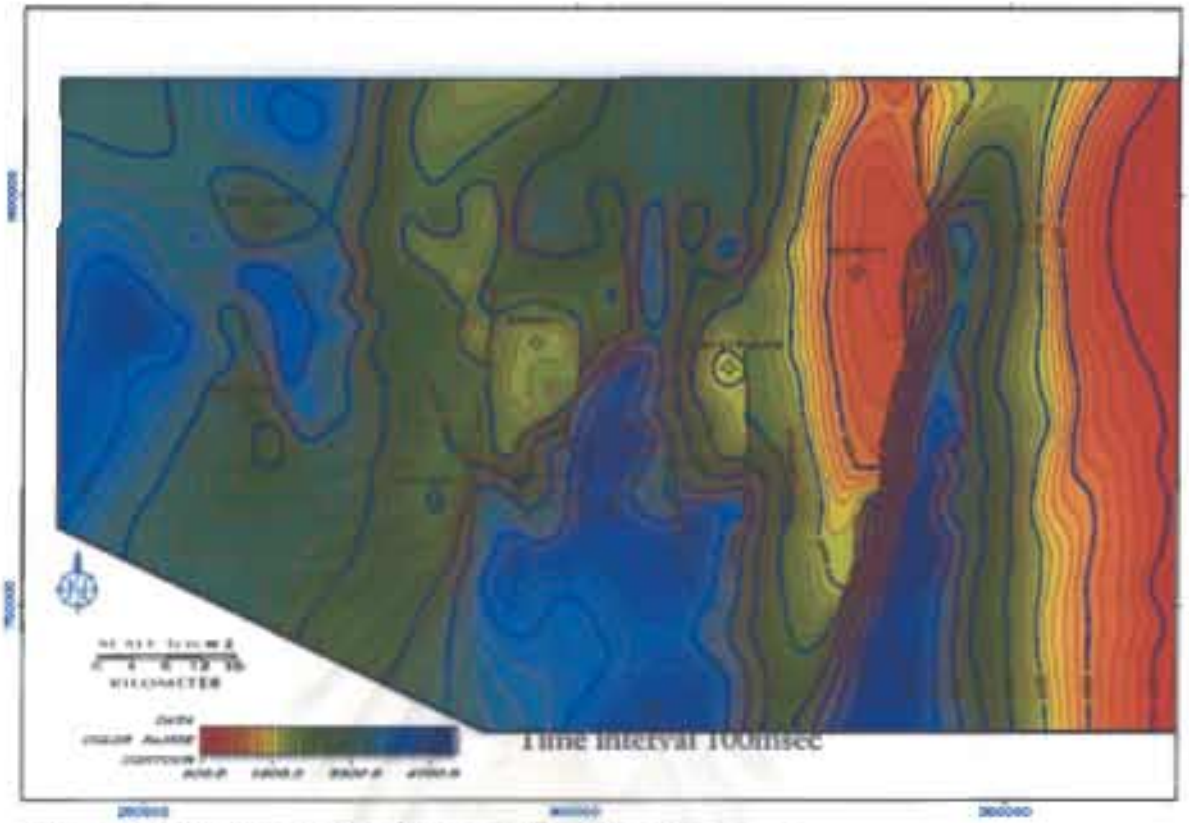

Figure 3.23 TWT structural map on the top of basement

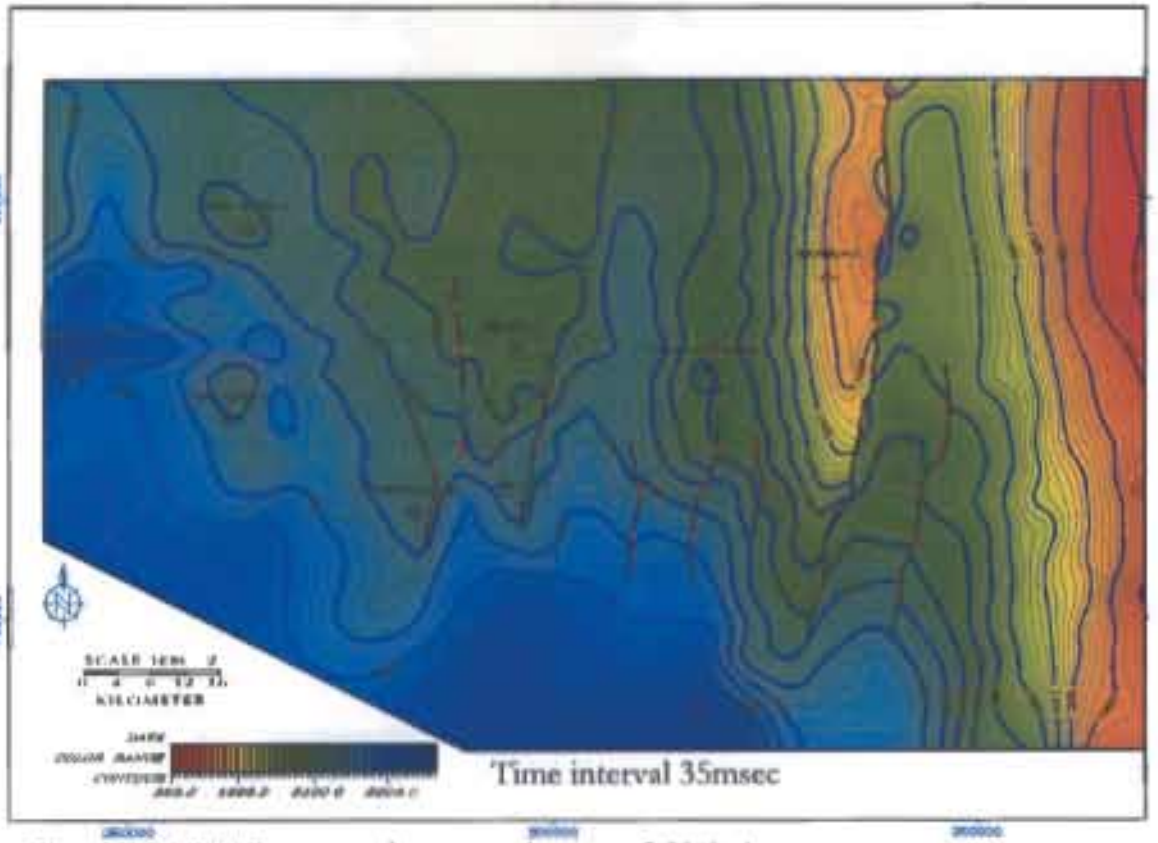

Figure 3.24 TWT structural map on the top of Unit A

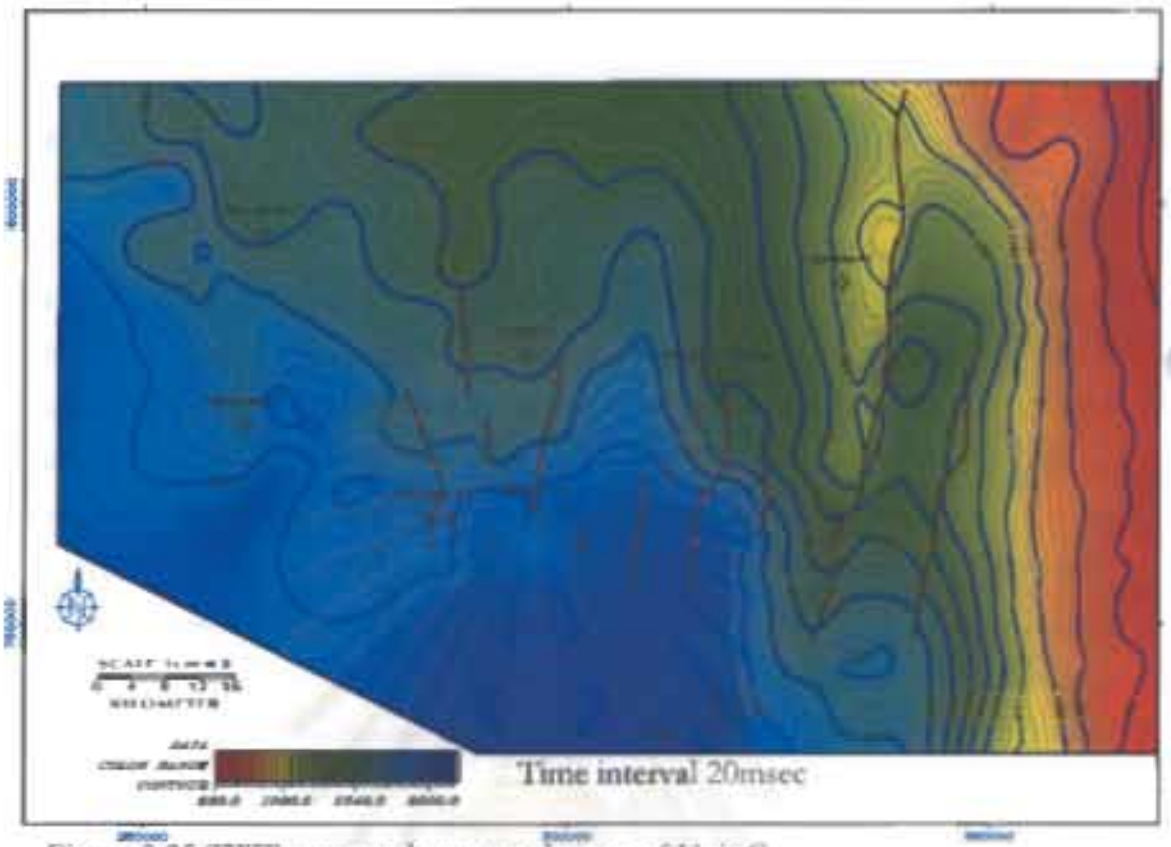

Figure 3.25 TWT structural map on the top of Unit C

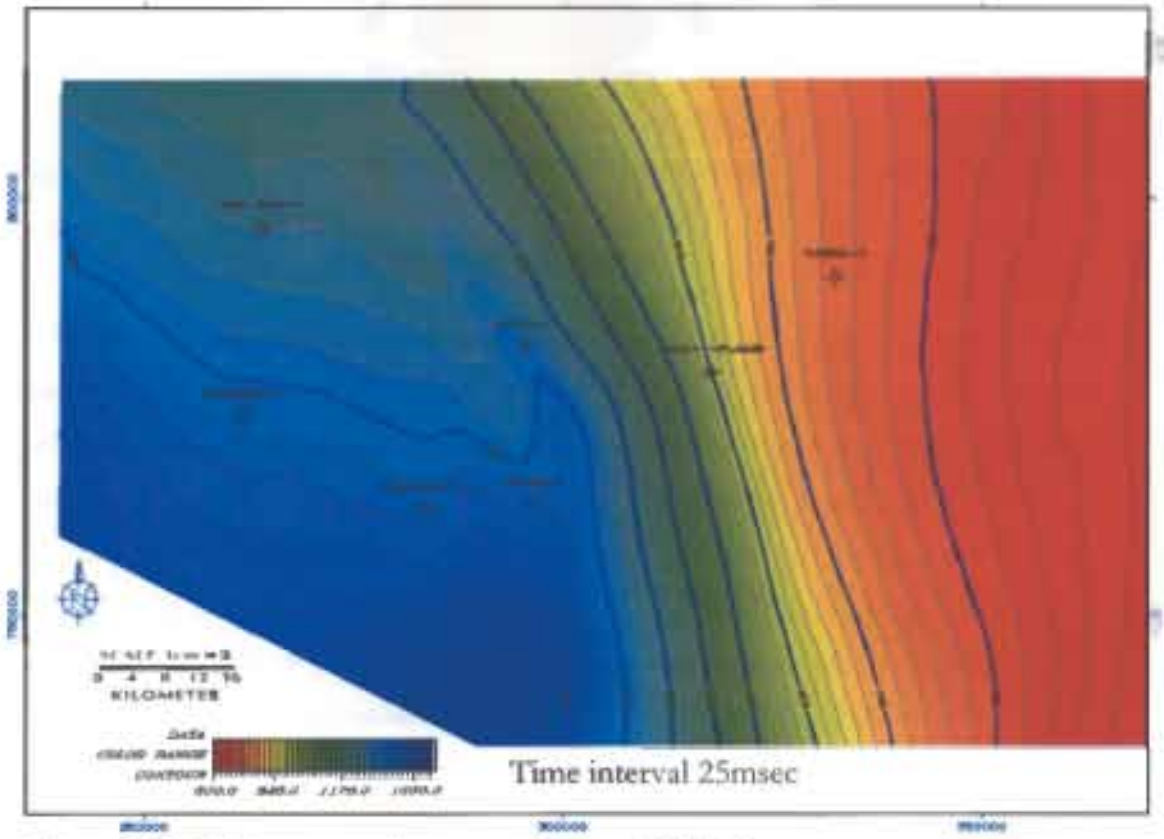

Figure 3.26 TWT structural map on the top of Unit D

turbidite and reef. The evolution of the southern part of Mergui basin is recognized into four period as follows:

Late Oligocene to Early Miocene

The northwards progressive collision of the Indian plate with Eurasion plate since 40-50 Ma (Polachan and Sattayarak, 1989) was cause increasingly oblique subduction of the Indian oceanic plate beneath the western edge of southeast Asia. It was resulted the major dextral movement along NNW-SSE trending Mergui fault zone and sinitral movement along Ranong-Klong Marui fault zone with NNE-SSW trending. That may be expected to cause the major extension of the Tertiary Mergui basin along the N-S orientation as follow the shear stress diagram that proposed by Polachan, (1988). The pre-tertiary basement was commence rifting as a half-graben and sediments was initials deposited. The microfossil that contain in the lowermost sequence of southern part of Tertiary Mergui basin suggest the oldest sediments are Late Oligocene and the depositional environment are deep marine on the west side of the study area that become shallow marine on the east side.

The stratigraphy of this period is based on interval A of the seismic sequence and the unit A of the sedimentary sequence. The divergent stratified configuration indicats varying rates of deposition caused by the tectonic tilting. The chaotic configuration also indicates the channel fill of submarine fans of sub-units A2-1 and A2-3 (Mitchum et al, 1977). Based on well data, two cycles of basinal shale are observed to deposit in upper to middle bathyal depth and then became shallower to outer neritic fine-grained clastics in the lower part, and progressively turned deeper into the low-fan turbidite in the middle part. As well the upper part comprises 3 cycles of outer neritic fine-grained clastic progressively become deeper into upper to middle bathyal depth of basinal plain of fine-grained clastics. Meanwhile, the shallow reeftal carbonate was formed in the lower part and then progressively become deeper into upper and middle bathyal depth of basinal plain of fine-grained clastics on Ranong trough. Sediments of A Unit deposited during the initial rifting of Mergui basin in Late Oligocene. This period represented predominantly of marine deposition during initial marine transgression and corresponded to major period of global eustatic sea-level rise.

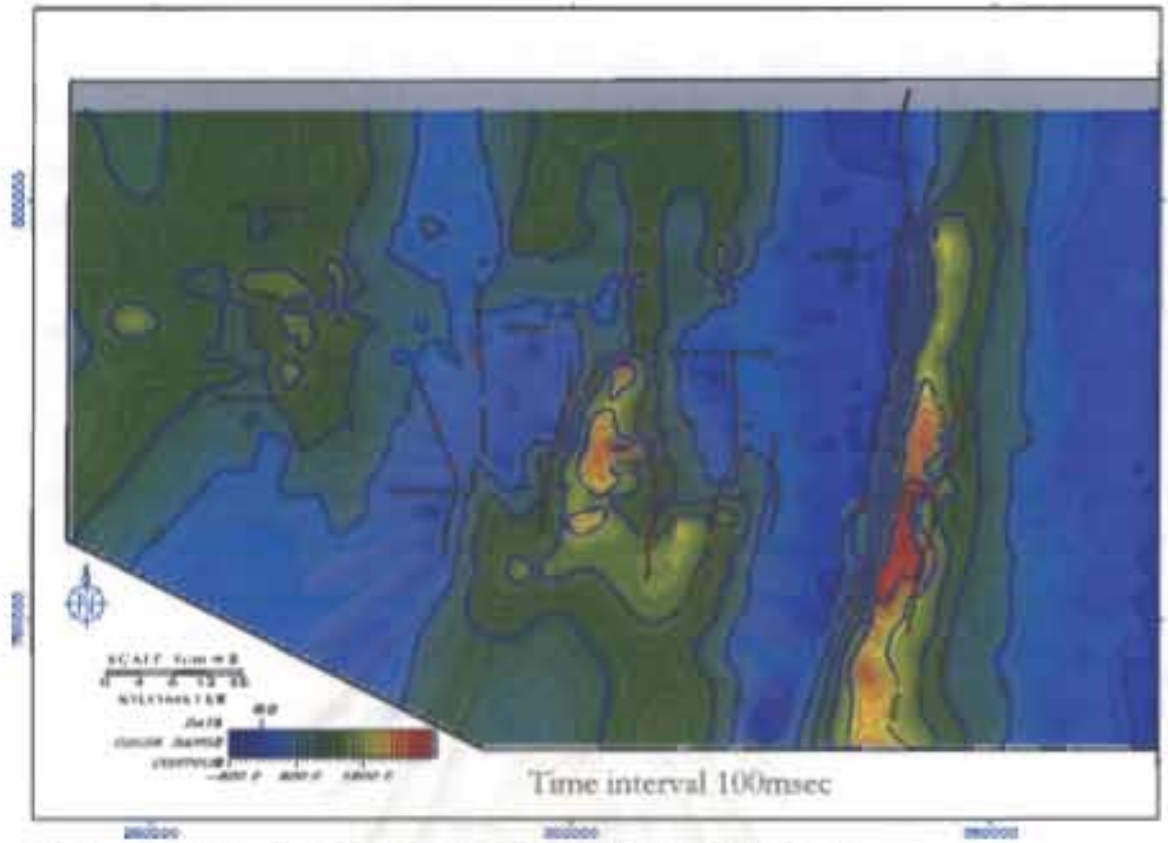

Figure 3.27 TWT isopach map of Unit A(with fault traces).

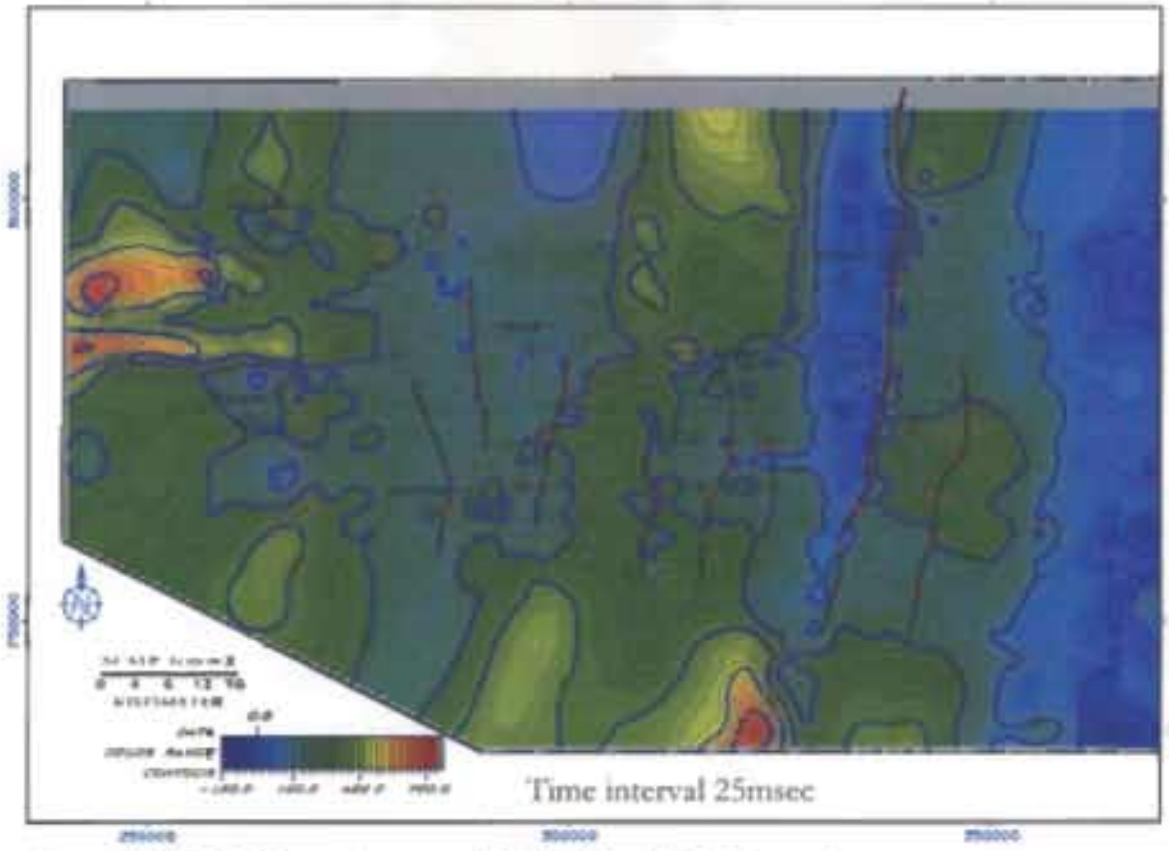

Figure 3.28 TWT isopach map of Unit C(with fault traces).

The isopach map of this interval in Figure 3.27 shows variation in range of thickness of sediments within deeper local sub-basin to thin sediment or starved in the Ranong ridge and Mergui shelf. The thickness was increased westward on the downthrown side of the east dipping normal fault as a wedge shape suggest this part was more subsidence than east part of subbasin and formed as depocenter of half-graben.

Early Miocene to Late Miocene

The stratigraphy of this period is based on interval B of the seismic sequence and the unit B of the sedimentary sequence. The divergent stratified configuration indicates the varying rates of deposition caused by the tectonic tilting. The parallel stratified reflection configuration also indicated uniform rates of deposition caused by the tectonic stability and uniform subsiding shelf setting (Mitchum et al, 1977). Based on the well data, basinal fine-grained clastics were deposited in upper to middle bathyal depth.

This period is represented by predominantly marine deposition during continued marine transgression and corresponds to major period of global eustatic sea-level rise.

Late Miocene to Pliocene

The stratigraphy of this period is based on interval C of the seismic sequence and the unit C of the sedimentary sequence. The parallel stratified reflection configuration indicated uniform rates of deposition caused by the tectonic stability and uniform subsiding shelf setting (Mitchum et al. 1977). Based on well data, bathyal fine-grained sediments were deposited in the eastern sub-basin and Ranong trough, while the palaeobathymetry suggested the continuation of deepening throughout this period whereas reeftal carbonate was initially formed in Ranong trough also suggests that Ranong trough is initially drowned at this time. Therefore, it suggests that the basin is deepened from southern and western part of the basin. The isopach map of this interval in figure 3.28 shows thin sediment strata or starved, toward the northern, eastern, and western directions, as well as thickening in the localized deeper Ranot and Ranong

troughs and the sediments supply were from basement high surrounding this deeper trough.

The early part of this period is represented the maximum marine transgression of the area as a result of Ranong ridge and Mergui shelf submerged.

Pliocene to Recent

The stratigraphy of an interval D of this period is based only on the seismic data only because it is lacking of the well data on this sedimentary. The downlap surface of prograding clinoforms as sigmoidal pattern lateral changes to concordant into basin at the lower boundary indicates low energy siliciclastic shelves of the basin. As well, the concordant surface at the base boundary with parallel to subparallel reflection configuration indicated the uniform rate of subsidence. The isopach map of this interval in the Figure 3.29 shows thickening in the southwestern direction and is absented in the northeastern part of the basin over the Mergui shelf.

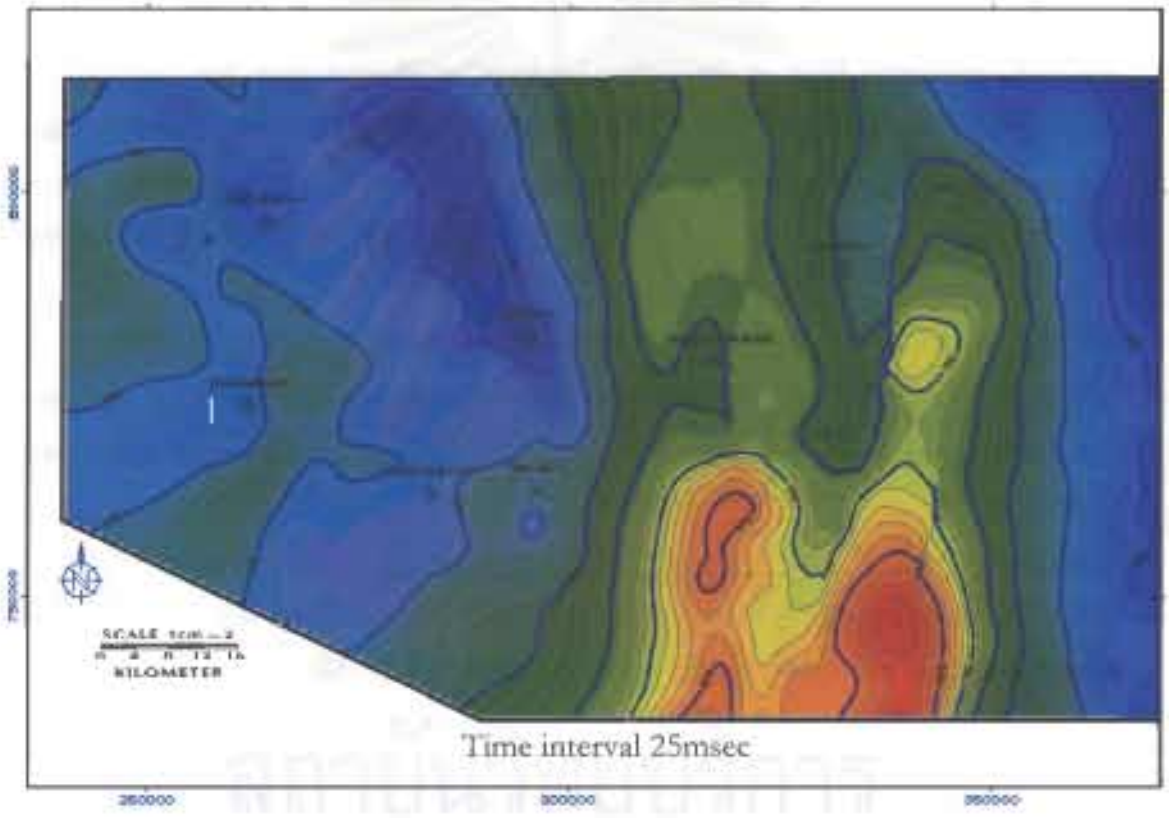

Figure 3.29 TWT isopach map of Unit D

CHAPTER IV

PETROLEUM POTENTIAL ASSESSMENTS IN SOUTHERN PART OF MERGUI BASIN

To search for petroleum, the petroleum geologists focus their attention on the geologic factors that combine to produce petroleum accumulation. These geological factors are the reservoir rock units that have suitable porosity to contain hydrocarbon and permeability to permit a fluid flow, organic-rich source rocks to generate hydrocarbon and must have been "cooked" sufficiently to yield petroleum. Also the regional seals or the impermeable cab rocks to prevent the upward escape of petroleum in the gross reservoir unit are as essential as the traps, stratigraphic or structural, that concentrate petroleum in specific places.

Thus, the petroleum potential assessments in southern part of Mergui basin are based on the structural and stratigraphic evolution of the depositional sequence within the basin as these provide most of the essential geologic factors as mentioned above.

In addition, the geochemical analysis information such as the total organic content (TOC) and pyrolysis are used for the assessments of petroleum source potential. Timing of oil generation was determined by Lopatin's method while the porosity was defined from the petrographic analysis.

4.1 Source rocks

The petroleum exploration in this area so far has not been successful. No commercial hydrocarbon has ever been found in Mergui basin. However, the result of the studies from the geophysical logs reveal that there is minor petroleum gas show and also the sedimentary sequence of marine shale and claystone has a potential to be the prospective source rocks.

A prospective source rock must contain adequate quantities of associated organic material, or organic richness, for the petroleum-generative potential. The total organic carbon content (TOC) is a simple measurement of carbon present in a rock in both insoluble (kerogen) and soluble (bitumen) forms which widely accepted as a rapid mean of characterizing the quality of potential source rock. Generally, the accepted source rock contains TOC at least 1% while the sediments in general contain less than 0.3% TOC. The good to very good source rock contains TOC between 1 % - 5% and greater than 5% is the excellent source rock. Petroleum is derived from organic material, the kerogen being contained in the sediment. Conventionally, three types of kerogen are classified according to their carbon indices, hydrogen indices and oxygen indices that cross-plot on a Van Krevelen diagram (Tissot and Welts, 1978). Type I kerogen is rich in lipids, predominantly of algal origin and is mostly oil prone. Type II kerogen is particularly good source of oil and is mainly derived from the organic matters of marine origin. Type III kerogen has a low oil potential but have high gas potential, and is derived from material of higher land plants.

The results of the geochemical analysis of the rock cuttings and sidewall core samples from the exploratory wells are summarized in Table 4.1. The study indicates that the organic richness of the exploratory wells is mostly determined as poor to fair with in a range 0.05% to 1.4%. The TOC determination considered to be source rock of minimum of 1% indicates such fairness in unit A in at Kraburi-1, Thalang-1 and Kantang-1A wells, particularly in the deeper parts of the basin. The Kathu-1 and Sikao-1 wells contain no source rock, as the results of TOC determination are less than 1%.

Geothermal gradient

Generally, the geothermal gradients are calculated by using the formation temperature received in the boreholes. The bottom hole temperature (BHT) is recorded during a geophysical logging operated in the well by the thermometers in a state of thermal disequilibrium. This is because the circulation of the drilling fluids thorough the well tends to cool the formation. Thus, the recorded bottom hole temperature is decreased to become less than the original true stabilized temperature. It is hence necessary to correct the recorded temperature to the true formation temperature by

Table 4.1 Geochemical analysis data of rocks.

Well	Rock type	Sedimentary sequence unit	Age	TOC % average	Korogen			Source rock type	Potential Petrolum Source Rock	Matuation
					I	II	III			
Thalang-1	Argillaceous	A	Oligocene	1.40			X	gas prone	fair	immature
						X	X	oil/gas prone	good	
Kangtang-1a	Argillaceous	A	Oligocene	0.96			X	gas prone	fair	immature
	limestone	A	Oligocene	0.20		X	X	oil/gas prone	very low	
Kraburi-1	Argillaceous	A	Oligocene	1.00			X	gas prone	fair	immature
Sikao-1	Clastic	B	Early Miocene	0.32		X	X	oil/gas prone	very low	immature
	limestone	A	Oligocene	0.10			X	gas prone	very low	
kathu-1	Clastic	B	Early Miocene	0.05			X	gas prone	very low	immature
	limestone	A	Oligocene	0.65			X	gas prone	very low	

using temperature recorded on each geophysical-logging run to be plotted on the Horner type plot proposed by Fertl & Wichmann, (1977). In this method, use the same equation for determining the increased pressure during Drill Stem Test when the drill hole was closed for a long time.

Following is an equation for calculating for the true formation temperature.

$$T_F = T_L + K \log \Delta t / (t_c + \Delta t)$$

T_F = True formation temperature(°F)

T_L = Bottom hole log temperature (maximum record temperature,°F)

Δt= Bottom hole circulation time (hours) after the formation was cut and before the mud pumps were shut off and the bit pulled.

t_c = Time interval between cessation of circulation and the measuring of T_L

K = Constant (Equal to 1 in this study.)

The maximum-recorded temperature (TL) on a linear scale in y-axis is plotted against $\Delta t / (t_c + \Delta t)$ ratio on logarithmic scale in x-axis (as shown in Figure4.1). Δt is time in hours of circulation at that depth and t_c is the number of hours since circulation stopped and logging. The true formation temperature (T_F) is reading as the intersection of the line with the y-axis for x = 1.

Once the corrected true formation temperature of each well is obtained, the geothermal can be determined from the following equation.

$$\text{Geothermal gradient} = \frac{T_F\ (°F) - \text{Ambient temperature } (°F)}{\text{Depth logger (ft)} - \text{Height above datum (ft)}}$$

The datum of geothermal gradient is at the seafloor or ground level, so the height above datum equals the sum of elevation of Kelly Bushing (K.B.) and ground level (G.L.) obtains from well log heading. In the present calculation, all wells are in the sea and the calculation is thus referred to the subsea levels with the surface temperature at seafloor being 8°C or 46.4°F (Hydrology Department, 1996).

The summary of the geothermal gradient of the exploratory wells is in Table 4.2. It must be noted that only 2 out of 5 exploratory wells could supply information for the geothermal gradient calculation as the other 3 wells have the incorrect data, either due to the malfunctioning of the temperature recorder or the shifting of the temperature recording depth

Table 4.2 Summary of the Geothermal gradient of exploratory wells.

a.Kraburi-1 well.

Log name	Time circulation (t_c, hr)	Time since stopped circulated (Δt, hr)	$\Delta t/(tc+\Delta t)$	TL (°F)	Depth of measurement (ft.)
AIT/CDL/CNL/ NGS/DSI	1	10.2	0.9107	238	9087
AIT/CDL/CNL/ NGS/DSI	1	6.03	0.8578	229	9087
AIT/CDL/CNL/ NGS/DSI	1	5.57	0.8478	221	9087

TF = 250 °F @ 9087 ft.

Elevation of K.B. = 83 ft. and G.L. =3272 ft.

Geothermal gradient = 2.261 °F/ft. or 4.122 °C/100m.

b.Kantang-1a well

Log name	Time circulation (t_c, hr)	Time since stopped circulated (Δt, hr)	$\Delta t/(tc+\Delta t)$	TL (°F)	Depth of measurement (ft.)
HALS/HILT/SP/ DSI	1	8.4	0.8936	215	6837.3
HALS/HILT/SP/ DSI	1	8	0.8889	212	6837.3

TF = 240 °F @ 6837.3 ft.

Elevation of K.B. = 83 ft. and G.L. =3561 ft.

Geothermal gradient = 2.866 °F/ft. or 5.225 °C/100m.

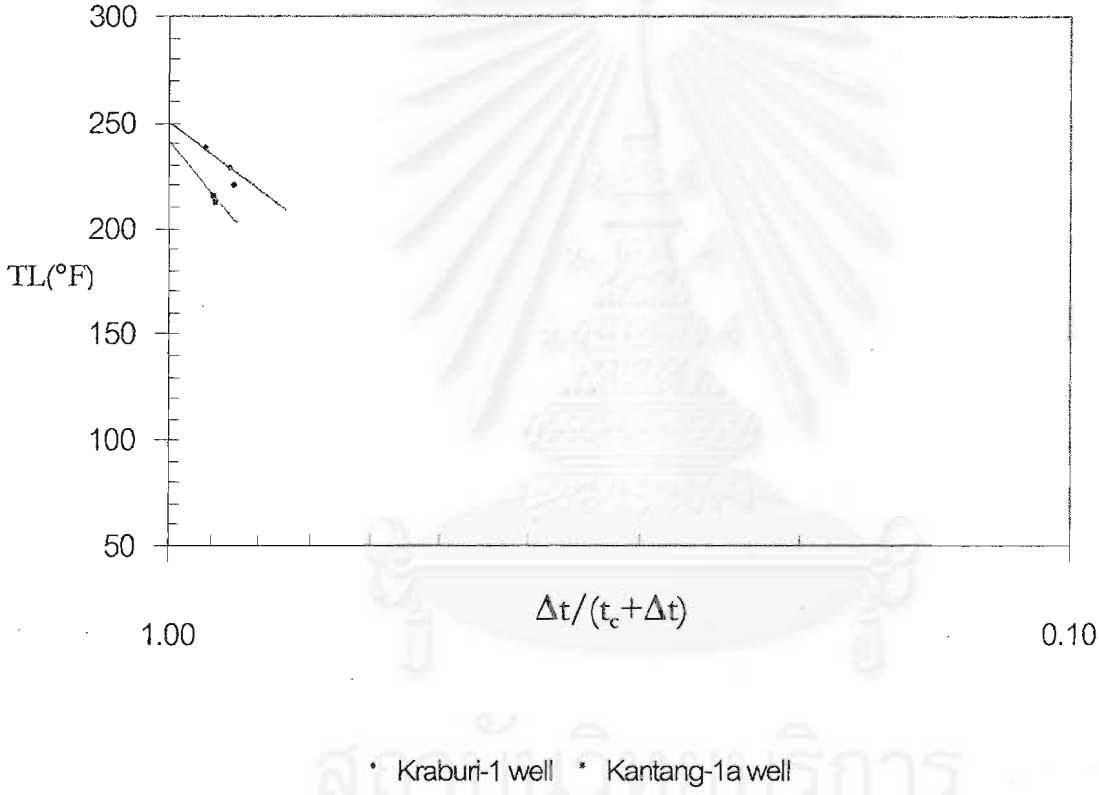

Figure 4.1 True formation temperature of each well within southern part of Mergui basin. The plots are according to the data in Table 4.2.

The geothermal gradient within the southern basin is concluded to range from 4.122 to 5.225 °C per 100 meters as shown in Table 4.2. The high gradient was observed in the deeper part of Eastern Mergui sub-basin margin.

Lopatin Method

Generally, the important factors in the process of oil generation and in the subsequence cracking of oil to methane are both time and temperature that could be interchangeable. A low temperature playing over a long time can have the same maturation effect as a high temperature playing in a short time. Lopatin has developed a "time-temperature index" of maturity (TTI) for the factors in thermal maturity of organic material in sediment or kerogen. The time-temperature index is based on the view that reaction rate is double for every 10°C rise in temperature.

Threshold values of Lopatin's time-temperature index of maturity (TTI) are as in Table 4.3.

Table 4.3 Threshold values of Lopatin's TTI.

Stage	TTI
Onset of oil generation	15
Peak oil generation	75
End of oil generation	160
Upper TTI limit for occurrence of oil with API gravity <40°	~500
Upper TTI limit for occurrence of oil with API gravity <50°	~1,000
Upper TTI limit for occurrence of wet gas	~1,500
Upper TTI limit for occurrence of dry gas	65,000

To determine TTI, the burial history is needed together with the temperature gradient. The following discussions are for the present study area. Firstly, the burial history of the geologic section was reconstructed by using the thickness of preserved stratigraphic unit which determined from the information of the exploratory wells and seismic data, geothermal gradient, sea floor temperature and age of each stratigraphic unit that is the relative age received from the biostratigraphic data. The burial history of

Kraburi-1 well starts with the deposition of Unit A of Late Oligocene sediment at the time approximately 32.8 m.y.B.P. at the sedimentary basinal surface (depth = 0).The sediment was continuously deposited at a varying rate to be buried to the present depth of 10,340 feet as the depth-time line that moving from left to right as illustrated in the Figure 4.2a. Similarly Unit B of Early Miocene epoch was commencing deposition at the time approximately 24.4 m.y.B.P. at the sedimentary basinal surface (depth = 0) and again was continuously deposited at a varying rate to be buried at the present depth 5,830 feet and its depth-time line is sub-parallel to that of Unit A as shown in Figure 4.2a. Unit C of Late Miocene sediments and Unit D of Pliocene sediments were commencing their deposition similarly at the time approximately 14.4 and 5.1 m.y.B.P., respectively at the sedimentary surface (depth = 0) and was continuously deposited at a varying rate to be buried to the present at depth 5,830 and 3100 feet respectively.

The burial history of Kantang-1a well (Figure 4.2b) could be explained in the same fashion.

Secondly, the temperature grid was reconstructed from the present-day geothermal gradients a series of 10 °C spacing lines of constant depth from the surface temperature of seafloor of 8°C or 46.4°F (Hydrology Department, 1996). The reconstruction is based on the assumption that both the gradient and the surface temperature have been constant throughout the time interval.

The time-temperature index (TTI) was calculated from the equation:

$$TTI = \sum_{nmin}^{nmax} (\Delta t_n)\,(r^n)$$

when Δt is the length of time spent by the sediment in the temperature interval I, nmax and nmin are the n-values of the highest and lowest temperature at 10°C interval, and r=2 as based on Arrhenius equation that states the rate of chemical reaction which is approximately double for every 10°C rise in temperature.

The time-temperature index studies indicate the depth for the oil generated is below deepest burial depth of the Late Oligocene units as resulted from the calculation

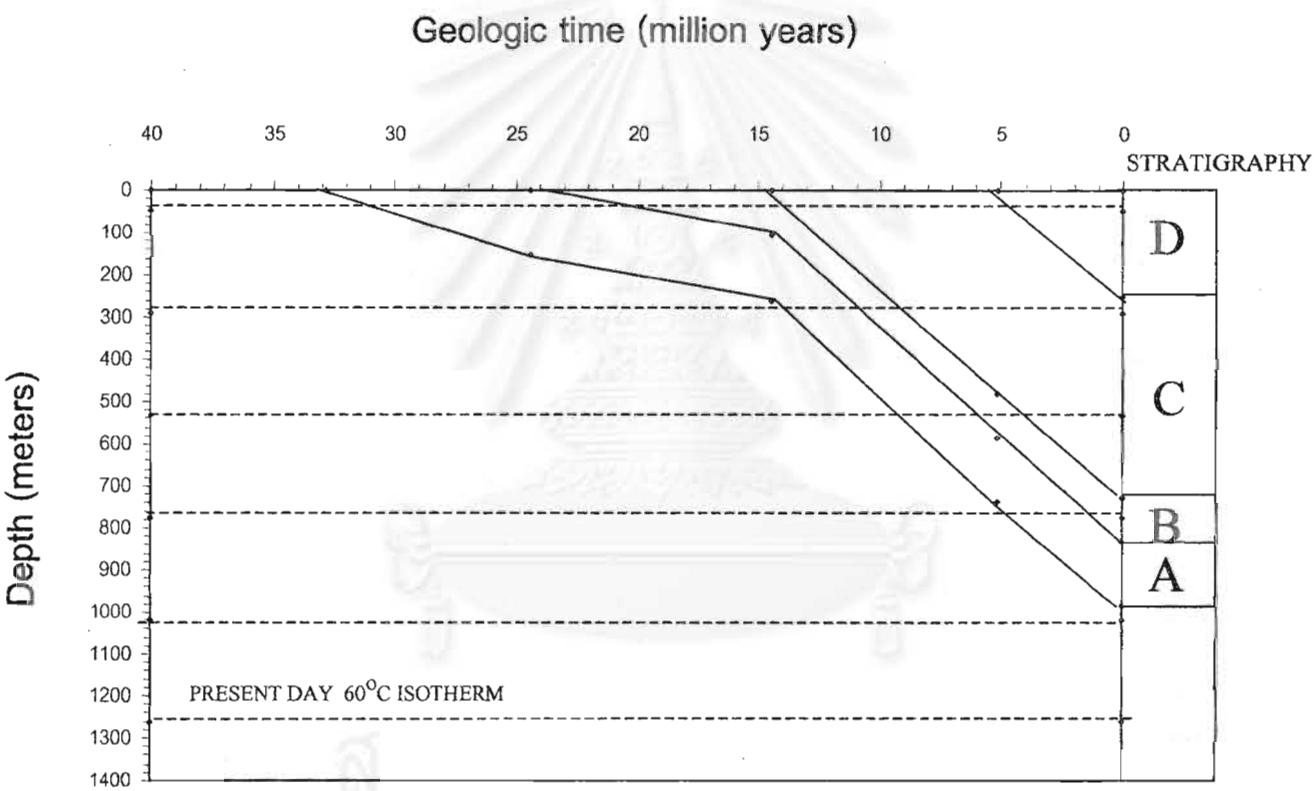

Figure 4.2. Burial history of exploratory wells.
a.Kraburi-1 well

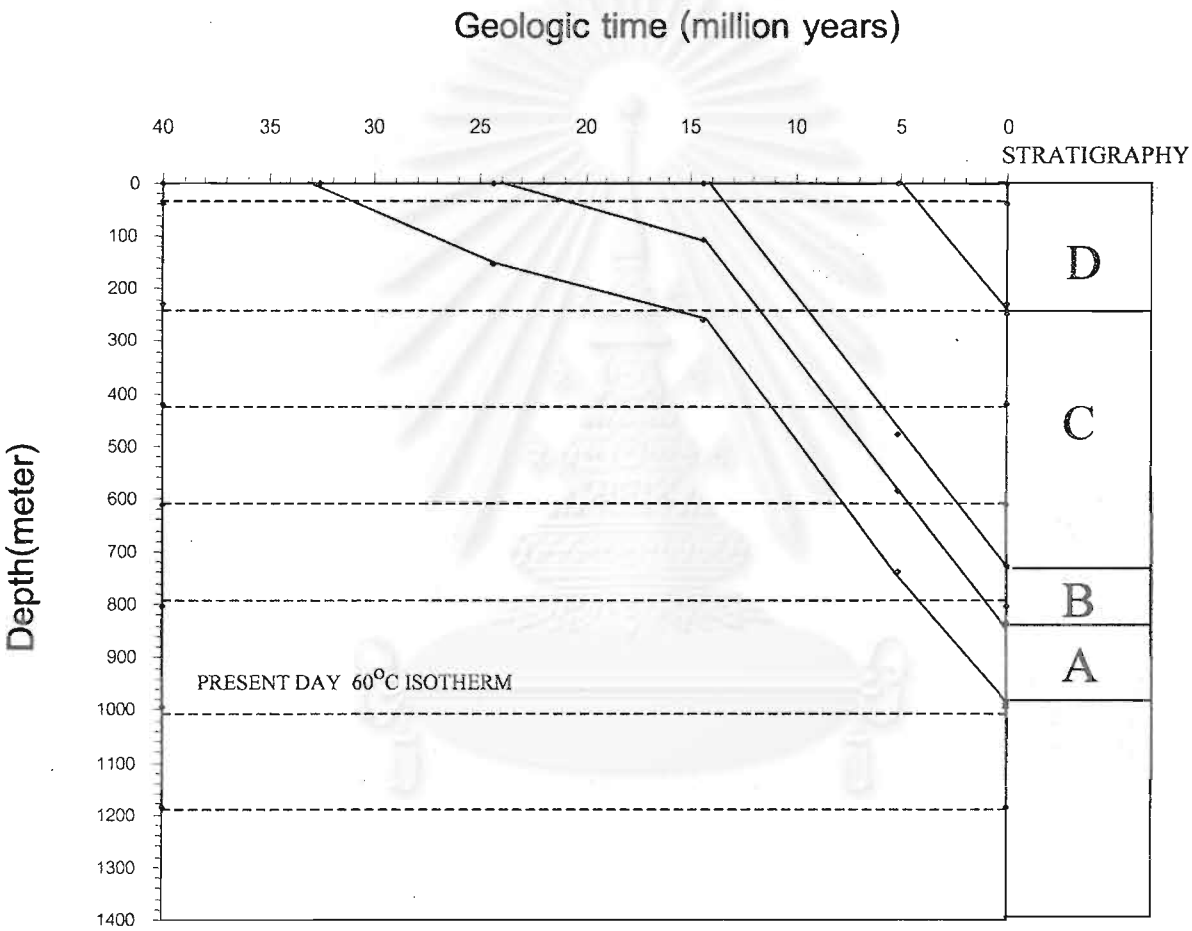

Figure 4.2. (Cont.) b.Kantang-1a well

sheet in Table 4.4. the present geothermal gradient also indicates the oil generation at a depth below the oldest sedimentary unit, 1000 meters in Kantang-1a well and 1200 to 1300 meters in Kraburi-1 well.

Table 4.4 Calculating of present TTI values of exploratory wells at shot point on seicmic section.

(a) Kraburi-1 well.

Temperature Inteval °C	Time my	Index Value n	Temperature factor g	Interval TTI	Total TTI
Horizon A					
0-10	2.60	-10	0.0009765625	0.0025390625	0.0025390625
10-20	16.20	-9	0.001953125	0.031640625	0.031640625
20-30	4.60	-8	0.00390625	0.01796875	0.04960938
30-40	4.80	-7	0.0078125	0.0375000	0.0871094
40-50	4.40	-6	0.015625	0.068750	0.155859
Horizon B					
0-10	4.60	-10	0.0009765625	0.0044921875	0.0044921875
10-20	8.90	-9	0.001953125	0.017382813	0.017382813
20-30	4.70	-8	0.00390625	0.01835938	0.03574219
30-40	6.20	-7	0.0078125	0.0484375	0.0841797
Horizon C					
0-10	1.00	-10	0.0009765625	0.0009765625	0.0009765625
10-20	4.60	-9	0.001953125	0.008984375	0.008984375
20-30	4.80	-8	0.00390625	0.01875000	0.02773438
30-40	4.00	-7	0.0078125	0.0312500	0.0589844

(b) Kantang-1a well.

Temperature Inteval C	Time my	Index Value n	Temperature factor g	Interval TTI	Total TTI
Horizon A					
0-10	2.10	-10	0.0009765625	0.0020507813	0.0020507813
10-20	13.00	-9	0.001953125	0.025390625	0.025390625
20-30	6.20	-8	0.00390625	0.02421875	0.04960938
30-40	3.70	-7	0.0078125	0.0289063	0.0785156
40-50	3.80	-6	0.015625	0.059375	0.137891
50-60	3.80	-5	0.03125	0.11875	0.25664
Horizon B					
0-10	4.30	-10	0.0009765625	0.0041992188	0.0041992188
10-20	8.10	-9	0.001953125	0.015820313	0.015820313
20-30	3.70	-8	0.00390625	0.01445313	0.03027344
30-40	3.70	-7	0.0078125	0.0289063	0.0591797
40-50	4.60	-6	0.015625	0.071875	0.131055
Horizon C					
0-10	4.40	-10	0.0009765625	0.0042968750	0.0042968750
10-20	3.80	-9	0.001953125	0.007421875	0.007421875
20-30	3.80	-8	0.00390625	0.01484375	0.02226563
30-40	2.40	-7	0.0078125	0.0187500	0.0410156

In addition, the hydrocarbon maturity of the sedimentary rocks can be determined from the empirical method as a function of sediment age and thermal history as proposed by Pigott (1985). The empirical method is as the follow equation.

$$T = 164.4 - 19.39 \ln t$$

T = Threshold temperature in °C

t = Sediment age in 10^6 years

$$D_{oc} = \frac{100(T-Ts)}{(dt/dz)}$$

D_{oc} = Depth in meters for the oil ceiling

Ts = Mean surface temperature

dt/dz = Geothermal gradient in °C/100m

From the age of sediment and geothermal gradient data within the southern part of Tertiary Mergui basin, the potential source rock buried in Late Oligocene epoch, approximately $32.8x10^6$ years thus gives the depth for the oil ceiling to be below 1660 meters as shown in Table 4.5.

Table 4.5 Calculation of oil ceiling depth.

a.Kraburi-1 well.

t	T	Ts	dt/dz	D_{oc}
32.8	96.721	10	4.122	2104
24.4	102.457	10	4.122	2243
14.4	112.682	10	4.122	2491
5.1	132.809	10	4.122	2979

b.Kantang-1a well.

t	T	Ts	dt/dz	D_{oc}
32.8	96.721	10	5.225	1660
24.4	102.457	10	5.225	1770
14.4	112.682	10	5.225	1965
5.1	132.809	10	5.225	2350

4.2 Reservoir

The reservoirs of the southern part of Mergui basin comprise two types of rock, limestones and sandstones. The limestone of carbonate buildups of the sub-unit A3 and unit C could be the one of prime targets for exploration. The carbonate build ups are clearly shown as the bright spots in the seismic profiles. These carbonate buildups occur in the basement high of the west flank of the Ranot trough and Ranong ridge. The depositional setting of these carbonate buildups is reef that deposited in Late Oligocene to Miocene time. From the petrography information, the porosity of carbonate reef buildups in Late Oligocene varies from 13 – 25 %, and that of the Miocene carbonate buildup is from 13 to 22%. These values are for the good quality reservoirs.

Secondly, the sandstones of the sub-unit A2-1 and A2-3 of the mid-fan turbidite depositional environment. These sandstones are found at the deeper part of the half-graben basin. These sandstones, are Late Oligocene in age. From the petrography information, the porosity of sandstones varies from 9 – 20 % indicating a fair quality reservoir potential. Thus this type of sandstone reservoir could be an interesting reservoir in the southern part of Mergui basin as well.

4.3 Seal

The effective hydrocarbon seals occur within all sequence in the southern part of Mergui basin. This is the marine shale or claystone which mostly deposited throughtout the basin from Late Oligocene till Recent. From an stratigraphic unit, the capabiliity hydrocarbon seals could be considered on the basis of prospect by prospect. For example, the bathyal shale of sub-unit A2-2 which is interbedded with sandstone is acting as source rock and seal at the same time.

The bathyal shale that overlies the limestone reservoir in sub-unit A3 and unit C is capable to be a good seal too. The bathyal shale or claystone of sub-unit Au that overlies sandstone reservoir in A2-3 could also prevent the upward escape of hydrocarbon.

4.4 Trap

The traps of the southern part of Mergui basin should be formed both structural and stratigraphic traps. The potential structural traps are along the N-S trending normal faults, the basement high which was formed during the initial rifting of the Mergui basin, and the rollover anticlines that occurred in the western flank of the Ranong trough and Ranot trough.

The reefs located on the isolate basement high have the potential to be the traps of both structure and stratigraphic types due to the reefs were drown and buried in the bathyal shale.

4.5 Migration

The presence of gas shows within the sedimentary unit C in Kantang-1a well which is thermally immature suggests an evident of migration from the thermally mature section that could be from the pre-Tertiary basement rock or the basinal shale in the deeper subbasin.

Hydrocarbon may be migrated up from basinal shale in the deeper subbasin along the fault planes and into sedimentary unit Au of Kantang-1a well and Sikao-1 well on the high side of the block. As well, it may migrate up from the adjacent pre-Tertiary basement which locates closer than from the deeper basinal shale.

CHAPTER V

DISCUSSION AND CONCLUSION

As mentioned earlier that the sedimentary sequence of Mergui basin is one of the prime targets for the petroleum exploration through time since 1975. The reasons could be that the basin is seemed to be continuing to North Sumatra basin which has a very promising petroleum potential there. Besides, Mergui basin and other sedimentary basin in Andaman Sea has a similar geologic condition. Mergui basin alone covers an area of about 100,000 square kilometers, with water depth of the sea floor from 200 to 2000 meters, and is where the Cenozoic sediments had accumulated down to the depth of approximately 8 kilometers. Several oil companies had tried the prospect of Mergui basin and unluckily had to retreat without success. However, more exploration data still become available, like these last ones of 5 new exploration wells and new seismic lines, altogether 10,648 meters in depth and 11,737 kilometers in length respectively. Thus a new attempt is done on these new data, aiming to judge for the petroleum potential of Mergui basin.

The present study which emphasizes on the age of deposition of the sedimentary units, which is Late Oilgocene as the oldest, also reveals the environment of deposition to be shallow marine which a continuous burial of the previously deposited sediments until Recent. The sedimentary units being recognized in this study consist of 4 stratigraphic unit, A, B, C, and D. The oldest unit, A, which is of the basinal, mid-fan turbidite, and reef depositional environment unconformably overlies the pre-Tertiary basement. The unit is composed of over 1000 meters thick of greenish gray shale or claystone, sandstone, and limestone. Unit B is composed of more than 1000 meters of basinal shale and is conformed to the underlying Unit A, Unit C which unconformably overlies Unit is made up with fine-grained clastic marine sediments, and above-lying Unit D is characterized by fine-to medium grained clastic marine sediments.

The study on the total organic carbon content (TOC) reveals that the marine clays and carbonate rocks in these sedimentary units especially A, B, C, and D is generally poor to fair. The korogen found in these units is commonly of type III which originated from the higher land plants. Perhaps during the accumulation of the organic

materials together with the inorganic mineral debris, the sedimentary basins did not locate very far from the land area so that the land could supply the land plant debris to these sedimentary accumulations by some methods of transportation.

The consideration of the maturation of the organic matters to general petroleum, either oil or gas, reveals that even the oldest Tertiary rocks here only stays at the beginning of the oil window zone. The time (age of deposition), temperature (geothermal gradient), and pressure (depth from surface to the sedimentary units) do not allow a good oil generation. This could explain why only trace of petroleum of uneconomic value were previously found in the exploratory wells. To look for a proper source rock, one should then pay more attention to the pre-Tertiary basement below.

As for the other essential factors for the petroleum accumulation, namely reservoir units, seals and traps, there are promising evidences for all these. Sandstones and carbonate buildups could be the good reservoir rocks while the fine-grained marine clays being found throughout the entire study area could play a role as the seals. The extensional N-S normal faults could create the structural traps while the basement-high formed during the continuous subsiding of the basement to form the half-graben sedimentary basins could create a perfect stratigraphic traps, together with the inclined porous sedimentary sequence.

REFERENCES

Allen, P.A., and Allen, J.R. 1993. Basin analysis: Principles and Applications. 3rd ed. London: Balckwell Scientific.

Anstey, N.A. 1977. Seismic Interpretation: the Physical Aspects. Boston: IHRDC.

Blow,W.H. 1969.Late Middle Eocene to Recent planktonic foraminiferal biostratigraphy. In bronniman, P., and Renz, H.H.(eds.) Proceedingss of the firsy international conference in planktonic microfossil. Leiden:E.J. Brill, 1, 199-421.

Bhuthuang, H. 1989. Subsurface Geology of some Upper Cenozoic Sediments in the Upper Gulf of Thailand with Special Reference to Off-Shore Hua Hin Basin. Master's Thesis, Department of Geology, Graduate School, Chulalongkorn University.

Chaodumrong, P. 1985. Sedimentological Studies of some Tertiary Deposits of Mae Moh Basin, Changwat Lampang. Master's Thesis, Department of Geology, Graduate School, Chulalongkorn University.

Curray, J.R., Moore, D.G., Lawver, L.A., Emmel, F.J. Raitt, Henry, M.and Kieckhefer, R.1978. Tectonics of the Andaman Sea and Burma. AAPG. Memoir29.

Dain, Y. A., Tapponnier, P., Molnar, P. 1984. Active Faulting and Tectonics of Burma and Surrounding Regions. J. Geophysical Research. Vol.89, No.31: 453-472.

Dowdle, W.L. and Cobb, W.M.1975.Static formation temperature from well logs an empirical method. J. petro. Tec. Nov: 1326.

Einsele, G. 2000. Sedimentary Basins: Evolution, Facies, and Sediment Budget. 2nd ed. Berlin: Springer-Verlag.

Geoservices Eastern Inc, 1996.Kraburi-1 Final well report. Bangkok: Thailand. (Unpublished Manuscript)

Geoservices Eastern Inc, 1996. Thalang-1 Final well report. Bangkok: Thailand. (Unpublished Manuscript)

Geoservices Eastern Inc, 1996. Kantang-1a Final well report. Bangkok: Thailand. (Unpublished Manuscript)

Geoservices Eastern Inc, 1996.Sikao-1 Final well report. Bangkok: Thailand. (Unpublished Manuscript)

Geoservices Eastern Inc, 1996.Kathu-1 Final well report. Bangkok: Thailand. (Unpublished Manuscript)

Gretener, P.E. 1981. Geothermics: Using Temperature in Hydrocarbon Exploration. Oklahoma: AAPG Bookstore.

Harding, T.P.1985. Seismic Characteristics and Identification of Negative Flower structures, Positive Flower Structures, and Positive Structure Inversion. AAPG. Bull., Vol 69 No.4: 582-600.

Ingersoil, R. V., 1988.Tectonics of Sedimentary Basins. Geol. Soc. Ame. Bull., Vol.100, pp.1704-1719.

Kaewsang, K. 1987. Sedimentary Facies Analysis of some Uppers Tertiary Deposits of Fang Basin, Changwat Chiang Mai. Master's Thesis, Department of Geology, Graduate School, Chulalongkorn University.

Khantaprab, C., and S. Sarapirome.1983. Geology Aspects of the Gulf of Thailand and Andaman Sea- A review. Conference on Geology and Mineral Resource of Thailand.Bangkok. Thailand.

Kosuwan, T. 1995. Evolution of Sedimentary Deposition and Assessment of Petroleum Potential of the Wichian Buri sub-basin, Changwat Phetchabun. Master's Thesis, Department of Geology, Graduate School, Chulalongkorn University.

Lekuthai, T. 1992. Geothermal Gradient in the Gulf of Thailand. Bangkok: Department of Mineral Resources.

Nakanart, A.., and Mantajit, N., 1983. Stratigraphic correlation of the Andaman Sea. Conference on Geology and Mineral Resources of Thailand, Bangkok, Thailand, 1-7.

Nelson, H.C., Nilson, H.T.,1989. Modern and Ancient Deep-Sea Fan Sedimentation. SEPM Short Course No.14.

Martini, E. 1971. Standard Tertiary and Quaternary calcareous nannoplanktonic zonation Proc. 2nd. Conf. Planktonic Microfossils. 2:739-786.

Mitchum, R.M., Jr., P.R. Vail, and J.B. Sangree, 1977. Stratigraphic Interpretation of Seismic Reflection Patterns in Depositional , in C.E. Payton(ed.)AAPG Memoir 26, P.117-133.

Mutti, E. and Ricci Lucchi, F.1972. Turbidites of the Northern Apennines:introduction to facies analysis. Translated by Nielson, T.H.1978. in International Geology Review, 20, No.2, 125-66

Packham, G. H. 1993. Plate Tectonics and the Development of Sedimentary Basins of the Dextral Regime in Western Southeast Asia. J. Southeast Asian Earth Sci. 8: 497-511.

Payton, C.E. 1977. Seismic Stratigraphy Applications to Hydrocarbon Exploration. AAPG. Memoir 26.

Pigott, J. D. 1985. Assessing Source Rock Maturity in Frontier Basins: Importance of Time, Temperature, and Tectonics. AAPG. Bull. Vol 69, No.8: 1269-1274.

Polachan, S. The Geological Evolution of the Mergui Basin, S.E. Andaman Sea, Thailand. Doctoral dissertation, Royal Holloway and Bedford New College. University of London, 1998.

Polachan, S. , and Racey, A., 1993. Lower Miocene Larger Foraminfera and Petroleum Potential of the Tai Formation, Mergui Group, Andaman Sea. J. Southern Asian Earth Sciences. Vol. 8: 487-496.

Posamentier, H.W., Summerhayes, C.P., Haq, B.U., and Allen, G.P. eds. 1993. Sequence Stratigraphy and Facies Associations. London: Blackwell Scientific.

Reading, H.G. ed. 1996. Sedimentary Environments: Processes, Facies and Stratigraphy. 3rd ed. London: Blackwell Science.

Reineck, H.E., and Singh, I.B. 1980. Depositional Sedimentary Environments: with Reference to Terrigenous Clastics. 2nd ed. Berlin: Springer-Verlag.

Rodolfo, K.1969. Bathymetry and Marine Geology of the Andaman Basin, and Tectonic Implications for Southeast Asia. Geological Society of America Bulletin., Vol 80 : 1203-1230.

Schumberger. 1985. Sedimentary Environments from Wireline Logs. Texas.

Selley, R.C. 1979. Dipmeter and log motifs in North Sea submarine-fans. AAPG. Bull. Vol 63 No.6: 905-917.

Sheriff, R.E. 1980. Seismic Stratigraphy. Boston: IHRDC.

Srigulwong, S. 1986. Structural Evolution and Sedimentation during the Oligocene Time in the Vicinity of the Well W9E-1, Mergui basin. Master's Thesis, Department of Petroleum Geology, University of Aberdeen.

Tissot, B.P., Pelet, R., and Ungerer, P.H., 1987. Thermal History of Sedimentary Basins, Maturation Indices, and Kinetics of Oil and Gas Generation. AAPG. Bull. Vol 71 No.12: 1445-1466.

Tissot, B.P., and Welte, D.H., 1978. Petroleum Formation and Occurrence. Berlin: Springer-Verlag.

Walker, G.R., 1978 Deep-water sandstone facies and ancient submarine fans: models for exploration for stratigraphic traps AAPG. Bull. Vol 62: 932-66.

Walker, G.R., 1984. Facies Model. 2nd ed. Ontario: Ainsworth Press.

Waples, D.W., 1980. Time and Temperature in Petroleum Formation: Application of Lopatin's Method to Petroleum Exploration. AAPG.Bull. Vol 64 No.6: 916-926.

Week, L.A., Harbison, R.N., and Peter, G., 1967. Island Arc System in Andaman Sea, AAPG. Bull. Vol. 51, No.9: 1803-1815.

APPENDIX

Appendix-1 Summary of petrographic analysis.

a.Kraburi-1 well

Depth	5831	7080	8190	8520	8812	8935	9163
Rock name	Lithic Arkose	litharenite	Lithic arkose/feldspar litharenite	litharenite	Lithic Arkose	litharenite	litharenite
Framwork grains							
Quartz	50	59	54	37	51	51	51
Monocrystalline	16	18	34	21	27	20	26
Polycrystalline	6	6	3	5	9	8	9
Feldspar	48	20	23	30	27	24	18
K. feldspar	11	5	7	8	7	7	7
Plagioclase	10	3	9	13	12	6	5
Lihic Fragments	2	22	23	33	23	25	31
Plutonic	1		2	7	4	5	5
Volcanic	5	1	3	2	1	1	2
Metamorphic	3	6	10	14	11	8	14
Chert	1	1	1	2	2	2	2
Mudstone	1	1	1	tr	1	2	1
Sandstone/siltstone	0	0	0	0	0	0	0
Limestone	0	0	0	0	0	0	0
Dolostone	0	tr	tr	0	0	0	0
Accessory grains	10	8	9	9	3	16	9
Muscovite	3	3	tr	3	tr	5	1
Biotite	7	5	9	6	3	11	8
Heavy mineral	tr	tr	tr	tr	tr	tr	tr
Enviroment indicator	3	7	tr	tr	tr	4	1
Plant fragments	3	6	tr	tr	tr	4	1
Glauconite	0	0	0	0	0	0	0
Fossils fragment	0	1	tr	tr	0	tr	0
Clay matrix	19	36	tr	1	2	6	7
Authigenic cement	6	3	8	10	21	11	10
Kaolonite/Dickite	0	tr	tr	tr	tr	tr	tr
Other pore-filling clay	tr	0	tr	tr	tr	tr	tr
Pore-filling clay	3	1	2	6	3	4	3
Quartz overgrowths	1	1	3	2	2	3	4
Calcites	0	0	3	1	15	2	1
Fe-Dolomite	0	0	0	0	0	0	0
Ankerite	0	0	0	0	0	0	0
Siderite	tr	0	tr	0	0	0	tr
Pyrite	2	1	tr	tr	tr	2	tr
Fe/Ti oxides	tr	tr	tr	1	1	tr	2
Barite	0	0	tr	0	0	0	0
Residual oil	tr	0	tr	tr	0	0	0
Porosity	9	5	14	10	3	8	5
Primary	8	1	12	5	2	4	2
Secondary	tr	1	1	1	tr	1	1
Microscopic	1	3	1	4	1	3	2
Total	100	100	100	100	100	100	100

Appendix-1 (cont.)

b.Thalang-1 well

Depth	7540	7560	7570	7608	7620	7630	7640
Rock name	Sublitharenite	Litharenite	Litharenite	Sublitharenite	Sublitharenite	Litharenite	Litharenite
Framwork grains							
Quartz	79	65	74	79	71	68	65
Monocrystalline	33	31	32	29	29	28	27
Polycrystalline	4	4	7	9	10	12	8
Feldspar	2	2	2	4	tr	5	2
K. feldspar	tr	tr	tr	tr	0	tr	0
Plagioclase	1	1	1	2	tr	3	1
Lihic Fragments	19	28	25	17	20	27	33
Plutonic	1	1	tr	1	tr	1	2
Volcanic	1	3	3	2	2	4	2
Metamorphic	5	9	8	3	6	7	11
Chert	tr	1	tr	tr	tr	tr	tr
Mudstone	1	1	1	tr	tr	tr	tr
Sandstone/siltstone	0	0	0	0	0	0	0
Limestone	0	0	0	0	0	0	0
Dolostone	0	0	0	0	0	0	0
Accessory grains	2	3	2	3	1	4	2
Muscovite	2	2	2	2	1	3	3
Biotite	tr	1	tr	1	tr	1	tr
Heavy mineral	tr	tr	tr	tr	tr	tr	tr
Enviroment indicator	tr	tr	tr	tr	tr	tr	tr
Plant fragments	0	0	0	tr	0	tr	0
Glauconite	tr	tr	tr	tr	tr	0	tr
Fossils fragment	0	0	0	0	tr	0	0
Clay matrix	1	0	tr	1	0	tr	tr
Authigenic cement	41	33	31	37	34	25	25
Kaolonite/Dickite	10	10	11	8	9	5	9
Other pore-filling clay	tr	tr	0	1	tr	tr	tr
Pore-filling clay	1	1	2	1	1	1	tr
Quartz overgrowths	1	2	2		3	1	3
Calcites	0	0	0	3	0	0	0
Fe-Dolomite	18	13	9	14	15	9	tr
Ankerite	0	0	0	0	0	0	0
Siderite	5	3	2	5	2	5	11
Pyrite	3	3	2	2	2	2	1
Fe/Ti oxides	3	1	2	2	1	2	tr
Barite	0	0	0	0	0	0	0
Residual oil	tr	tr	1	1	1	tr	tr
Porosity	9	13	14	11	15	12	20
Primary	1	3	5	2	7	4	9
Secondary	3	5	3	5	4	4	5
Microscopic	5	5	6	4	4	4	6
Total	100	100	100	100	100	100	100

Appendix-2 Summary of sidewall core description.

a. Thalang-1 well

No	Depth (ft)	Lithology	Description
1	8408	sandstone	olive grey, light grey very fine grained, poorly sorted, subangular calcareous, trace chlorite coal
2	8392	shale	dark grey, light grey, fissil, slightly to non calcareous firm
3	8313	silty shale	dark grey, grey, occ silty to very fine, occ rock fragments, locally fissil, trace chlorite, strongly
4	8200	shale	dark greenish grey, fissile, platy, modderately to slightly calcareous firm trace chlorite
5	8042	silty shale	dark green grey, olive grey occ silty to very fine, fissile, platy, slightly calcareous
6	7845	silty shale	olive grey, light grey occ silty to very fine, trace chlorite, strongly calcareous
7	7694	Bullet lost	
8	7660	shale	brownish grey, play, fissile, strongly calcareous, trace chlorite, trace coal
9	7640	sandstone	greenish grey, very fine to fine grained, quartz white, milk, transparent, translucence, moderately to
10	7630	sandstone	greenish grey, very fine to fine grained, moderately to poorly sorted, sub-angular to sub-round,
11	7620	sandstone	greenish grey, very fine to fine grained, quartz clear, sub-angular to sub -round, soft to friable,
12	7608	sandstone	greenish grey, very fine to fine grained, milky, clear quartz, sub-angular, friable, poorly-moderately
13	7570	sandstone	light grey, very fine to fine grained, milky, clear quartz, sub-angular, firm, common mica, chlorite,
14	7560	sandstone	medium grey, very fine to fine grained, sub-angular, firm, poor to mod sorted, strongly calcareous,
15	7540	sandstone	medium grey, very fine to fine grained, sub-angular, firm, occ mica, chlorite, trace feldspar

Appendix-2 (cont.)

a. Thalang-1 well (cont.)

No	Depth (ft)	Lithology	Description
16	7480	Bullet lost	
17	7354	Bullet lost	
18	7205	silty shale	medium grey, light grey, occ silty, fissile, firm, trace mica, slightly calcareous
19	6968	silty shale	medium to dark grey, occ silty, firm, abundant chlorite, strongly calcareous
20	6800	silty shale	olive grey, occ silty, minor very fine sands, firm ,occ mica, common feldspar, strongly calcareous
21	6708	shale	brownish grey,light grey,occ silty, trace mica, chlorite absent, strongly calcareous
22	6647	shale	brownish grey, light grey, occ very fine sands, silty, fissile, trace pyrite, strongly calcareous
23	6480	shale	brownish grey, light grey, occ very fine sands, silty, common coal, trace mica, pyrite, strongly
24	6280	shale	brownish grey, light grey, strongly calcareous, trace chlorite, mica, pyrite, coal
25	6250	shale	brownish grey, sub-fissile, moderately calcareous, trace feldspar coal
26	6141	shale	brownish grey, sub-fissile, moderate calcareous, trace feldspar coal
27	6044	shale	light brown grey, strongly calcareous, trace, mica
28	5978	shale	light brown grey, olive grey, strongly calcareous, trace, mica, coal
29	5763	Bullet lost	
30	5701	Bullet lost	

Appendix-2 (cont.)

b.Kraburi-1 well

No	Depth (ft)	Lithology	Description
1	10122	silty shale	dark grey, sub-fissile, moderate coal, moderately calcareous
2	9972	silty shale	dark grey, soft-firm, moderate silty, moderately coaly, calcareous
3	9785	silty shale	dark grey, locally very fine sands, silt, platy, moderately coaly calcareous
4	9585	silty shale	dark grey, soft to firm, locally very fine sands, silt, trace coal calcareous
5	9469	silty shale	dark grey, firm, silty, trace sands, trace coal, trace rock fragments, strongly calcareous
6	9425	silty shale	dark grey, soft to firm, silty, trace sands, calcareous
7	9314	silty shale	dark grey, soft, silty, trace very fine sands, trace coal, moderately calcareous
8	9205	silty sand	dark grey, very fine sands, silty, sub-round too sub-angular, poorly sorted, friable, common coal, trace mica, chlorite, moderatelly calcareous
9	9195	Sandstone	dark grey, very fine to fine grained, locally silty, clay, sub-round to round, friable, moderate chlorite, common coal, trace rock fragments trace
10	9163	Sandstone	dark grey, very fine to fine grained, locally silty, clay, sub-angular to sub-round, friable, trace chlorite, common coal, trace rock fragments
11	9150	Sandstone	dark grey, very fine to fine grained, silty, locally clay, angular to sub-angular,friable, trace rock fragment, moderate chlorite common coal,
12	9090	Sandstone	dark grey, very fine to fine grained, silty, locally clay, sub-round to round, friable, trace chlorite, common coal, trace rock fragments,
13	9010	Sandstone	greyish black, locally silty, firm, sub-fissile, plate, moderately calcareous
14	8980	Sandstone	dark grey, very fine to fine grained, silty, sub-round to round, friable,trace chlorite, common coal, trace rock fragments, moderrately calcareous
15	8950	Sandstone	dark grey, very fine to fine grained, silty, sub-round to round, friable,trace chloritetrace mica, common coal, trace rock fragments, moderately
16	8935	Sandstone	dark grey, very fine grained,silty, sub-angular to sub-round, friable, common coal, moderately calcareous
17	8910	Sandstone	dark grey, very fine to fine grain, silty, sub-angular, friable, trace mica, trace chlorite, trace coal , trace dolomite, moderately calcareous
18	8880	Sandstone	dark grey, very fine to fine grain, silty, sub-angular to sub-round, friable, common chlorite, common coal, trace rock fragments, trace
19	8812	Silty Sand	dark grey, very fine to fine grained, silty, angular to sub-angular, friable, poorly, sorted, common chlorite, common coal, trace, rock fragment
20	8685	Sandstone	dark grey, very fine to fine grain, silty, angular to sub-angular, friable, poorly sorted, trace mica, moderate chlorite, common coal, moderately
21	8590	Sandstone	dark grey, very fine to fine grain, silty angular to sub -angular, firm, poorly sorted, trace chlorite, common coal, calcareous
22	8520	Sandstone	dark grey, very fine to fine grain, silty, angular to sub-angular, firm, poorly sorted, trace feldspar, common coal, trace dolomite moderately
23	8460	Sandstone	dark grey, very fine to fine grain, silty, angular to sub-angular, firm, poorly sorted, trace feldspar, common coal, trace dolomite moderately

Appendix-2 (cont.)

b.Kraburi-1 well(cont.)

No	Depth (ft)	Lithology	Description
24	8385	Sandstone	dark grey, very fine to fine grain, silty , angular to sub - angular, firm, poorly sorted, common mica, common chlorite, moderate feldspar,
25	8190	Sandstone	medium dark grey, very fine to fine , locally medium grains, angular to sub-angulae, firm, poorly sorted, trace mica, moderate chlorite, trace
26	8020	Shale	olive black, locally silty , firm, strongly calcareous
27	7978	Silty Shale	olive black, locally silt, firm, sub-fissile, strongly calcareous
28	7805	Silty Sand	medium grey, locally very fine to fine sands, angular to sub-round poorly sorted, firm, moderate mica, trace chlorite, moderate coal , trace rock
29	7710	Silty Shale	dark grey, sub-fissile, firm, strongly calcareous
30	7618	Silty Shale	dark grey, firm , platy, trace mica, strongly calcareous
31	7505	Silty Shale	dark grey, firm, platy, tace mica, moderate coal, strongly calcareous
32	7435	Silty Shale	dark grey, firm, sub-fissile,moderate coal, strongly calcareous
33	7316	Silty Shale	dark grey, firm, moderate mica, moderate coal, trace pyrite
34	7215	Silty Shale	dark grey, firm, sub-fissile, trace mica, strongly calcareous
35	7160	Silty Shale	medium grey, firm , trace mica, trace chlorite, trace coal
36	7080	Sandstone	medium grey, very fine to fine, locally medium grain, angular to sub angular, poorly sorted , firm, moderate mica, moderate chlorite, common
37	6955	Silty Shale	dark grey, locally very fine sands, firm, platy, moderate coal, trongly calcareous
38	6895	Silty Shale	olive grey, locally very fine sands, firm, platy, moderate coal, strongly calcareous
39	6680	Silty Shale	olive grey, locally very fine sands, firm, sub--fissile, moderate coal, strongly calcareous
40	6355	Silty Shale	dark grey, silty, firm , sub -fissile, strongly calcareous
41	6252	Silty Sand	medium grey, very fine to fine grain, angular to sub-angular, poorly sorted, friable, moderate mica, trace chlorite, common coal, calcareous
42	6163	Silty Shale	dark grey, locally silt, sands, friable, trace mica, common coal, strongly calcareous
43	5965	Silty Shale	dark grey, locally silt, sands, friable, moderate coal, strongly calcareous
44	5831	Sandstone	mediun grey, very fine to fine, locally medium grain, angular to sub-angular, friable, poor to moderately sorted, moderate mica, moderate
45	5500	Silty Shale	ddark grey, soft, sub-fissile, trace mica, trace coal, strongly calcareous

Appendix-2 (cont.)

c. Kantang-1a well

No	Depth (ft)	Lithology	Description
1	6472	silty shale	brownish grey, olive grey, sub-fissile, mottled, firm , common coal, very strongly calcareous
2	6433	silty shale	brownish grey, olive grey, sub-fissile, mottled, firm , common coal, very strongly calcareous
3	6390	silty shale	olive grey, fissile, mottled, moderate coal, common fossils, very strongly calcareous.
4	6338	silty clay	olive grey, fissile, mottled, firm, common coal, very strongly calcareous.
5	6300	silty clay	olive grey, no-fissile, mottled, firm, common coal, strongly calcareous.
6	6265	silty clay	olive grey, no-fissile, mottled, soft, common coal, strongly calcareous.
7	6222	silty clay	olive grey, no-fissile, mottled, firm, moderate coal, strongly calcareous.
8	6182	Bullet Lost	
9	6130	Silty Clay	Olive grey, no-fissile, trace coal, local calcite, strongly calcareous
10	6083	Claystone	olive grey, no-fissile, soft, trace coal, trace carbonate fragments, strongly calcareous.
11	6052	silty clay	olive grey, no-fissile, soft, trace coal, strongly calcareous
12	6002	Claystone	olive grey,trace coal,locally carbonate fragments,strongly calcareous
13	5957	Claystone	olive grey, soft,sticky,trace coal,strongly calcareous
14	5907	Claystone	olive grey, soft,sticky,trace coal,strongly calcareous
15	5862	Claystone	olive grey, soft,trace coal,strongly calcareous
16	5810	Claystone	olive grey, soft,no coal,rare silt, strongly calcareous
17	5801	Claystone	olive grey, soft,no coal, strongly calcareous
18	5778	Claystone	olive grey, soft,trace coal,locally silt, strongly calcareous
19	5757	Claystone	olive grey, soft,trace coal,trace pyrite, trace carbonate fragments, strongly calcareous
20	5698	Bullet Lost	
21	5640	silty clay	light olive grey, silty, firm,mottled, trace coal,trace carbonate fragments, moderately calcareous
22	5600	silty clay	light olive grey, silty, firm,mottled, trace coal,trace carbonate fragments, strongly calcareous
23	5570	clayey silt	medium to dark grey grey, silty, moderate caly, hard, abundant coal, trace mica , strongly calcareous
24	5532	clayey silt	medium to dark grey grey, silty, moderate caly, friable, abundant coal, trace mica , strongly calcareous

Appendix-2 (cont.)

c. Kantang-1a well (cont.)

No	Depth (ft)	Lithology	Description
1	6745	limestone	white, milky, firm-hard, friable,chalky
2	6740	limestone	white, milky, firm-hard, friable,chalky
3	6735	limestone	white, milky, firm-hard, friable,chalky
4	6730	limestone	white, milky, firm-hard, friable,chalky
5	6723	limestone	white, milky, firm-hard, friable,chalky
6	6720	limestone	white, milky, firm-hard, friable,chalky
7	6715	limestone	white, milky, firm-hard, friable,chalky
8	6711	limestone	white, milky, firm-hard, friable,chalky
9	6705	limestone	white, milky, firm-hard, friable,chalky
10	6700	limestone	white, milky, firm-hard, friable,chalky
11	6695	limestone	white, milky, firm-hard, friable,chalky
12	6690	limestone	white, milky, firm-hard, friable,chalky
13	6685	limestone	white, milky, firm-hard, friable,chalky
14	6677	limestone	white, milky, firm-hard, friable,chalky
15	6670	limestone	white, milky, firm-hard, friable,chalky
16	6664	limestone	white, milky, firm-hard, friable,chalky
17	6659	limestone	white, milky, firm-hard, friable,chalky
18	6653	limestone	white, milky, firm-hard, friable,chalky
19	6644	limestone	white, milky, firm-hard, friable,chalky
20	6634	limestone	white, milky, firm-hard, friable,chalky
21	6627	limestone	white, milky, firm-hard, friable,chalky
22	6620	limestone	white, milky, firm-hard, friable,chalky
23	6615	limestone	white, milky, firm-hard, friable,chalky
24	6610	limestone	white, milky, firm-hard, friable,chalky
25	6599	limestone	white, milky, firm-hard, friable,chalky
26	6594	limestone	white, milky, firm-hard, friable,chalky
27	6590	limestone	white, milky, firm-hard, friable,chalky
28	6586	limestone	white, milky, firm-hard, friable,chalky
29	6582	limestone	white, milky, firm-hard, friable,chalky
30	6578	limestone	white, milky, firm-hard, friable,chalky
31	6571	limestone	white, milky, firm-hard, friable,chalky
32	6566	limestone	white, milky, firm-hard, friable,chalky
33	6560	limestone	white, milky, firm-hard, friable,chalky
34	6556	limestone	white, milky, firm-hard, friable,chalky
35	6553	limestone	white, milky, firm-hard, friable,chalky
36	6547	limestone	white, milky, firm-hard, friable,chalky
37	6543	limestone	white, milky, firm-hard, friable,chalky
38	6538	limestone	white, milky, firm-hard, friable,chalky
39	6517	limestone	white, milky, firm-hard, friable,chalky
40	6400	limestone	white, milky, firm-hard, friable,chalky

Appendix-2 (cont.)

d.Sikao-1 well

No	Depth (ft)	Lithology	Description
1	5625	Granite	green, hard, non-calcareous, translusent quartz
2	5581	Limestone	white, light grey, firm, fair porosity
3	5566	Limestone	white, light grey, firm, fair porosity
4	5555	Limestone	white, light grey, firm, fair porosity
5	5540	Limestone	white, light grey, firm, fair porosity
6	5530	Limestone	white, light grey, firm, fair porosity
7	5520	Limestone	white, light grey, firm, fair porosity
8	5513	Limestone	white, light grey, firm, fair porosity
9	5500	Limestone	white, light grey, firm, fair porosity
10	5495	Limestone	white, light grey, firm, fair porosity
11	5485	Limestone	white, light grey, firm, fair porosity
12	5470	Limestone	white, light grey, firm, fair porosity
13	5457	Limestone	white, light grey, firm, fair porosity
14	5447	Limestone	white, light grey, firm, fair porosity
15	5440	Limestone	white, light grey, firm, fair porosity
16	5430	Limestone	white, light grey, firm, fair porosity
17	5427	Limestone	white, light grey, firm, fair porosity
18	5400	Limestone	white, light grey, friable, fair porosity
19	5390	Limestone	white, light grey, friable, fair porosity
20	5379	Limestone	white, light grey, friable, fair porosity
21	5373	Limestone	white, light grey, friable, fair porosity
22	5366	Limestone	white, light grey, friable, fair porosity
23	5360	Limestone	white, light grey, friable, fair porosity
24	5334	Limestone	white, light grey, friable, fair porosity
25	5326	Limestone	white, light grey, friable, fair porosity
26	5317	Limestone	white, light grey, friable, fair porosity
27	5309	Limestone	white, light grey, friable, fair porosity
28	5302	Limestone	white, light grey, friable, fair porosity
29	5297	Limestone	white, light grey, friable, fair porosity
30	5293	Limestone	white, light grey, friable, fair porosity
31	5285	Limestone	white, light grey, friable, fair porosity
32	5271	Limestone	white, light grey, friable, fair porosity
33	5264	Limestone	white, light grey, friable, fair porosity
34	5258	Limestone	white, light grey, friable, fair porosity
35	5252	Limestone	white, light grey, friable, fair porosity
36	5244	Limestone	white, light grey, friable, fair porosity
37	5236	Limestone	white, light grey, friable, fair porosity
38	5229	Limestone	white, light grey, friable, fair porosity
39	5192	shale	olive grey, firm, calcareous
40	5066	-	

Appendix-2 (cont.)

e.Kathu-1 well

No	Depth (ft)	Lithology	Description
1	3278	Basement	Tool failed
2	3270	Limestone	Light grey, hard, vuggy porosity (5x5mm)
3	3261	-	
4	3254	Limestone	white, light grey, friable, soft
5	3250	-	
6	3241	Limestone	white, light grey, friable, soft
7	3235	Limestone	white, light grey, friable, soft
8	3230	Limestone	white, light grey, friable, soft
9	3225	-	
10	3222	Limestone	white, light grey, friable, soft
11	3218	Limestone	white, light grey, friable, soft
12	3211	Limestone	white, light grey, friable, soft
13	3206	Limestone	white, light grey, friable, soft
14	3200	Limestone	white, light grey, friable, soft
15	3186	-	
16	3176	Limestone	white, light grey, friable, soft
17	3170	Limestone	white, light grey, friable, soft
18	3114	Limestone	white, light grey, friable, soft
19	3155	-	
20	3055	Shale	olive grey, too soft to recover
21	2890	Shale	olive grey, too soft to recover

BIOGRAPHY

Miss Praphaporn Khrusida was born in Unbonrachthani in 1972, she studied at Nareenukul school for the pre-university education in Unbonrachthani between 1984 and 1990. She graduated with the B.Sc. in Geotechnology from Khonkean University in 1994. After graduation, she worked with the Bangkok Engineering Consultant Co., Ltd. for one year, In 1996, she worked with the Samart Project Consultant Co., Ltd. In 1998, Geotechnical & foundation Engineering Co., Ltd. employed her, At present, she is studying the M.Sc. degree in Geology at Chulalongkorn University.